

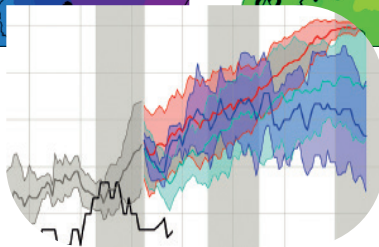
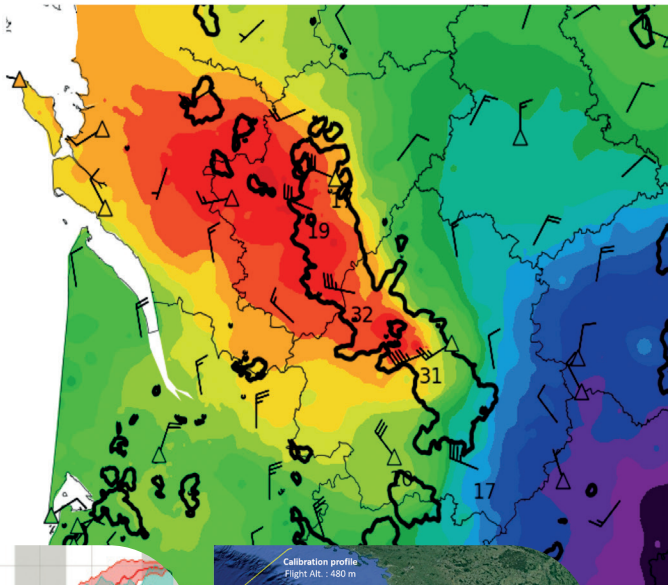
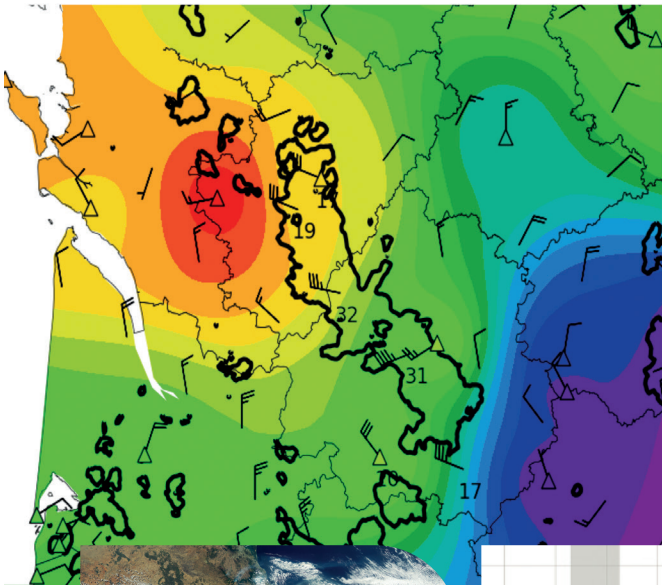
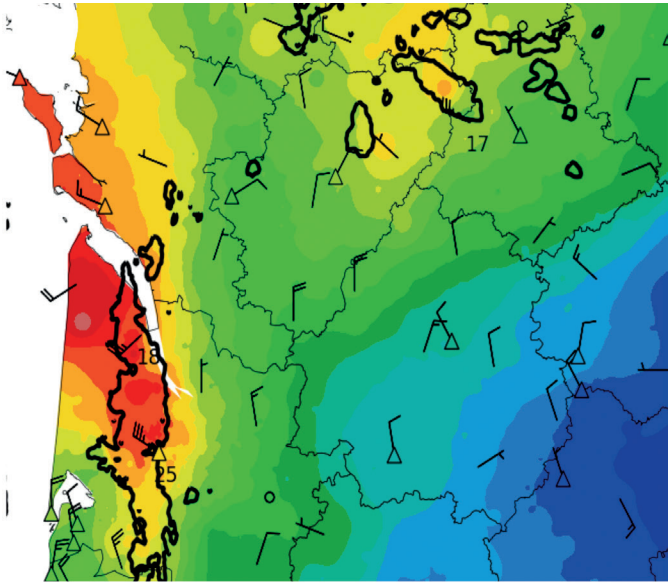
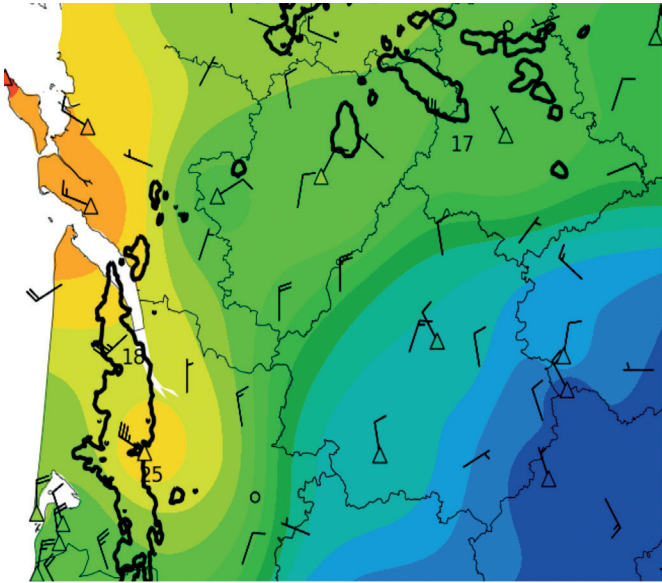


RÉPUBLIQUE
FRANÇAISE

*Liberté
Égalité
Fraternité*



METEO
FRANCE



Research Report 2019

Research Report 2019

Table of contents

Numerical weather prediction and data assimilations ● page 6

Process studies and modelling ● page 14

Climate ● page 20

Climate modelling
Diagnostic, study and impacts
Seasonal forecast

Chemistry, aerosols and air quality ● page 30

Snow ● page 34

Oceanography ● page 38

Engineering, campaigns and observation products ● page 42

Observation engineering and products
Campaigns

Research and aeronautics ● page 50

Appendix ● page 54



Research occupies a privileged place within Météo-France as it supports all of the Establishment's missions. It is the source of the progress that is implemented in terms of observation, numerical weather and climate forecasting. It enables the Establishment to constantly improve the quality of its operational products and to open new projects to meet the expectations of society and the public authorities.

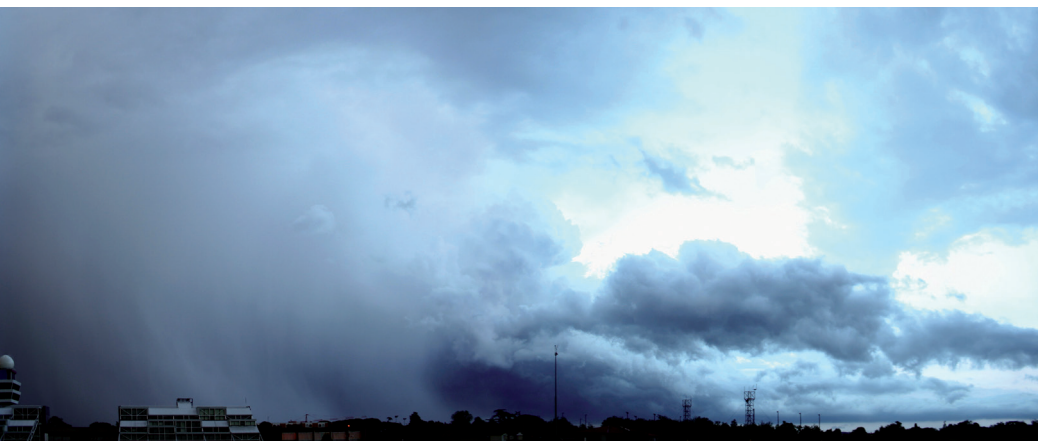
It has been guided over the last few years by the document "Scientific Strategy Météo-France 2013-2020". The year 2019 was therefore the year of reflection to build the major scientific orientations of the Establishment for the new decade 2020-2030. This Scientific Strategy 2020-2030 was discussed within the COMSI (Scientific Committee) 2019 of Météo-France. The numerous debates help to enrich a new version that will be finalised during 2020. The year 2019 will also have been the year of the HCERES evaluation of the CNRM which is the major and essential research entity of Météo-France. A great effort has been made by the members of the CNRM. The very positive evaluation of the HCERES Committee is an encouragement to continue in the proposed scientific directions and its valuable advice should be considered.

At the international level, Météo-France wishes to amplify its policy of privileged cooperation with the ECMWF around the global Arpège/IFS model and to consolidate the rapprochement with the Aladdin and Hirlam consortia within which the developments of high-resolution regional models are shared. In addition, Météo-France is pursuing its policy of active participation in Eumetsat and ESA programs and in enhancing the value of various space missions. In particular, ADM-

Aeolus (assimilation of wind profiles in the global model), CFOSAT (assimilation of wave observations in the sea surface state model) and the preparation of the future MTG and METOP-SG satellites, which will carry new high-potential instruments. Météo-France is also continuing its strong participation in European projects such as Copernicus.

At the national level, Météo-France maintains its involvement in the scientific community, which manifests itself through various links with numerous actors including the CNRS, CNES, Universities and through its participation in AllEnvi. The MISTRALS program, in particular the HyMeX project, which Météo-France has particularly supported for its interest in forecasting Mediterranean events, is coming to an end. The success of this program is already guaranteed by the positive scientific feedback. The Establishment is also a stakeholder in the Data Terra Research Infrastructure with its Data and Services Poles AERIS and THEIA, in Kalideos-Alpes under the aegis of the CNES, and participates in the construction of the ACTRIS-FR and CLIMERI-France Research Infrastructures. In particular, AERIS is an opportunity and a vector to facilitate the access of the research world to the operational data of the Establishment. Météo-France will also support, alongside SAFIRE's supervisory bodies, the CNRS and the CNES, the steps taken to replace the Falcon 20 high-altitude research aircraft.

In terms of its internal priorities, Météo-France will accentuate the long-term orientation of its various digital tools towards a single "seamless" system from the mesoscale to the global scale, integrating all the compartments of the Earth System:



atmosphere, waves, ocean, ice, continental surfaces including hydrology, chemical composition of the atmosphere, and the carbon cycle for the climate. The first priority is to set up a joint "atmosphere-continental surface" assimilation system in order to take full advantage of our knowledge of the surface for the benefit of numerical weather prediction. All the main work carried out in the two laboratories CNRM and LACy, as well as in the thematic directions of the Establishment is detailed in this document. Nevertheless, we can mention the major axes that are the forecasting of highly precipitating events, phenomena with a strong impact on our Mediterranean regions, the forecasting of cyclones, the forecasting of fog, a phenomenon with high stakes for civil aviation and which was the subject of a dedicated campaign during the winter 2019-2020. At the other end of the spectrum, under the leadership of the IPCC, the CNRM carries out the simulations of the CMIP-6 exercise with a new version of the CNRM-CM6 climate model and an Earth System model including the CNRM-ES carbon cycle. The aim is also to take into account the prospects offered by artificial intelligence, in order to make better use of overall forecasts, and to make the most of the numerous observations of connected objects, so that today we can better observe and understand hectometric scale phenomena and tomorrow we can better predict them.

In the perspective of the exascale, Météo-France will participate in the European dynamics for the development of a modeling framework adapted to future supercomputer architectures. For the time being, Météo-France, which has seen an increase in the power of its computers in 2016 (2 x 2.5

Pflops), notes, both with satisfaction and concern, that the implementation of all the scientific advances is leading to saturation of both machines. The project to renew our computing resources in 2020, but also our storage resources in 2021, are major challenges, in order to continue to convert our research work into progress in our digital systems, and in fine, to predict and prevent ever better.

Before concluding, it should also be mentioned that Météo-France, after setting up a Research Department in 2018, also wanted to associate its National School of Meteorology in a single Higher Education and Research Department (DESR) to strengthen synergies between teachers and researchers.

This editorial can neither cover nor summarise all of the subjects dealt with in this 2019 Research Report. The detailed articles that follow are fascinating and perfectly illustrate the broad spectrum of our research activities, all of which are essential to the Institution and its future.

Enjoy reading them.

Marc Pontaud,
director of Research

Numerical weather prediction and data assimilations

Representation of observation error spatial correlations

The objective of this research project is to drastically improve the spatial density of the observations exploited in the numerical prediction systems ARPEGE and AROME. This requires accurately representing the observation error correlations. To this end, we use a technique coming from the field of oceanography, based on the solution of a diffusion equation, which we decide to apply on unstructured meshes. A first study dealing with scalar data makes use of the finite element method. It provides a way to represent horizontal error correlations for scalar data, such as brightness temperature from satellite data.

Experimental validation was achieved using measurements from the infrared imager MSG/SEVIRI, which are assimilated both in ARPEGE and AROME.

We propose to extend this method to the representation of wind error correlations. These are vectorial data, meaning that every observation location is associated with two values, zonal and meridional. We focus specifically on scatterometer measurements, that are available every 25km but only assimilated every 100km.

First, the wind field is decomposed into one divergent component and one rotational component. Then, the scalar correlation

operator is applied to each component. Then, the wind field is reconstructed while maintaining the symmetry and the positivity of the correlation operator. Experiments show agreement with the analytical results. In the future, all types of observations will be considered, whether or not they are conventional, and we will extend the method to the three dimensional case to address the specific case of radars for instance.

1

Assimilation of microwave radiances affected by clouds and precipitation within ARPEGE

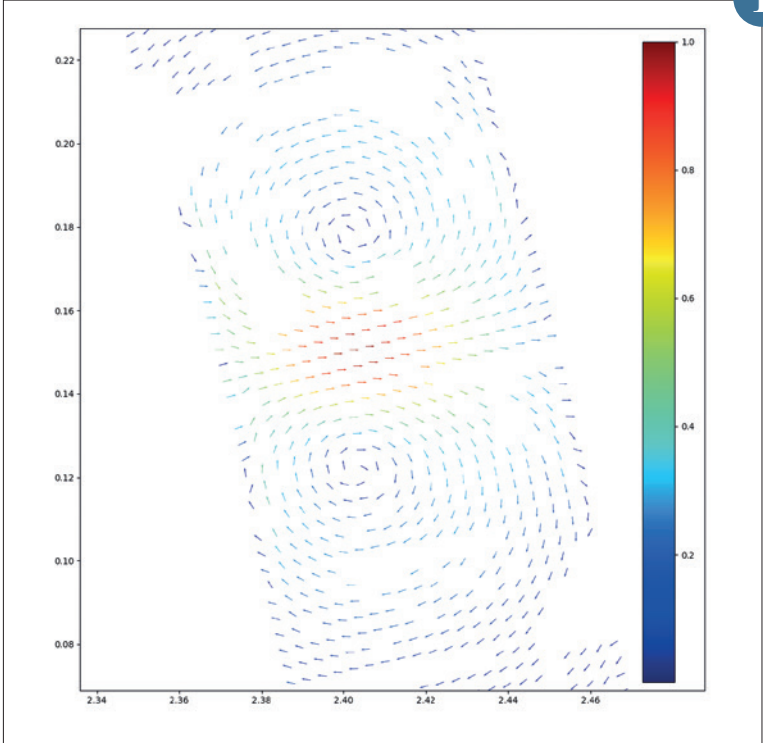
Presently, data from twenty microwave sounders and imagers on-board low Earth orbiting satellites are assimilated within the operational weather forecasting systems of Météo-France. These observations (radiances), are characterized by a very useful information content on vertical profiles of temperature and humidity for constraining the initial conditions of atmospheric models. They remain under-used within the current version of our systems because all the observations affected by clouds and precipitation are discarded from the assimilation process, which leaves only the clear sky observations.

After several years of investigations, a methodology was defined, which permit the use of microwave observations within clouds and precipitation in our system. This work leads to significant improvements of large-scale scores of the global model ARPEGE, as well as on its forecast skills of extreme events like tropical cyclones. The figure shows an example of forecast for the Typhoon Shanshan which occurred with the Western Pacific Ocean. Its forecast is improved by roughly 100km at +72h range by assimilating the cloudy and rainy radiances of the Indo-French satellite Megha-Tropiques.

For the moment, this method was adapted to five instruments of the constellation. After transfer to operations of this first group of instruments, the rest of the constellation will be progressively included toward the use of the full fleet of twenty sounders and imagers.

2

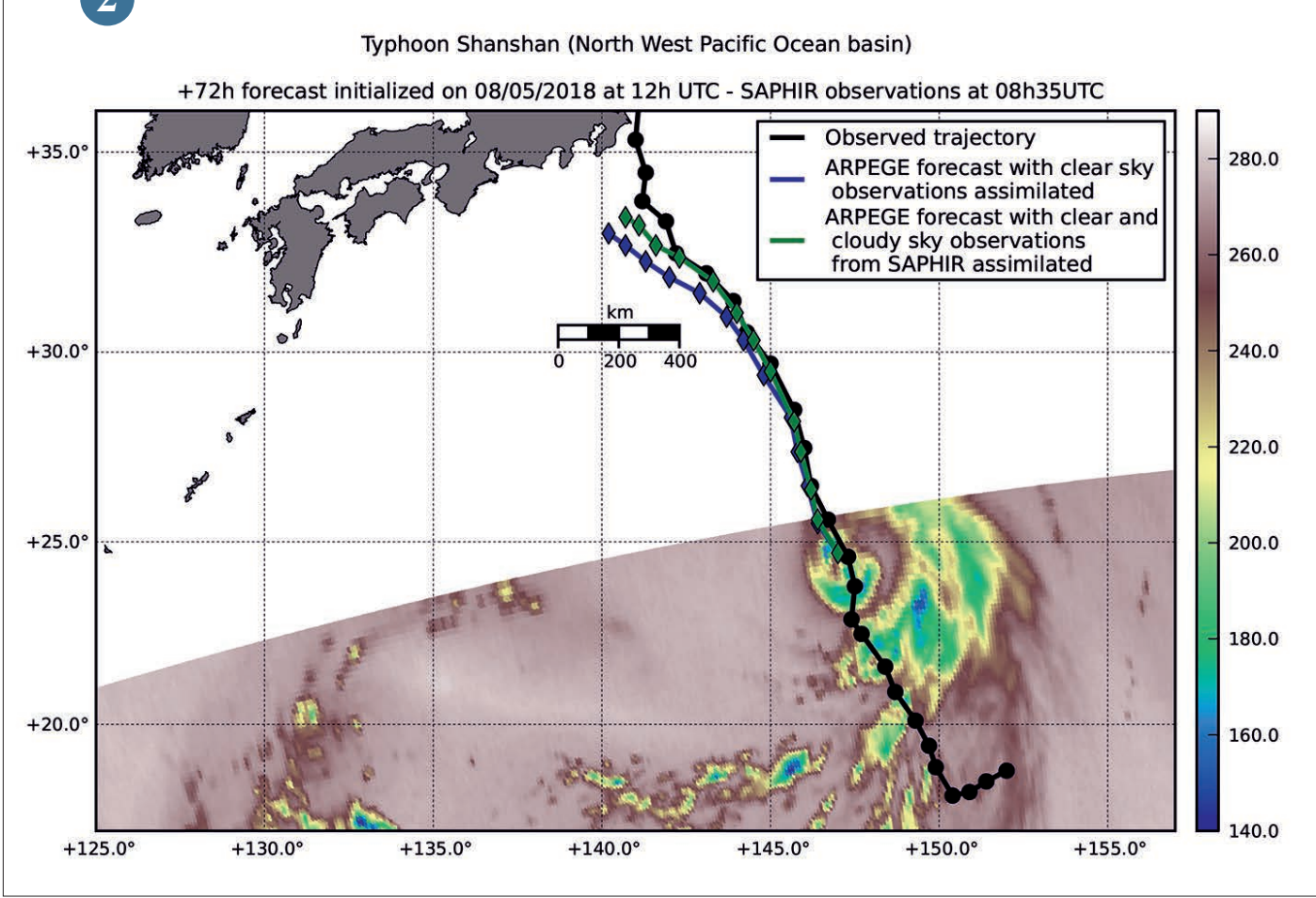
1



Typical impulse response of the wind correlation model to a zonal forcing in the non divergent case.

Observed trajectory of Typhoon Shanshan (black line). Trajectory forecasted by the ARPEGE global model on August 5th, 2018 at 12h UTC, up to a +72h forecast range, for a version of ARPEGE with clear sky observations only (blue trajectory) and with cloudy observations added (green trajectory). In the Southern part of the map, a fraction of the swath of the SAPHIR instrument onboard the Megha-Tropiques satellite is visible; the colors represent the measured brightness temperatures, with the coldest values corresponding to geographical areas which are characterized by high solid hydrometeors content (snow and ice).

2

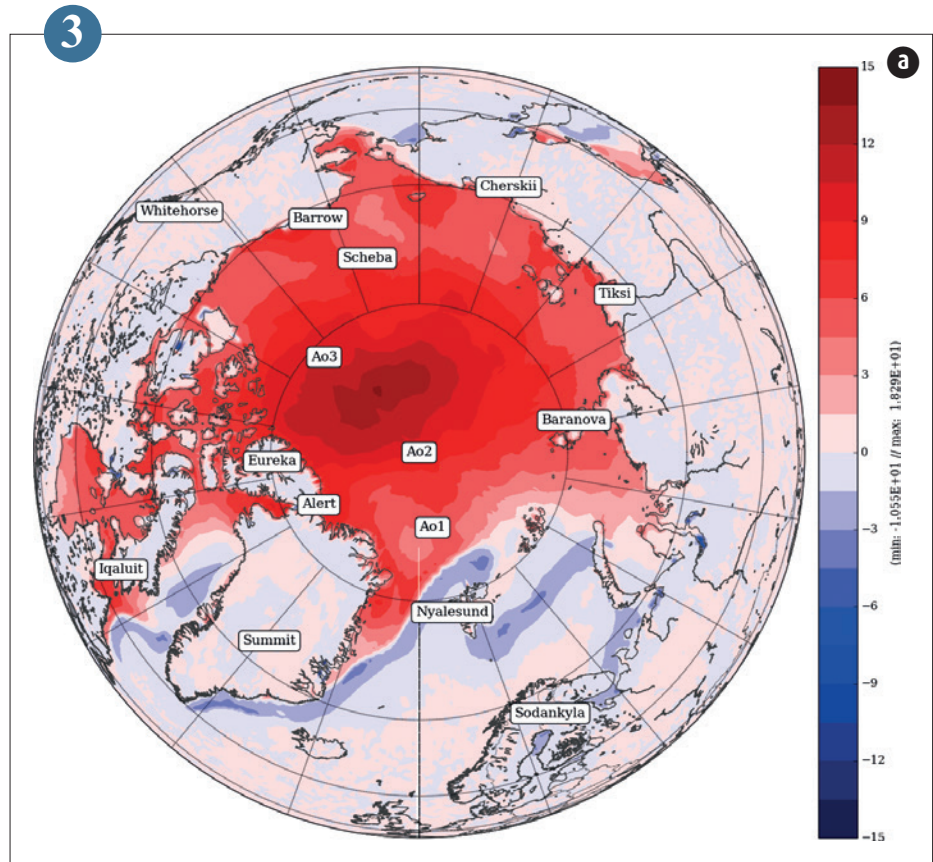


Impact of a sea-ice model for global weather forecast

So far, sea-ice has not been modeled in operational weather forecasts at Météo France. The sea ice temperatures needed to calculate the fluxes of moisture and heat into the atmosphere have been based on historical climatologies. This has not allowed for a realistic representation throughout the forecast because they can be strongly biased and also because it implies that the temperature is constant throughout the forecast.

Recent developments aim to activate the 1d sea-ice model GELATO developed by CNRM, only used for now in climatological forecasts. Results show a strong impact on surface temperatures (specifically, the two meter temperature field) since physical processes are now represented (Fig. 1). Note that the inclusion of GELATO on average leads to an increase of the surface temperature. Comparisons to ERA5 were done and show a clear improvement of simulated two meter temperatures above sea-ice in terms of bias and variability.

3



(a) Two meters temperature difference between Arpege-Gelato and Arpege-Oper (average over march 2018).

Changes in the convection scheme for the new resolution of ARPEGE

The new version of the ARPEGE forecast model implemented in 2019 has seen its horizontal resolution increased by 50%, with an increased risk of Grid Point Storms (GPS), which are specific to any numerical weather forecast system, due to the lack of vertical mixing in the convection scheme. Urgent and mandatory action was needed to address this risk, which is very embarrassing for forecasters on a daily basis.

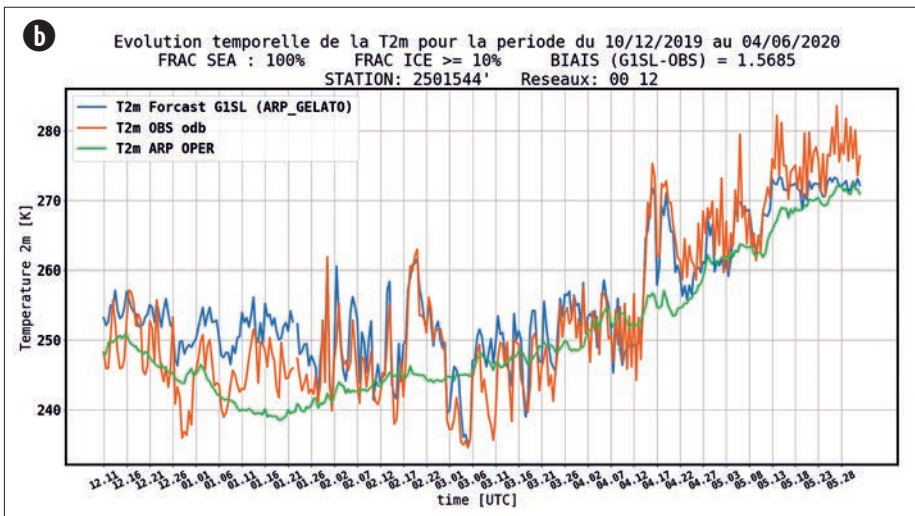
The current convection scheme includes an action since 2012 to limit the number of GPSs. After numerous unsuccessful tests and attempts, the developments finally concerned an increase in the activity of this "anti-GPS" action, continuing an action abandoned in 2013 which consisted in

temporarily adding, at the beginning of the convection scheme, the impact of humidity convergence on the energy equation (this action currently concerns the equation for humidity). Most of the work consisted of correcting parasitic oscillations that appeared in the tropics when the energy equation was modified.

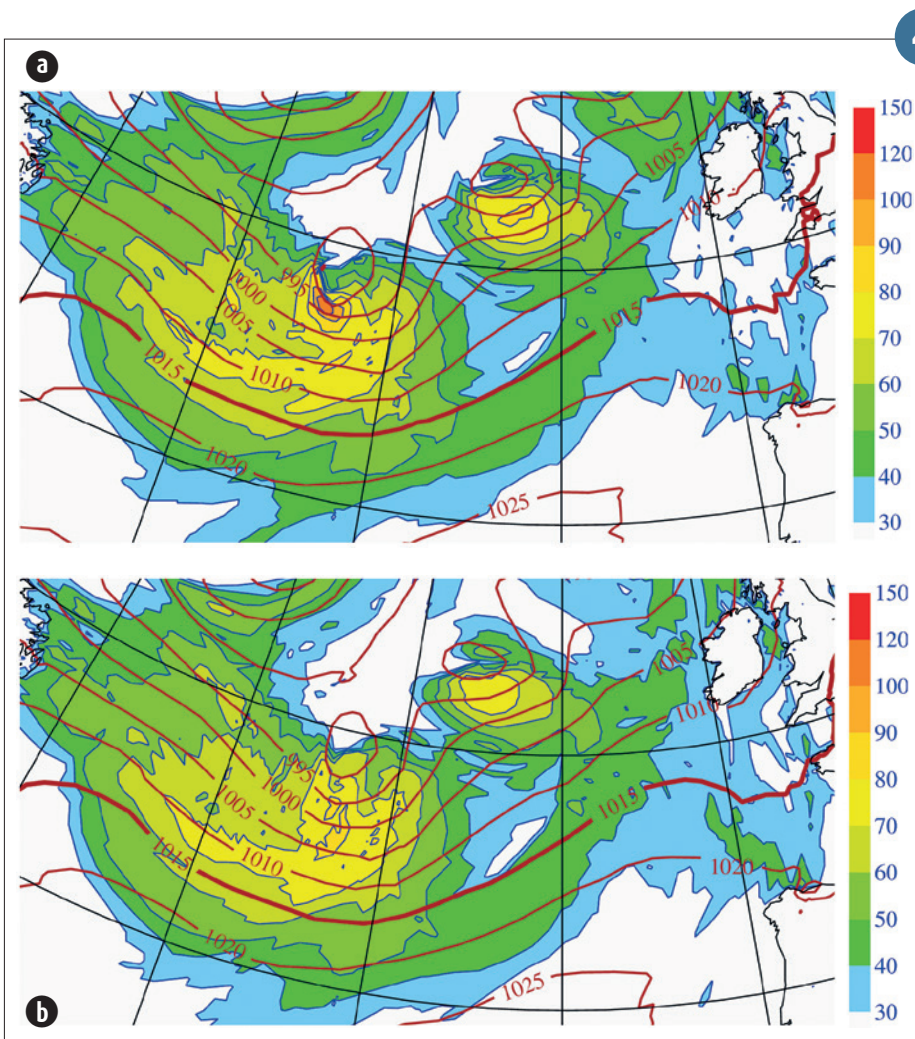
Figure "a" shows a GPS in the central North Atlantic that results in a marked tightening of isobars and average winds above 100 km/h, expected to induce higher gusts and possibly reaching the vigilance threshold. Figure "b" shows that the new version of the anti-GPS eliminates the unrealistic area of strong winds and tightening of the isobars.

The next step will not be to continue to improve the "anti-GPS" action for the current convection scheme, but rather to move towards the use of a new convection scheme that can be of better quality and induce less risk for GPS.

4



(b) Two meters temperature from december 2019 to may 2020 of the buoy 2501544 (6h time step). Operational configuration (green), GELATO (blue) and measurement (orange).



(a) A map plotted with the ARPEGE model for the high-resolution version of the March 8, 2017 forecast at 72h. The isolines of mean sea level pressure (in birste, every 5hPa) are superimposed on the 10m wind module (in coloured ranges, in km/h). (b) The same forecast as in figure "a", but with the new version of the anti-GPS.

A more stable formulation for the Non-hydrostatic "constant-coefficient semi-implicit" dynamical core of AROME system

Despite its proven robustness and accuracy for NWP purposes at kilometric scales, the currently used "constant-coefficient" linear approach for solving the system of Euler equations with a semi-implicit scheme may suffer from serious weaknesses when severe high-resolution flows and steep orography are at stake. Actually, the possible inconsistency in the lower boundary treatment between the horizontally homogeneous implicit linear part and the non-linear explicit part of the model, and the absence of implicitly treated orographic metrics terms arising from the use of terrain-following coordinate, may jeopardise the stability of the system at very high-resolution. A bespoke solution alleviating these two issues without relaxing the constant-coefficient assumption is proposed. This solution consists of the use of a new prognostic variable that automatically guarantee a consistent space-and-time vertical lower boundary treatment, and the design of a specific linear semi-implicit operator that somehow takes into account a relevant piece of information about the terrain's slope. The resulting formulation leads to a substantial gain in term of stability for the constant-coefficient semi-implicit dynamical core of AROME model.

5

Process-oriented evaluation of AROME-OM

The final goal of this work is to assess the ability of the French cloud resolving model AROME-OM West Indies to represent the various cloud regimes (deep, shallow, precipitating or not), the different types of weather (dry / wet season, intensity of the trade winds) as well as the mesoscale cloud organization.

Since February 2016, the AROME-OM model has been available in overseas territories with a resolution of 2.5km against 1.3km in France. The scientific questions that arise in the Tropics are different: i) to what extent this new generation of models significantly improves the forecast in the Overseas ii) these simulations represent a huge reservoir of data and therefore an opportunity to study the major processes that govern the shallow convection, in terms of organization or regime (precipitating or not).

To analyse the performance of the model, we use different types of observations, namely i) 5 radiosoundings spawned on the West Indies arc; ii) the Barbados Cloud Observatory equipped with instruments documenting the cloud stratification (<https://barbados.mpimet.mpg.de/>); iii) observations of the GOES East geostationary satellite.

In this work, we focus on the process-oriented evaluation of AROME-OM over the Antilles through the study of links between large scale dynamics, surface forcing and the macro and microphysical properties of

boundary layer clouds. The Antilles area has been chosen as in January-February 2020 the EUREC4a international measurement campaign (<http://eurec4a.eu/>) will take place off the island of Barbados (13N, 57W). To ease the follow-up of the AROME-OM Antilles model, we developed a website (http://intra.cnrm.meteo.fr/moana/AROME_OM/). A study conducted in January-February 2018 at the Barbados site shows the good skill of the AROME-Antilles model to represent the double peak of cloud fraction with one peak located at the base of the cumulus and the other at the trade-wind inversion (Figure); those two peaks are associated with the presence of very shallow cumulus and much thicker cumulus that reach 3km with a frequent occurrence of an anvil at this altitude. This is a good skill for the model since with a resolution of 2.5km, it should be noted that the processes associated with trade wind cumulus remain parameterized. However, the cloud base is higher in the model (900hPa) than that estimated by the cloud radar (920hPa), which can partly be associated with a boundary layer that is too cold and too dry.

6

SAR (Synthetic Aperture Radar) Surface Wind Data Assimilation in AROME for Tropical Cyclone Forecasting in the Indian Ocean

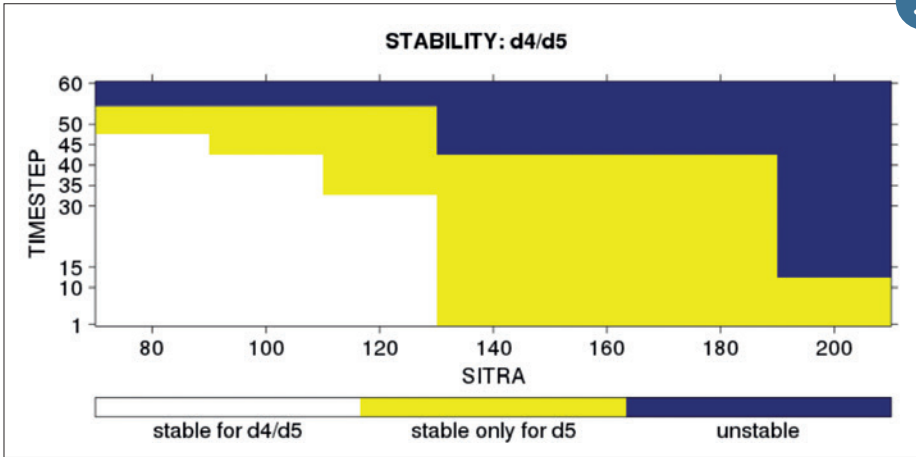
SAR active sensors, embedded in Sentinel-1A/B satellites, are able to estimate, from the roughness of the ocean surface, the intensity of surface winds with high spatial resolution (1-3 km) without any threshold effect, which represents considerable progress in comparison with data from ASCAT scatterometers. During the 2018-2019 cyclone season, as part of the ReNov'Risk campaign, a few dozen images of tropical cyclones were acquired in the South West Indian Ocean Basin (SWIO), several of which captured the eyewall and the strong winds associated.

In a basin where the network of in situ observations is very sparse, the assimilation of these data in AROME 3D-Var Indian (research version) should have a significant impact on tropical cyclone analysis and forecast in term position, intensity and structure.

On the tests carried out for Tropical Cyclone IDAI, SAR data assimilation produces analysis increments in wind, temperature and humidity on the surface but also in low and middle troposphere, notably in the area close to the eye of the cyclone. The figure shows that the position and structure of the tropical cyclone in the background are corrected by SAR data assimilation.

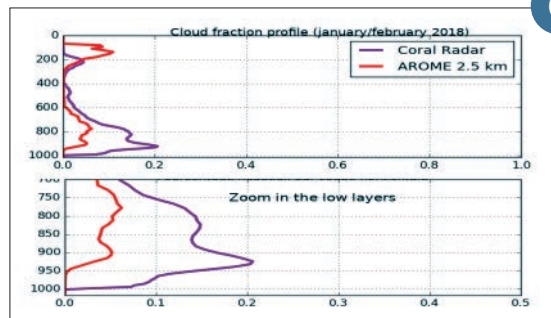
We are now exploring new ways to make the most of the information provided by SAR images, especially those for the strongest winds. A simulation covering a large part of the 2018-2019 cyclone season in the SWIO will be used to assess whether the assimilation of these data has statistically a positive impact on tropical cyclone analysis and forecasts.

7



5

Stability diagram comparing the current formulation "d4" to the new formulation termed as "d5" under similar numerical settings. This outcome results from a series of AROME experiments at 375 m of horizontal resolution over a domain including the Alps mountains with a observed maximum slope of 57°. The chosen meteorological pattern corresponds to strong winds travelling across the Alps on the date of 3.10.2015. The calculations are deemed to be stable if the run terminates after 24 hours of forecast.

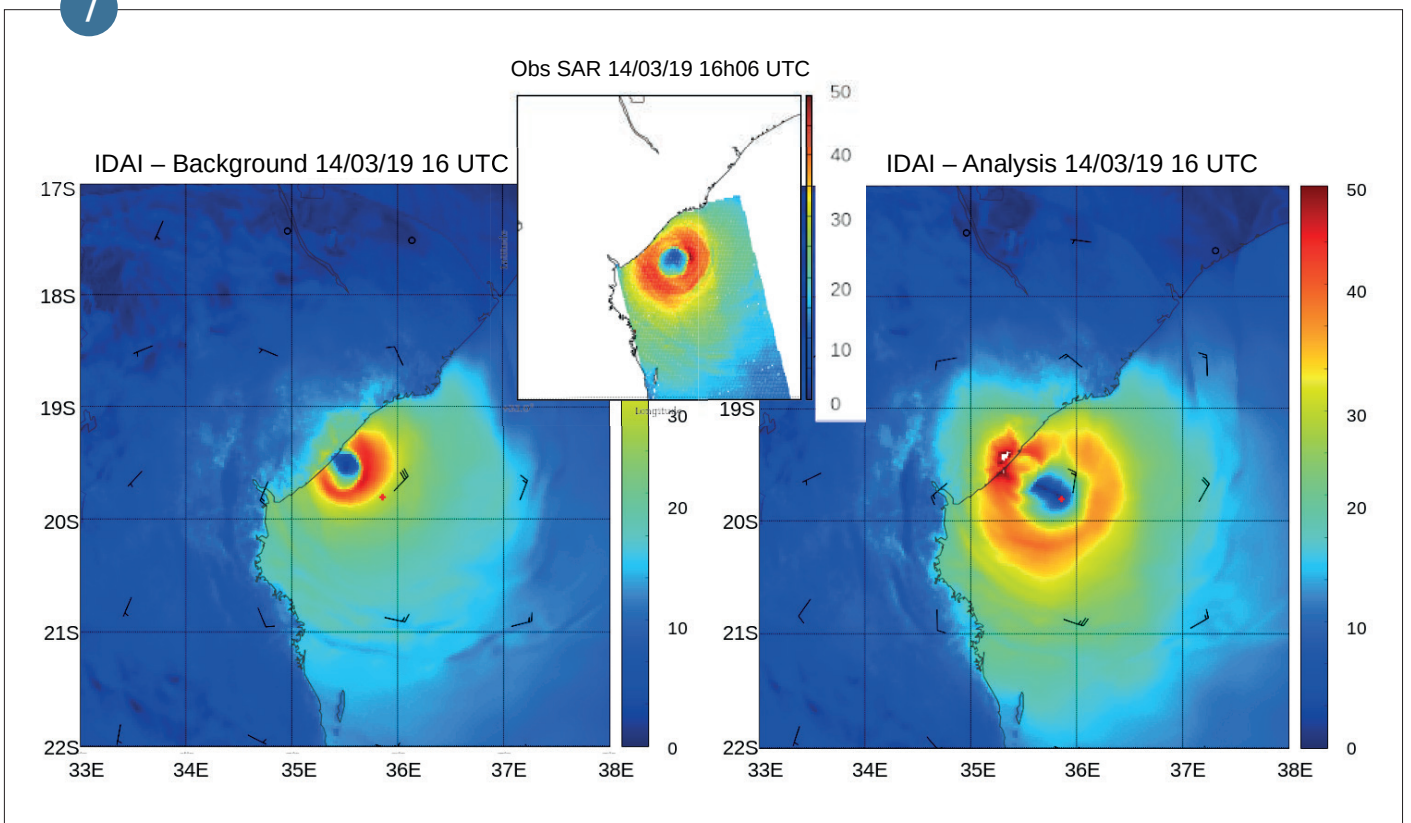


6

Vertical profile of cloud fraction from AROME-OM (red) and radar observations (purple).

Surface winds (in m/s) modelled by AROME 3D-VAR Indian on March 14, 2019 at 16 UTC in background (left) and in analysis (right) for tropical cyclone IDAI. In the middle, surface winds from a SAR image acquired on March 14, 2019 at 16:06 UTC. The position of the centre of the cyclone estimated by the RSMC La Réunion is marked by the red cross.

7



Identification of tropical cyclones by deep learning

The automatic identification of tropical cyclones in the outputs of numerical weather prediction models has existed since the late 1980s; it is useful to provide information both in real time, such as the predicted trajectory or the extension of the strongest winds, and also after the event for the evaluation of these models. These algorithms are based on the identification of a center, from which other characteristics are deduced, such as the maximum wind radius, which translates the size of the eye of the cyclone.

A new approach, based on a convolutional neural network, is under development at the CNRM. It consists in directly identifying the structure of the predicted cyclones, without prior knowledge of the center. Currently, the maximum wind zone and the zone of winds exceeding 120 km/h (force 12) are treated.

A learning base of 150 cases of cyclones with various characteristics has been manually created from the Arome-Antilles model forecasts. These data allowed to obtain a first version of a network capable of identifying a cyclone from two fields forecasted by

AROME: the wind strength at 10m and the geopotential at 850 hPa. The structures obtained are close to those labelled by hand, even when two cyclones are present simultaneously (see figure, cyclones Irma and Jose). The direct application of this network on the AROME-Indian outputs also provided satisfactory identifications.

These promising results will be further developed in 2020. This will include consolidating the learning base, training the network to handle forecasts from other models, and developing a time tracking module. Ultimately, this approach to identifying and tracking cyclones will be operational, with reduced computing time and the possibility of creating innovative products for probabilistic cyclone forecasting.

8

Convective area forecast with PEARP

Deep convection is a major risk for air transport. A new diagnosis of deep convection has been developed as a result of the Arpege ensemble forecast (PEARP). This product is a synthesis of several recent research studies. First it is based on the diagnosis of top convective cloud pressure which is produced by the different versions of Arpege. This diagnosis has been operational since July 2, 2019.

The information provided by the 35 pressure fields at each PEARP lead time is then synthesized using the similarity-based method developed at the CNRM. This method detects physically coherent structures or "objects". The method makes works independently of the underlying grid. It has also been constructed to take into account uncertainties. To reflect location

uncertainties, the boundary between "inside" and "outside" an object is of variable thickness (or fuzzy). Results of the method are probability maps of belonging to a convective object of different levels of severity. The 35 series of grid point values are replaced by collections of structures hierarchized by both intensity and probability of presence. The method has a high potential for automatic zoning. An application of this method could be the drawing of TEMSI maps. This work is being carried out within the framework of the European SESAR initiative.

10

Extension of the RTTOV radiative transfer model to the far infrared for the FORUM mission

The fast radiative transfer model RTTOV used primarily for the assimilation of satellite observations in the infrared (3 - 20 μm) and in the microwave (20 - 200 GHz) spectral ranges has recently been extended to the far-infrared wavelengths up to 100 μm , bringing the gap between the two spectral ranges.

This work has been developed as part of the preparatory studies for the future space mission FORUM (Far-infrared Outgoing Radiation Understanding and Monitoring) which has recently been selected to be the Earth Explorer 9 observation mission of ESA, scheduled for launch in 2026, and which will fly jointly with Metop-SG.

The FORUM hyperspectral instrument will measure radiances at the top of the atmosphere between 100 and 1600 cm^{-1} (equivalent to 6.7 and 100 μm) with a spectral sampling of 0.5 cm^{-1} (see figure in brightness temperature for clear and cloudy sky cases at three incidences with a surface temperature of 292 K and an optical thickness of the ice cloud of 2 at 10 μm).

To simulate these observations, RTTOV has been adapted in all components of radiative transfer: gas absorption using the LBLRTM line-by-line model, optical properties of clouds and aerosols from existing models, and surface emissivity. It is interesting to note that these future observations will validate several unknowns of far-infrared radiative transfer modelling such as water vapour spectroscopy, temperature dependence of ice crystal scattering properties and surface emissivities in polar regions.

9

Forecast of a set of rain scenarios to anticipate rapid floods (PICS project)

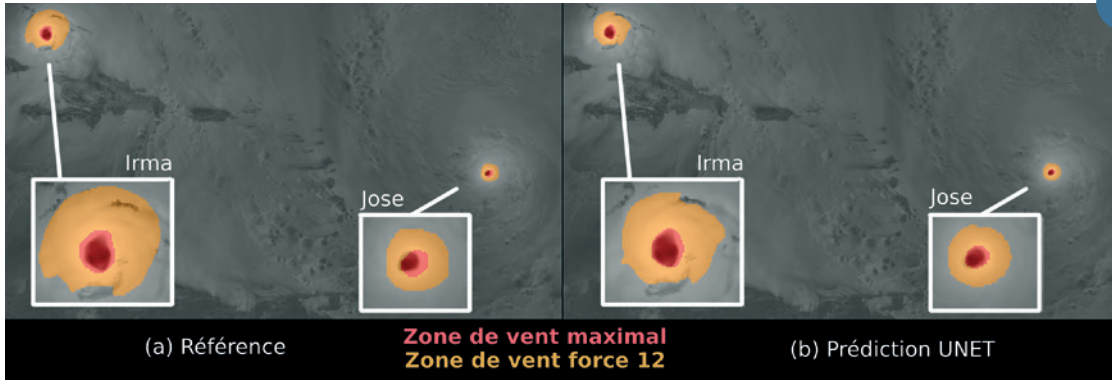
Flash-flood prediction is usually based on observations of precipitation and water levels. For more timely warnings, high resolution rain forecast scenarios are needed in a form suitable for hydrological models. Until now these forecasts have been available as extrapolated radar images or as numerical model output that may not cover all required forecast ranges. To better

integrate these diverse data sources, we have developed temporally consistent rain forecast scenarios, as consistency is essential for depicting peak precipitation events. The scenarios are presented as an ensemble forecast that is suitable for modelling uncertainty propagation in hydrometeorological prediction systems. Forecasts can be quickly refreshed using

the latest observations. The potential of this approach is under evaluation with flood forecasting institutes as part of an ANR-funded project, with the intent of making it operational.

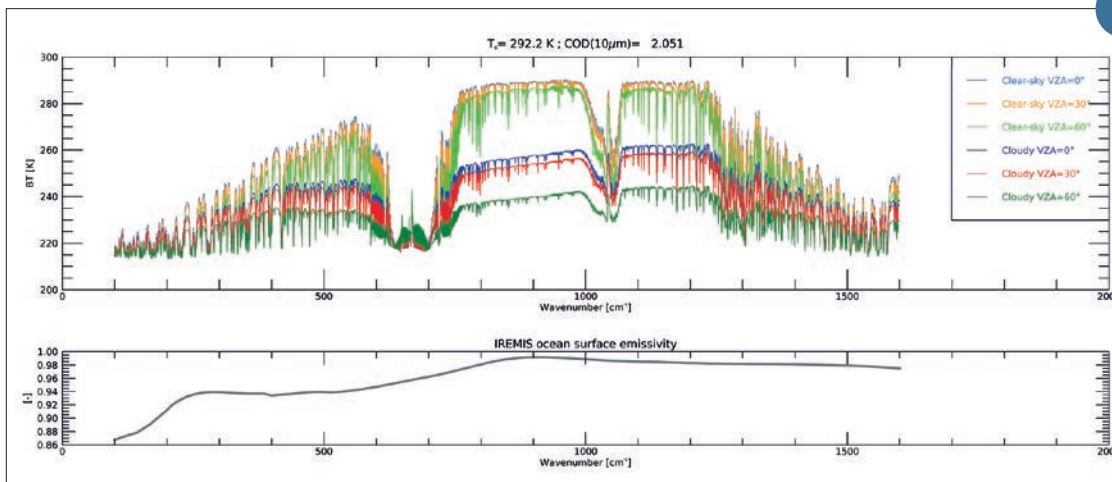
11

8



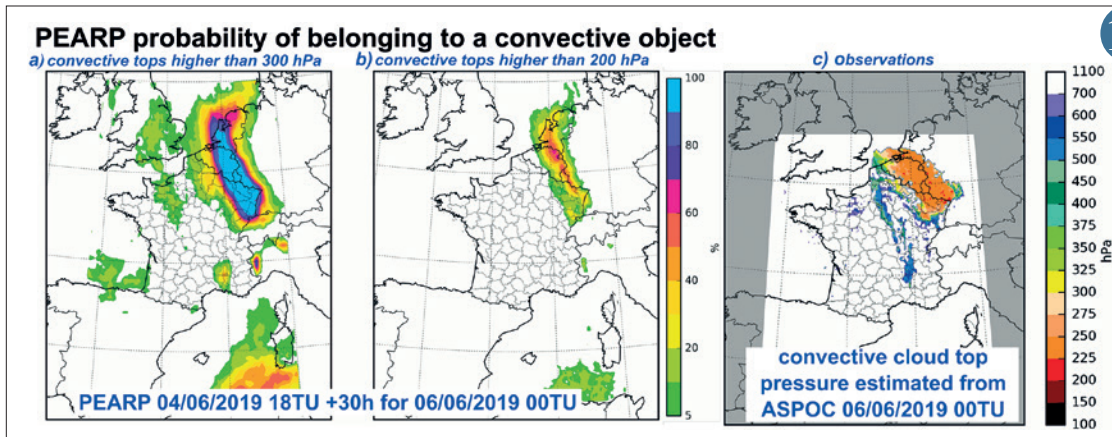
Forecast wind strength at 10m from Arôme Antilles during the 2017 hurricane season, with the presence of the two hurricanes Irma and Jose. On the left are represented the cyclonic structures labeled by hand, and on the right those identified by the UNET network.

9



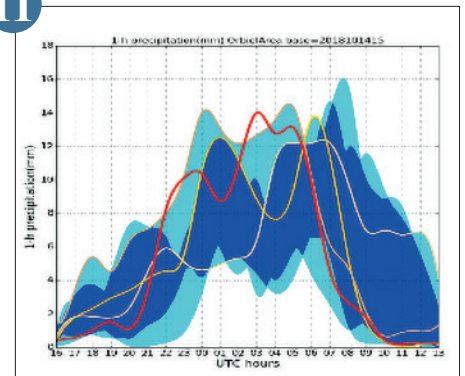
Brightness temperatures simulated with the RITOV model for the FORUM instrument for three cases of clear sky with different satellite zenith angles and three cases of cloudy sky containing ice crystal with an optical thickness at 10 µm of 2. The surface temperature is 292 K on an ocean surface whose spectral emissivity is shown below.

10



Left: probabilities of belonging to a convective object with cloud top pressure (used as an intensity indicator) exceeding (a) 300hPa and (b) 200hPa. These probabilities are deduced from the realization of the Arpege PEARP ensemble forecast of 04/06/2019 18TU, with a time horizon of +30h. The stakes of the forecast may be different depending on the point of view, airspace or pilot. By choosing an appropriate probability threshold, we obtain an outline of the objects. Thus the information is summarized in a compact way. (c) Observation of cloud top pressure estimated from satellite and lightning data, on 06/06/2019 00TU.

11



Rainfall ensemble prediction available a few hours before a catastrophic flash-flood event: in red, observed hourly rain totals in the affected area; in blue, range of ensemble forecasts from a high-resolution numerical weather prediction system (AROME-EPS); in yellow, some of the predicted rain scenarios, suitable for driving hydrological models.

Process studies and modelling

Researches on process knowledge aim at a better understanding and modelling of meteorological phenomena in numerical weather prediction (NWP) and climate models. The overarching goal is to develop efficient weather and climate services, and new applications. The methodologies implemented to advance our understanding of processes are generally based on the combine use of observations, from satellite and field campaigns, and numerical experiments, especially at very high resolution, as illustrated below.

The LDAS-Monde data assimilation system integrating satellite-derived observations of vegetation and soil moisture allows to represent the phenology and to evaluate the impact on vegetation of the heat waves. In the same field of continental surfaces, progress in the understanding and modelling of processes requires consideration of anthropogenic factors affecting the water cycle. The CTRIP routing model, which has been refined in resolution over France, offers to take into account impacts of lakes and dams on the continental water cycle.

At more extreme latitudes such as in Antarctica, measurements over Dome C made it possible to quantify the radiative impact of supercooled liquid water clouds, thus highlighting the underestimation of downward radiative fluxes by NWP models, for which the representation of supercooled cloud water is always difficult.

Icing by supercooled water is also crucial for aviation forecasting, just like fog. Fog modelling at much finer scales such as metric resolution, validated from the LANFEX measurement campaign over the United Kingdom, allows to better understand the important processes driving its life cycle and to improve the representation of the process activation of aerosols into droplets in the models.

This same high-resolution Meso-NH research model was also coupled with a wind turbine model, paving the way for innovative studies of dynamical interactions induced by the wake effect of wind farms, such as in offshore areas.

Impact of heat waves over land surface conditions

Researches on process knowledge aim at a better understanding and modelling of meteorological phenomena in numerical weather prediction (NWP) and climate models. The overarching goal is to develop efficient weather and climate services, and new applications.

The methodologies implemented to advance our understanding of processes are generally based on the combine use of observations, from satellite and field campaigns, and numerical experiments, especially at very high resolution, as illustrated below.

The LDAS-Monde data assimilation system integrating satellite-derived observations of vegetation and soil moisture allows to represent the phenology and to evaluate the impact on vegetation of the heat waves. In the same field of continental surfaces, progress in the understanding and modelling of processes requires consideration of anthropogenic factors affecting the water

cycle. The CTRIP routing model, which has been refined in resolution over France, offers to take into account impacts of lakes and dams on the continental water cycle.

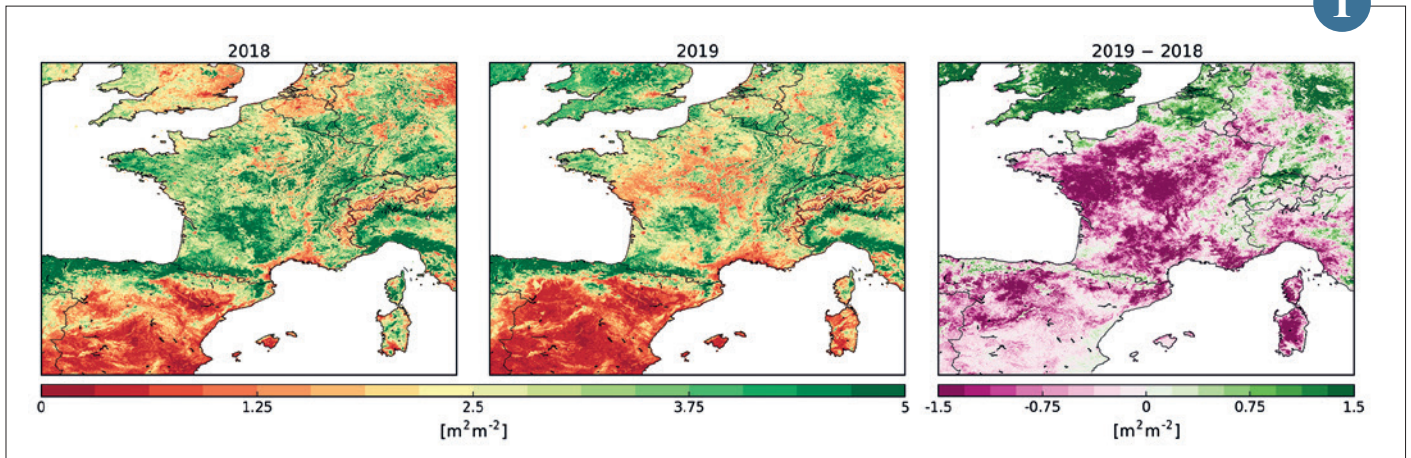
At more extreme latitudes such as in Antarctica, measurements over Dome C made it possible to quantify the radiative impact of supercooled liquid water clouds, thus highlighting the underestimation of downward radiative fluxes by NWP models, for which the representation of supercooled cloud water is always difficult.

Icing by supercooled water is also crucial for aviation forecasting, just like fog. Fog modelling at much finer scales such as metric resolution, validated from the LANFEX measurement campaign over the United Kingdom, allows to better understand the important processes driving its life cycle and to improve the representation of the process activation of aerosols into droplets in the models.

This same high-resolution Meso-NH research model was also coupled with a wind turbine model, paving the way for innovative studies of dynamical interactions induced by the wake effect of wind farms, such as in offshore areas.

1

1



Effect of the 2018 and 2019 heatwaves on vegetation. The leaf area index for vegetation for the month of July is displayed for 2018 and 2019. This is a value that was simulated by Météo-France's ISBA model using satellite data from the Copernicus Global Land service. The difference between these two maps illustrates the very marked droughts that affected southern England, Belgium, the Netherlands and Lower Saxony in 2018 (green), and almost all of France, northern Spain and Sardinia in 2019 (purple).

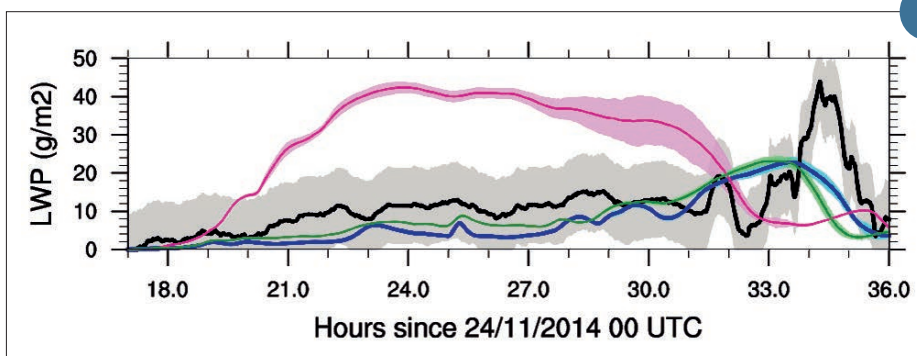
Impact of microphysics on the simulation of a radiative fog

CNRM has developed a data assimilation system able to work at a global scale for any vegetation type (grasslands, crops, forests, savannas). This tool is called LDAS-Monde (www.umr-cnrm.fr/spip.php?article1022). It is based on the SURFEX modelling platform (www.umr-cnrm.fr/surfex/). It can integrate satellite-derived observations of vegetation and soil moisture into a model of the soil-plant system called ISBA. As opposed to satellite data, ISBA is able to continuously provide time series of various land surface variables (vegetation biomass, water deficit

or excess, evapotranspiration, carbon fluxes, surface temperature) in a consistent way. Satellite observations are used to improve the quality of the simulated variables. The model is forced by meteorological data available at low spatial resolution at a global scale (10 to 25 km). LDAS-Monde uses data produced by the Copernicus Global Land service: leaf area index and a soil moisture index. Since these products have been available for several years, soil moisture and vegetation growth anomalies can be derived. When LDAS-Monde is used at a global scale, it can detect drought

events. At a regional scale, atmospheric variables are available at a better spatial resolution. For example, the AROME-France numerical weather forecast system produces such data at a spatial resolution of 1.3 km over a large part of western Europe. This set of tools was used to analyse the impact on vegetation of the heat waves of 2018 and 2019.

2



Liquid water path (in $\text{g}\cdot\text{m}^{-2}$) from observation (in black) and simulations with the standard version of LIMA (in pink), with the prognostic supersaturation (in green) and with an improvement of the activation parametrization (in blue). Grey area corresponds to the uncertainty of measurements, and colour area to the variability over the simulated domain.

Simulations of the meteorological impacts of off-shore wind farms at ultra-high resolution

A collaboration engaged 4 years ago between Météo-France and IFPEN with the objective to improve the knowledge on interactions between wind farms and local meteorology. For example, to improve the setting of wind turbines, it is necessary to finely simulate the air flow within the wind farm, taking into account the real meteorological conditions. During the first PhD thesis on the subject, a wind turbine model of IFPEN has been coupled into the high-resolution atmospheric model MesoNH, jointly developed by Météo-France and Laboratoire d'Aérodynamique, Toulouse. The coupled model determines the wind turbine plume induced by the interactions of the aerodynamical efforts they produce and the wind, the latter being of course also influenced by meteorological processes. This study allowed to better understand the phenomenon of condensation, that can lead to fog, observed in the Horns Rev off shore Danish wind farm (picture 1). Because of their rotation, the wind turbines mix the atmospheric boundary layer. The meteorological conditions can therefore

be modified downwind of the turbines, and in specific conditions, lead to such phenomenon. This research will continue by studying the impact of giant wind turbines that can reach the inversion layer of the marine atmospheric boundary layer and impact the free atmosphere above, through gravity waves.

Thanks to their respective expertise's, IFPEN and Météo-France propose here the first open-source simulation code able to explain the interactions of a wind farm with the local meteorology, at a resolution as high as 5m.

3

The CTRIP routing model has a global 1/12° hydrographic network

The Earth system model developed at the CNRM incorporates a hydrological component to represent the transfer of water from rivers to the oceans, and thus close the water balance at the global scale. The CTRIP routing model coupled to the SURFEX platform mainly represents the propagation of flows within the hydrographic network. It has been used for several years at the CNRM at the global scale at a resolution of 0.5°, with very satisfactory performances in terms of its ability to simulate discharge at the outlet of large basins. However, at this resolution, only large rivers can be represented. With the increase in resolution of atmospheric and surface models, the low resolution of CTRIP can become penalizing for the representation of mesoscale processes.

The CTRIP-12D version of the model has recently been implemented at a resolution of 1/12° (about 6-8km in France). This work is based on the development of a global hydrographic network, derived from the hydrology-corrected high resolution (90m) MERIT-DEM Digital Terrain Model, which describes the flow direction of each pixel of continental surfaces (Figure a). After a detailed validation of the quality of the network, including the shape and structure of the major basins of the globe, CTRIP-12D parameters such as length of river stretch, slope, width, roughness, etc., have been calculated. The first global scale simulations showed a very good capacity of the model to reproduce the flows on all the continents, with performances better than with the low resolution version (Figure b). In addition CTRIP-12D should make it possible to take into account new processes such as the impact of lakes and dams on the continental water cycle.

4

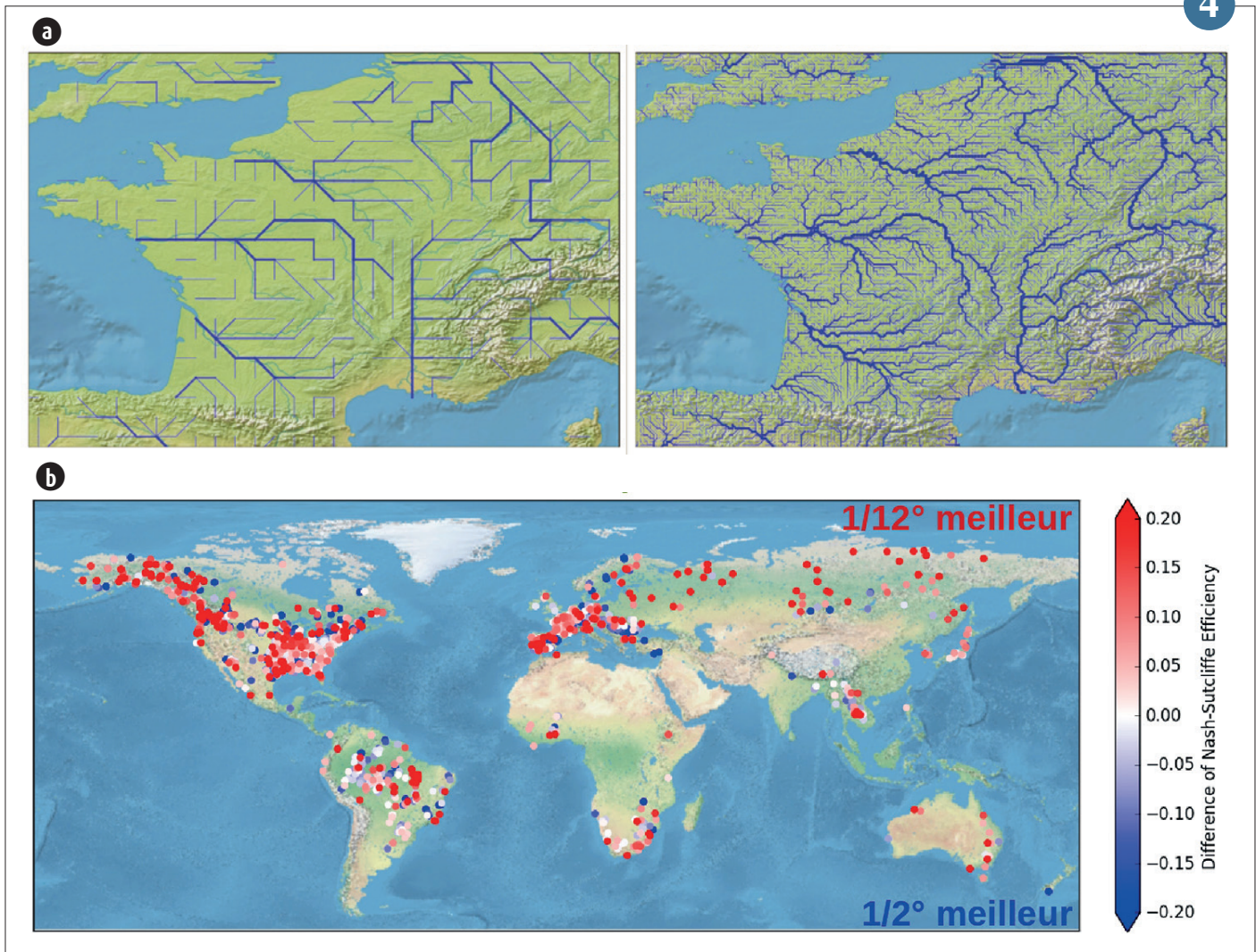


◀ (a) Offshore wind farm of Horns Rev 1 (12/02/2008)
©Vattenfall.
(b) Numerical Simulation on supercomputer
with the ultra-high-resolution atmospheric model
MesoNH.



3

4



▲ (a) Comparison of hydrographic networks at 0.5° (left) and 1/12° (right) in metropolitan France.
(b) Comparison of performances (simulated discharge vs observed discharge) between CTRIP simulations at 0.5° and 1/12°.

Analysis of supercooled liquid water clouds over Dome C, Antarctica

Antarctic clouds play an important role in the climate system by influencing the Earth's radiation balance, both directly at high southern latitudes and, indirectly, at the global level through complex teleconnections.

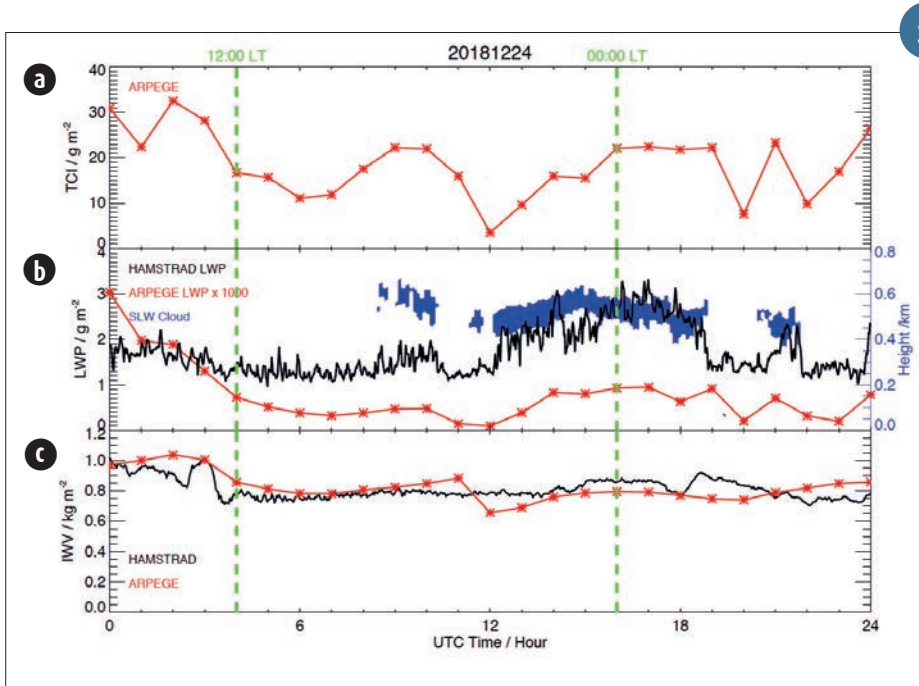
A comprehensive analysis of the water budget over the Dome C station (Concordia, Antarctica) has been performed during the austral summer 2018-2019 as part of the YOPP international campaign. Thin (~100-m deep) supercooled liquid water (liquid water present at temperatures below 0°C) clouds have been detected and analysed using remotely sensed observations at the station (LIDAR, microwave radiometer HAMSTRAD, net surface radiation from BSRN), radiosondes and

using satellite observations (CALIOP/CALIPSO) combined with the Numerical Weather Prediction model ARPEGE (Figure 1).

On 24 December 2018, our study showed that supercooled liquid water clouds were observed at Dome C in the entrainment zones at the top of the planetary boundary layer. ARPEGE was not able to correctly estimate the ratio of liquid to solid water inside the clouds. The lack of simulated supercooled liquid water in the model impacted the net surface radiation that was 20-30 W m⁻² higher in the BSRN observations than in the ARPEGE calculations. This is mainly attributable to longwave downward surface radiation from BSRN being 50 W m⁻² greater than that of ARPEGE (Figure 2).

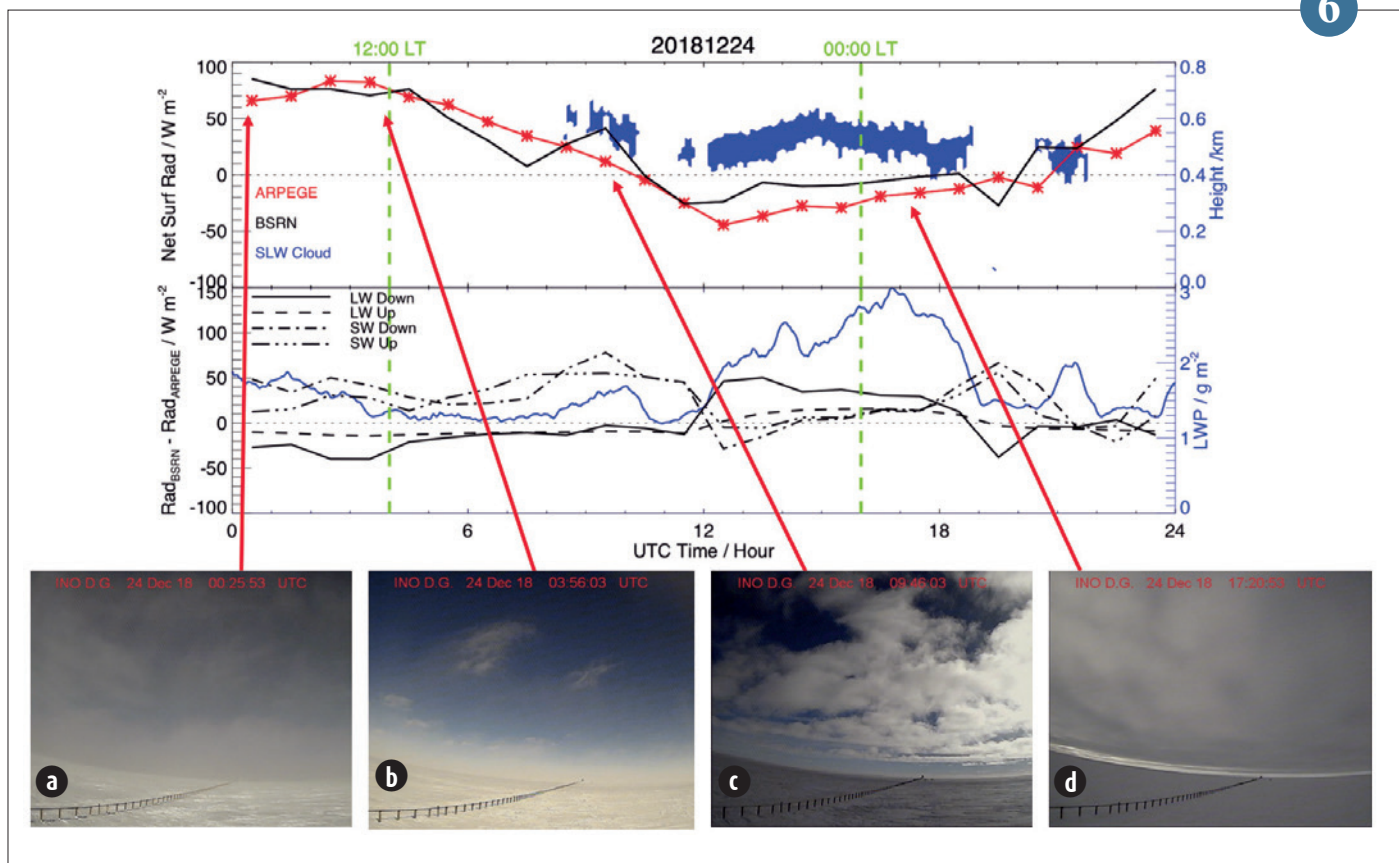
The absence of supercooled liquid water clouds in numerical weather prediction models over Antarctica may indicate an incorrect simulation of the radiative budget of the polar atmosphere.

5



5

Diurnal variation on 24 December 2018 (UTC Time) of: (a) the Total Column of Ice (TCI) (g m⁻²) calculated by ARPEGE (red crossed line), (b) the Liquid Water Path (LWP) measured by HAMSTRAD (g m⁻², black solid line) and calculated by ARPEGE (x1000 g m⁻², red crossed line) and (c) the Integrated Water Vapour (IWV, kg m⁻²) measured by HAMSTRAD (black solid line) and calculated by ARPEGE (red crossed line). Superimposed to panel b) is the supercooled liquid water cloud thickness (blue area) deduced from the LIDAR observations (blue y-axis on the right of the Figure). Note LWP from ARPEGE has been multiplied by a factor 1000. Two vertical green dashed lines indicate 12:00 and 00:00 LT (Local Time).



▲ (Top) Diurnal variation of the net surface radiation ($W m^{-2}$) observed by BSRN (black solid line) and calculated by ARPEGE (red crossed line) on 24 December 2018 in UTC Time. Superimposed is the supercooled liquid water cloud altitude (blue) deduced from the LIDAR. (Middle) Diurnal variation of the difference between surface radiation ($W m^{-2}$) observed by BSRN and calculated by ARPEGE on 24 December 2018 for longwave downward (black solid), longwave upward (black dashed), shortwave downward (black dashed dotted) and shortwave upward (black dashed triple dotted) components. Superimposed is LWP (blue) measured by HAMSTRAD. (Bottom) Four webcam images showing the cloud coverage at: (a) 00:25 UTC and (b) 03:56 UTC (cirrus clouds, no supercooled liquid water cloud), (c) 09:46 and (d) 17:20 UTC (supercooled liquid water cloud). Two vertical green dashed lines indicate 12:00 and 00:00 LT (Local Time).

Climate

The year 2019 was marked in France by two exceptional heat waves in June and July. On 25 July, temperatures measured at numerous weather stations in the north of France exceeded 40°C for the first time on record, even reaching 43°C locally. The link between these heat waves and anthropogenic climate change is clear: attribution studies have shown that they are now at least 5 to 10 times more likely to occur than in 1900, and could be 4 times more frequent in 2040 than they are now.

Thanks to its research and observation activities, Météo-France is one of the few national meteorological services with all the tools and expertise needed to qualify such events in near-real time. In terms of observations, it is more crucial than ever to have quality data on the current period, but also to pursue data rescue in order to assess long-term changes and climate variability. On the research side, as a contribution to the IPCC 6th assessment report, CNRM has done most of the largest set of global climate simulations ever produced on Météo-France's supercomputers. However, analysis of the simulations produced by numerous international global models, including CNRM-CM, revealed an increased sensitivity to the increase in atmospheric CO₂. Assessing and understanding this climate sensitivity is a major research challenge.

The fine-scale regional climate models covering mainland France and the overseas territories are fed by global model outputs and complement them, as they make it possible to represent orography and phenomena unresolved at large scale. They provide essential information for public and private stakeholders to make decisions on assessing the impacts, risks and adaptation measures associated with climate change. This year has seen an increase in the use of AROME at a resolution of 2.5 km for climate studies. This model, which is used daily for weather forecasting, has demonstrated its excellent capacity to simulate events such as intense rainfall or thunderstorms. Météo-France also provides information to anticipate climate variability on time scales ranging from a few weeks to a few months. The subseasonal and seasonal forecasting systems are based on CNRM-CM. Once corrected and formatted, the production of these systems contributes in particular to optimising water resource management, agricultural practices or the production of weather-sensitive energy.

1

Climate modelling

Fast forward to perturbed equilibrium climate

Determining the response of the climate system to an imposed external perturbation is a major challenge in climate science. The equilibrium climate sensitivity, i.e. the global-mean surface temperature change in response to a doubling of the carbon dioxide concentration is a widely used metric in climate change studies. Its exact value is rarely known because its estimation is computationally expensive: it requires a long integration time of several thousand years of coupled atmosphere-ocean general circulation models.

Recently, we have proposed a method to estimate an accurate value of the equilibrium response from fully coupled climate models at a reasonable computational cost. Using this method, our state-of-the-art climate model CNRM-CM6-1 reaches a stationary state after only few hundreds of years of integration. This 'Fast-Forward' method consists of an optimal two-step forcing pathway designed using the framework of a two-layer energy-balance model.

This method can be applied easily to any coupled climate model and can improve our capacity in developing next generation of climate models.

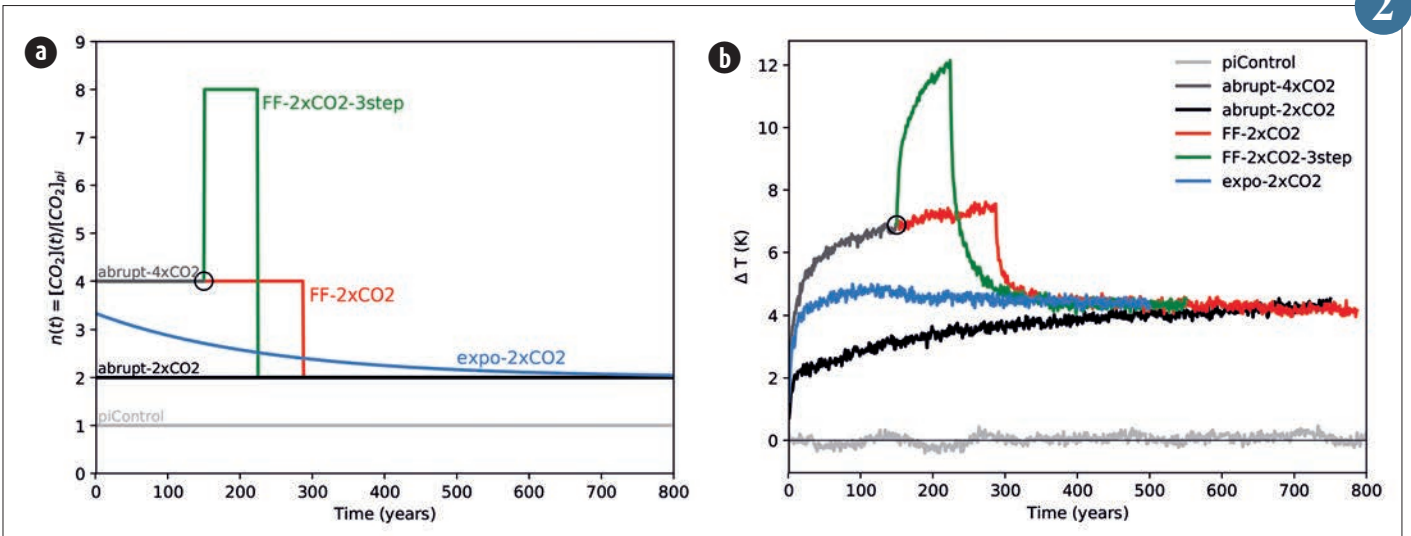
2

1



▲ Heatwave in Paris (Trocadéro). © Pascal Taburet – Météo-France.

2



▲ Temporal evolution of (a) CO₂ concentration in the step-forcing and Fast-Forward experiments and (b) corresponding global-mean surface-air temperature responses (deviation from the temporal mean of the piControl experiment). The black circle denotes year 150 of the abrupt-4xCO₂ experiment. See details in Saint-Martin et al (2019).

ISBA-CTRIP: the new land surface modelling system for global climate applications

During the last decade we developed an ambitious land surface modelling system designed to realistically represent the water and carbon cycles on all continents. In this system (Fig. a), the surface model ISBA gives a detailed representation of the water and energy exchanges in the soil-snow continuum by explicitly solving Darcy's and Fourier's laws. ISBA also represents atmospheric CO₂ assimilation by plant photosynthesis, plant respiration, the evolution of plant biomass and leaf area index, natural large-scale forest fires, land cover changes, soil organic carbon accumulation and decomposition by micro-organisms, and dissolved soil carbon. ISBA calculated runoff and dissolved soil carbon are transferred to CTRIP to simulate river discharge and dissolved organic carbon concentration in the rivers over all continents. We also developed a real two-way coupling between ISBA and CTRIP. This coupling allows the use of a dynamical river flooding scheme

that describes the interaction between the flooded plains, the soil and the atmosphere through evaporation and re-infiltration of surface water. Aquifer physics and their coupling with superficial soil and rivers are also represented by a two-dimensional diffusive aquifer scheme. This new system called ISBA-CTRIP, (<http://www.umr-cnrm.fr/spip.php?article1092&lang=en>) has shown far better performances than its previous versions at simulating for instance the discharge of the world large rivers or the CO₂ assimilation by plant photosynthesis (Fig. b).

3

Development of CNRM global climate models and their CMIP6 contribution

In the context of the 6th phase of the coupled model inter-comparison project (CMIP6), three versions of the CNRM-CM climate model have been developed and provide data to the CMIP international database: (1) the standard model at 100km resolution, (2) the high resolution version (50km) and (3) the Earth System version based on the standard model on which are added the full carbon cycle representation, the land use changes, the stratospheric ozone chemistry and the interactive aerosol scheme.

These three versions share the same physical model basis and their tuning is identical. This consistent ensemble of model allows to assess in an objective way the impact of increased complexity versus the increased resolution on the representation of the 20th century climate and on future projections. Climate projections under a business as usual emission scenario show that the warming simulated by the standard and the high resolution models is of similar amplitude whereas it is reduced by 10% in the Earth System version. This weaker warming has been attributed to vegetation carbon flux impacts and to aerosols feedbacks.

The Earth system version and the high resolution version computational cost is respectively two and ten times larger than for the standard version. Even if they enable to address new scientific questions regarding climate variability and changes, their computational cost limits the capacity of performing large ensemble simulations and/or very long run. This consistent ensemble of model configurations constitutes a novel and valuable contribution from CNRM to the CMIP6 effort. This will allow to derive wider and more relevant information on their scientific usefulness in regard to their numerical cost.

5

Mediterranean events and climate change: contribution of CNRM-AROME

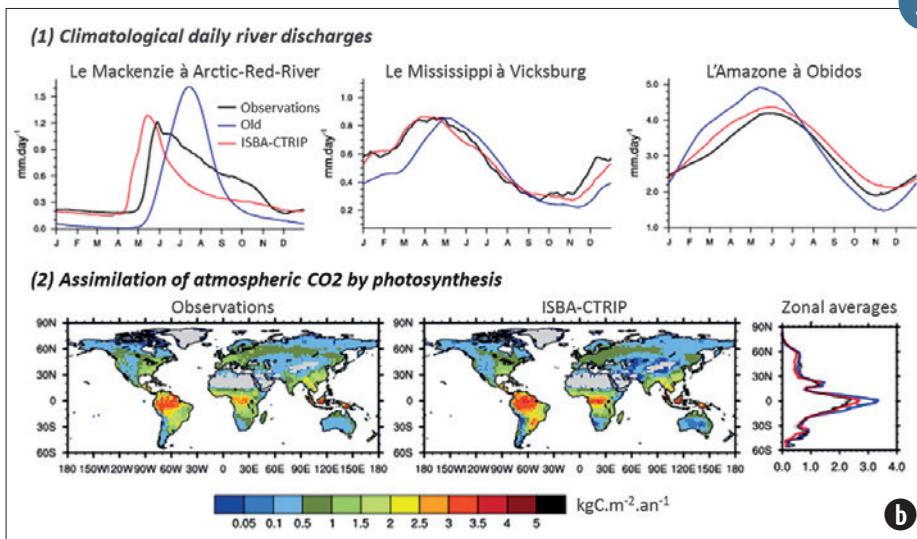
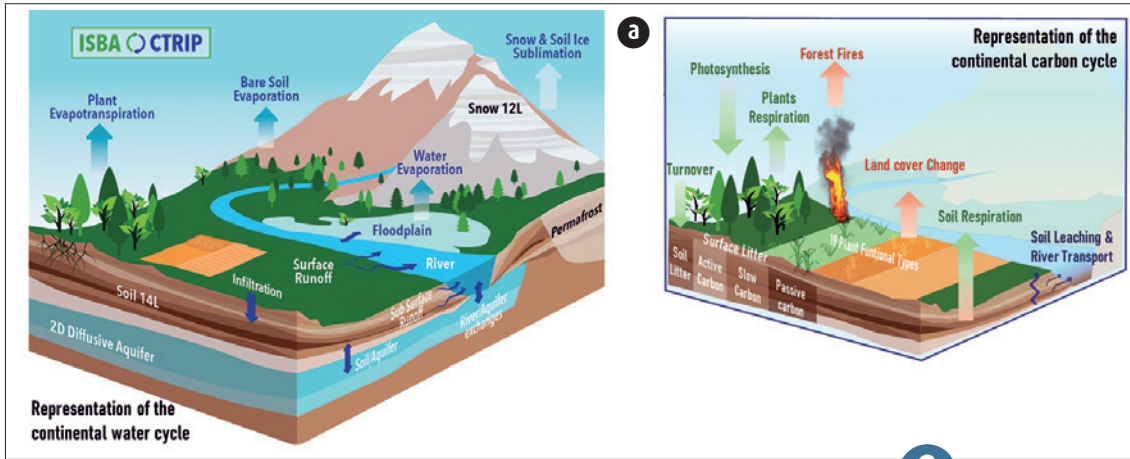
South East France is often affected by intense rainfall episodes called "Mediterranean episodes" generating flash floods causing major material damage and sometimes loss of life. For these reasons, studies on the evolution of these Mediterranean episodes in a context of global warming are of major importance for our society.

Until now, the climate change projection simulations used for this type of study in South East France have been carried out using Regional Climate Models (RCMs) with parameterized convection and a horizontal resolution not exceeding 12.5km. With the recent increase in computing capabilities, it is now possible to perform very high resolution (2-3km) climate simulations with Explicit Deep Convection Regional Climate Models such as CNRM-AROME.

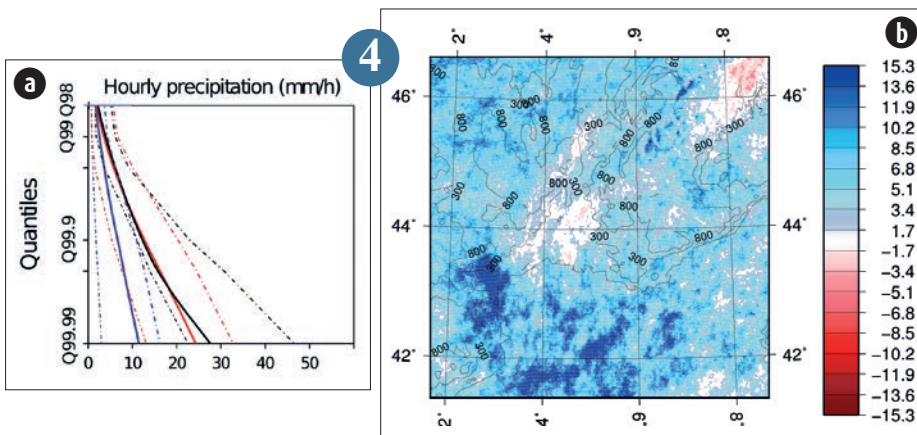
The use of the AROME model in climate mode has shown a high added value in the representation of extreme precipitation compared to the ALADIN RCM with parameterized deep convection (Fumière et al. 2019). This added value is significant on the representation of daily extreme precipitation, but also and especially on hourly extremes where the intensity of precipitation in convective systems is better represented (see Figure a).

The first climate projections with CNRM-AROME over 30-year periods were made following the IPCC's greenhouse gas emission scenario RCP8.5. By 2100, projections show a decrease in average autumn precipitation and an increase in extreme daily and hourly precipitation in south-eastern France. Note that this intensification is more pronounced in Roussillon (see Figure b).

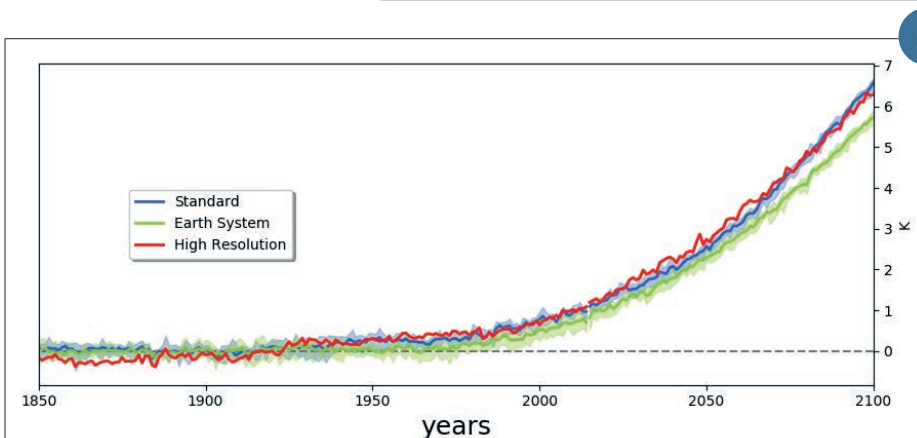
4



(b) Comparison of ISBA-CTRIP simulated versus observed river discharge and photosynthesis. (1) The top panel shows the average seasonal cycle of daily river discharge (in mm per day) simulated and observed for years 1979-2010 at the gaging stations near the outlet of the Mackenzie, Mississippi and Amazon rivers. Observations are in black, results from the previous model version used in the early 2010s are in blue, and ISBA-CTRIP results in red. (2) The bottom panel represents the spatial distribution of CO₂ assimilation by photosynthesis (in kg of carbon per m², per year) derived from spatialized in-situ observations (left) and simulated by ISBA-CTRIP (middle) for years 1980-2013. The corresponding zonal means (mean of the values at all longitudes per latitude band) are shown on the right. Observations are in black, results from the previous model version used in the early 2010s are in blue, and ISBA-CTRIP results in red.



(a) Cumulative Density Function (CDF) of hourly precipitation over the Cevennes in south-eastern France. The black curve represents Comephore observations, the blue curve represents precipitation simulated by ALADIN and the red curve represents precipitation simulated by the CNRM-AROME model. The discontinuous curves represent the 90% confidence interval of each data series. (b) Map of differences in the quantiles 99.9 of hourly precipitation over South East France between the historical (1976-2005) and future (2071-2100) periods according to the IPCC's RCP 8.5 greenhouse gas scenario. The differences in percentages are represented by degree of warming.



Evolution of the global mean near surface temperature in anomaly to the preindustrial climate. For the period 1850-2014, the external natural anthropogenic forcings are derived from observations while over 2015-2100, they are taken from the business as usual emission scenario, named ssp585. The blue line is for the standard model, the green line for the Earth system version and the red line for the high resolution version, lines indicate the multi-members average while the shading indicates the inter-members range (6 members are considered here both for the standard version and the Earth System model).

Diagnostic, study and impacts

The climate of Paris and its conurbation: long-term analysis based on observations and very high resolution climate modeling

The limited area model AROME is now used as a convection-permitting regional climate model with a horizontal resolution of 2.5 km. Coupled with the TEB urban canopy model, it allows to simulate the interactions between urban surfaces and the atmosphere, and the potential feedbacks of the city on the local and regional climate. AROME's ability to simulate urban climate characteristics was evaluated with Paris as a case study. Upstream, a climatological study was carried out using long series of spatialised observations of day and night surface temperatures from MODIS satellite products, daily minimum and maximum air temperatures by spatialisation of RADOME data, and cumulative daily precipitation derived from COMEPHORE rainfall hourly reanalyses. Urban climate indicators were deduced to qualify the urban heat island in terms of air and surface temperature, and the effect of the city on precipitation (Fig 1). Especially, daily precipitation were found to be 29% higher on average downstream of the city.

Driven by ERA-Interim and ALADIN over the period 2000-2015, the AROME model reproduces a good climatology of the nighttime urban heat island which remains positive all year round with maxima in summer, as well as realistic differences in precipitation accumulation upstream and downstream of the city (Fig 2). AROME is now applied for 10-year climate simulations by middle and end of the 21st century for impact studies over Paris city.

6

Climate Data rescue from French lighthouses 1881-1940

In 1881, the lighthouse weather service *Service météorologique des phares et balises* organised the climatological network of the French lighthouses, composed by 21 lighthouses. These lighthouses contributed to the French climatological network of the National weather service *Bureau central météorologique de France* from 1882. The lighthouse keepers had to take observations of atmospheric pressure, wind, temperature and rain and to record them in a climatological formular, according to detailed instructions. A copy of this monthly formular, dedicated to lighthouse weather records, should be sent, each month, to the services *Bureau central météorologique de France* and then *l'Office national météorologique*.

Research in the deposit from Météo-France at the French National Archives permitted to find formulars prior to 1941 for 25 French lighthouses, of which 12 long-term series for 1881-1940.

Cataloguing, analysing the climatological value and imaging the records, products of the collaboration between the French National Archives and Météo-France, are completed. Recovery of around 2 million observations of atmospheric pressure and wind data, taken 3 times during the night, at 9 p.m., midnight and 3 a.m., will be carried out by the DCSC during the next two years.

The International Data Rescue Portal (I-DARE) allows to follow the progress in the climate data recovery from lighthouses between 1881 and 1940 (<https://www.idare-portal.org/>).

7

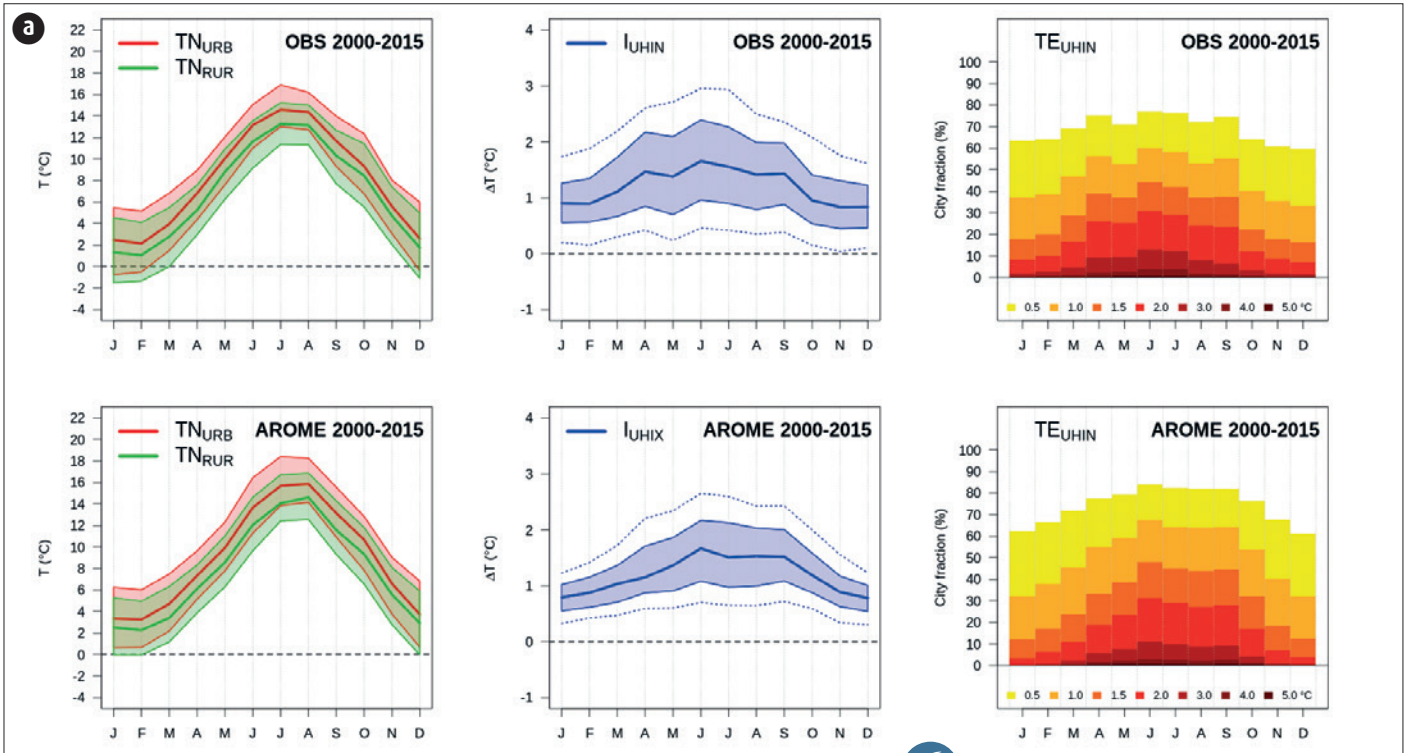
Evolution of cyclonic activity in the SW Indian Ocean basin: first results of the ReNovRisk program

One of the objectives of the "ReNovRisk Cyclones and Climate Change" research programme (INTERREG-V Indian Ocean 2014-2020) is to assess the evolution of cyclonic activity in the South-Western Indian Ocean (SWIO) basin at the end of the century. The analysis of global (Arpege-Climat; 10-30 km resolution) and regional (Aladdin-Climat, 12 km resolution) climate simulations (RCP 8.5) carried out specifically for this programme shows that global warming could have significant repercussions on both the frequency and intensity of tropical cyclones developing in this part of the world.

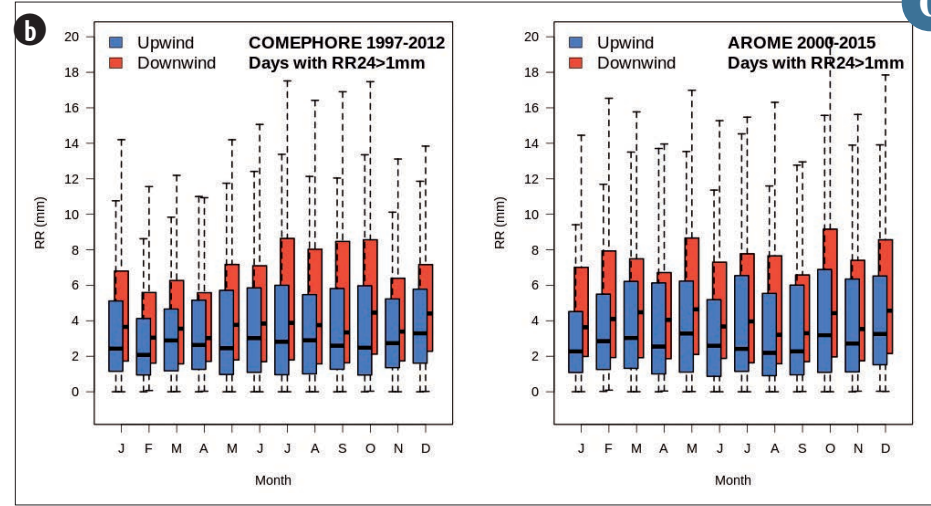
Climate simulations, carried out over the period 2051-2094, first suggest that the cyclone season, which nowadays starts around mid-November, could be delayed by about a month in a few decades. Models also suggest a significant decrease in the

number of low-pressure systems at the basin scale, nevertheless combined with an increased number of intense and very intense systems. Finally, one also notice a marked southward shift in the position of the maximum intensity (LMI) reached by tropical cyclones that develop in the SWIO. Overall these projections suggest that the cyclone risk could increase significantly in the Mascarene Archipelago (Reunion, Mauritius) with more intense systems in the vicinity of Reunion concentrated over a shorter period of time.

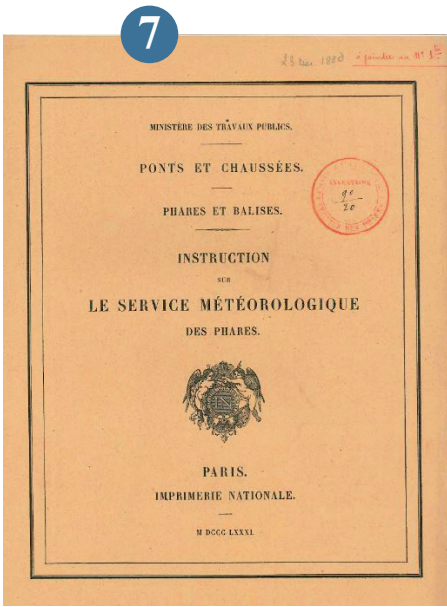
8



6



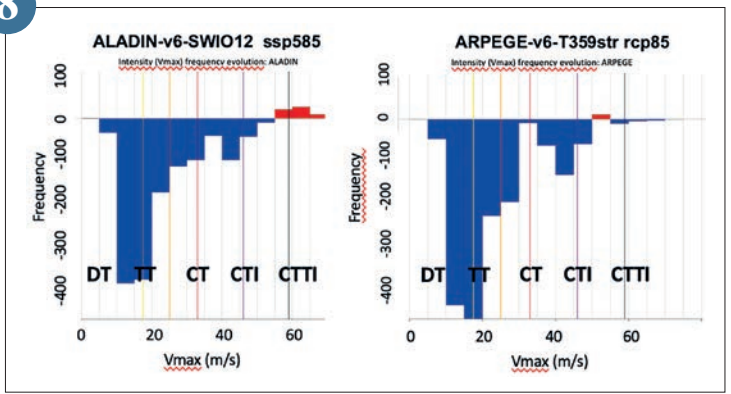
(a) Comparison of monthly averages over the period 2000-2015 of urban and rural temperatures observed and simulated by AROME (left), of the associated urban heat island (middle), and of the city fraction impacted by different urban heat island intensities (right). (b) Comparison of the monthly evolution of the daily precipitation rates from COMEPHORE reanalysis (left) and AROME simulation (right) over upwind and downwind areas.



Instruction for the French lighthouse weather service, 1881. Archives nationales (France).

Frequency evolution of tropical depression system intensity in the SW Indian Ocean basin on the horizon (2051-2094), classified by type of system: DT depression; TT storm; CT cyclone; CTI Intense Cyclone; CTTI very intense cyclone.

8



Climate projections and their impacts on agriculture in Guadeloupe

Climate change puts pressure on both the environment and human lifestyles, and its impact on the agricultural sector can already be felt. The French Antilles are particularly vulnerable because of their insular nature and a poorly resilient agricultural sector. In this context, the EXPLORER project lead by INRA and co-funded by ERDF and ADEME, of which Météo-France's DIRAG is a partner, aims at proposing an integrated approach of agriculture in Guadeloupe to address the issues of adaptation to climate change, reduction of greenhouse gas emissions, and improvement of food security. On the other hand, climate projections have been performed for Guadeloupe with ARPEGE-Climat and corrected with long series of observed temperature and precipitation in the framework of the ERDF C3AF project. These projections are being used in the framework of EXPLORER, namely with the computation of climate indices specific to the agricultural sector and to the study region. The analysis, which focuses on the future evolution of both mean climatology and weather events, aims at the definition of a vulnerability profile for agriculture in Guadeloupe. The results show strong year-round warming and significant wet-season drying that are already evident by the half of the century. They would be associated with more frequent heat waves and droughts, yet less frequent heavy precipitation events and tropical cyclones in the vicinity of Guadeloupe, with likely adverse impacts on water resource management and agriculture.

9

Seasonal forecast

Improving sub-seasonal precipitation forecasts in New Caledonia through a statistical-dynamical approach

S2S (Sub-seasonal-to-seasonal) systems provide ensemble climate forecasts at a global scale and at forecast times ranging from two weeks to two months. In some regions, they are able to provide relevant information about forthcoming precipitation anomalies (drier or wetter than normal) up to a few weeks in advance. However, their raw precipitation forecasts need to be post-processed either by calibration, or bridging with large-scale climate features that impact rainfall and are better predicted than precipitation itself.

These two aspects have been merged into a statistical-dynamical approach designed to improve sub-seasonal precipitation forecasts from the Météo-France S2S system, based on the CNRM-CM general circulation model. This method has been applied to the southwest tropical Pacific basin, where precipitation exhibits some sub-seasonal predictability on account of El Niño Southern Oscillation (ENSO) and the Madden-Julian Oscillation (MJO). A particular focus was put on New Caledonia, a territory prone to both drought and heavy rainfall spells.

A Bayesian approach uses predictors coming from the dynamical S2S system (raw precipitation output, climate indices related to ENSO and the MJO) to infer corrected precipitation thanks to a statistical model that is fitted on a reforecast period. This approach leads to more reliable probabilistic forecasts and enhances the ability to detect weekly spells of heavy rainfall up to four weeks in advance.

10

Seasonal hydrological predictability for Ebro and Po catchments (MEDSCOPE project)

The MEDSCOPE project aims to strengthen the use of seasonal forecasts in the Mediterranean area with a particular interest in the seasonal management of water resources, in a climate context increasingly marked by drought events.

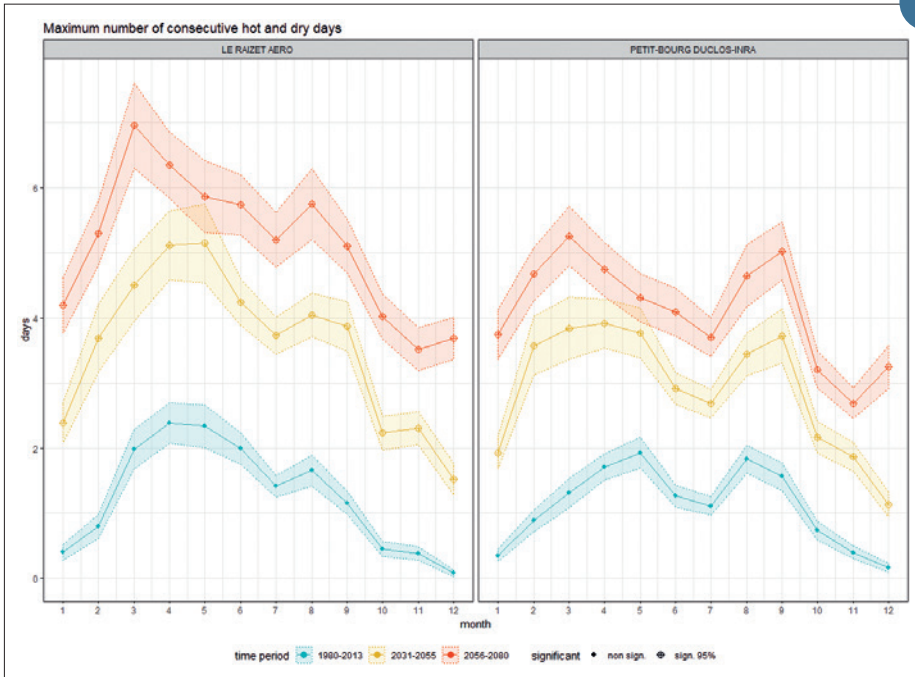
In this context, Météo-France is extending its hydrological seasonal forecasting capacity to the southern part of Europe. The new chain is fed by an atmospheric seasonal forecast model (Météo-France System 6 and later other models of the European portal C3S) whose data are debated by the ADAMONT downscaling method (see article dedicated in this report) from the new European UERRA re-analysis at a 0.05° resolution. The seasonal forecast is also compared to climatological forecasts, based on a set of historical simulations. These datasets then feed the SURFEX-CTRIP model, which calculates from the initial state of the considered year the seasonal evolution of the hydrological

components of the watersheds: soil water content, snow water equivalent, river flows, level of watertable.

Case studies were drawn up with the project partners, notably on the Ebro basins in Spain (with AEMET and the Ebro Hydrological Confederation) and the Po basin in Italy (with the CMCC and the Arpa-Simc). The objective is to develop and evaluate indicators of seasonal management of water resources with local partners and managers of these basins (see attached figure).

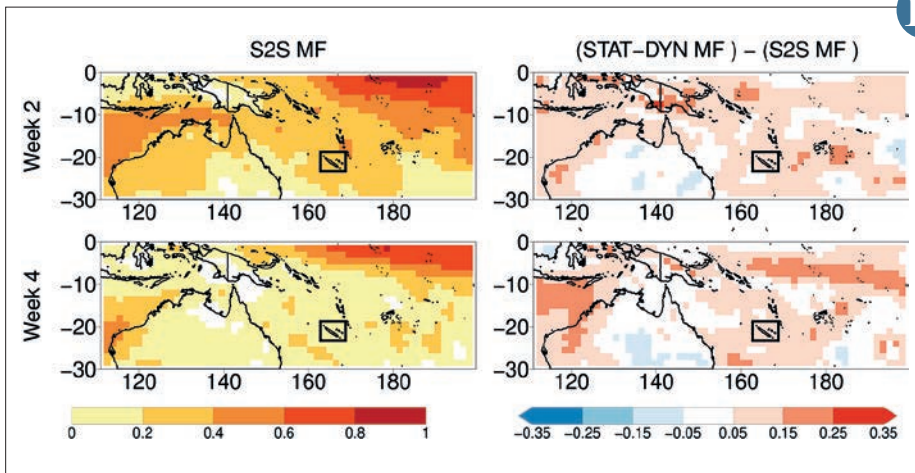
11

9



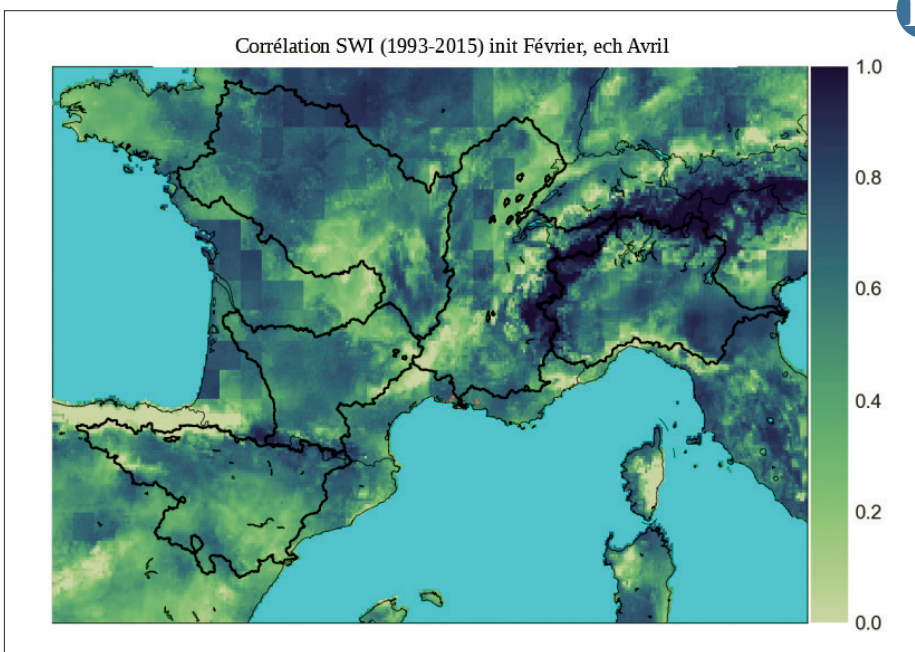
Changes in the maximum number of consecutive hot and dry days by respectively 2055 and 2080 for two locations representative of the low lands of Grande-Terre (Le Raizet) and the high lands of Basse-Terre (Petit-Bourg) in Guadeloupe. The projected changes are robust (significant at the 95% level) whatever the calendar month, future period (2031-2055 or 2056-2080), or considered location.

10



Left: ROC score (discrimination of the occurrence of an event) for the upper quintile of weekly precipitation in the Météo-France S2S system before application of the statistical-dynamical scheme. Right: Difference between the ROC score obtained after and before applying the statistical-dynamical scheme to the Météo-France S2S system. The rectangular box indicates the location of New Caledonia.

11



Correlation map of soil water index (SWI). Climatic forecast initialized on February 1st - Lead time 2 months (April) - Period 1993-2015.

Forecast in West Africa at seasonal and sub-seasonal in the framework of the CREWS-Burkina Faso project

The CREWS program aims to strengthen information and early warning systems in the most vulnerable countries. CREWS-Burkina Faso is a pilot project (2018-2020) for the Sahel climate zone in which Meteo-France has been entrusted with the development of the seasonal to sub-seasonal forecasting component.

Meteo-France uses several European models for the seasonal scale and the Ensemble Prediction System (EPS) of the European centre (ECMWF) for the sub-seasonal scale with the aim of predicting the most significant events at these time scales (such as drought or heavy rainfall events).

Products have been developed at Meteo-France for the entire Sahel to document the important elements of the monsoon and to make the best use of variables with better predictability than rain, like the precipitable water. The Burkina Faso agency has also contributed to the evaluation of forecast products through a network of rain gauges now counting more than 150 stations.

During this first year of the project, weekly briefings have involved Meteo-France and the meteorological services of Burkina Faso, Senegal, Niger and Mali in order to appropriate and evaluate the products developed and to share the expertise of each of the centres. This year, the seasonal forecast has showed an extremely dry start to the season on Senegal which was well observed. On a sub-seasonal scale, a highly precipitating event in Mali as well as an exceptionally late and wet monsoon season end could be expected up to four weeks in advance.

In 2020, the project will continue with the different partner departments, including a plan to transfer the expertise developed during the project.

12

Selection of the new set of regional simulations debiased in France for the DRIAS portal

The DRIAS portal, opened in 2012, aims to provide regionalized and debiased climate projections for France. The current reference set is mainly based on a EURO-CORDEX set defined in 2014, which has been updated as part of the climate services agreement with the MTES.

Over the past five years, the number of simulations available on EURO-CORDEX has increased significantly and allows a better assessment of model uncertainties. However, the number of simulations currently available, about 30 pairs of GCM/RCM per climate scenario, raises problems of volume and data processing. In addition, it appears that anomalies have been detected on more than half of the old EURO-CORDEX simulations currently available on the portal.

Based on this observation, a set of selection criteria has been defined to achieve a robust set: diversity of representation of GCMs and RCMs, elimination of GCMs/RCMs with anomalies, availability of at least two RCP scenarios. The new set was also defined to allow the model uncertainties and their diagnostic implications on temperatures and precipitation in France to be represented as accurately as possible (See Figure).

This new set of regional simulations corrected with the ADAMONT method will include 42 simulations, 12 over the historical period, 12 projections on the RCP8.5, 10 for RCP4.5 and 8 for RCP2.6 and will be posted on the DRIAS portal in mid-2020.

14

Adaptation of the ADAMONT downscaling method to seasonal forecast

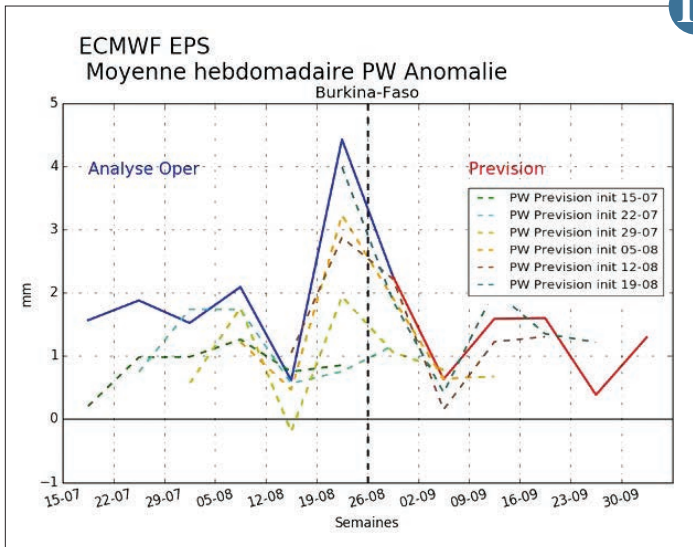
Climate services at seasonal scale are booming these last years in Europe. Traditional sectors like energy or water management are expecting such innovations, but new sectors like tourism too.

Most of these services rely on impact models. They allow to deliver forecasts of variables or indicators directly usable to decision makers. These impacts models can't be fed by raw seasonal forecast data. As a matter of fact, raw seasonal forecasts are affected by bias, moreover their temporal and spatial resolution are too coarse. This is where downscaling tools come in.

This issue arose in the development of two specific services: hydrological forecast in the framework of MEDSCOPE project, and snowpack forecast in the framework of PROSNOW project. For both applications, the ADAMONT method (initially developed by CNRM for downscaling climate scenarios over mountainous areas) has been adapted by DCSC (Directorate of Climatology and Climate Services) to deal with seasonal forecast.

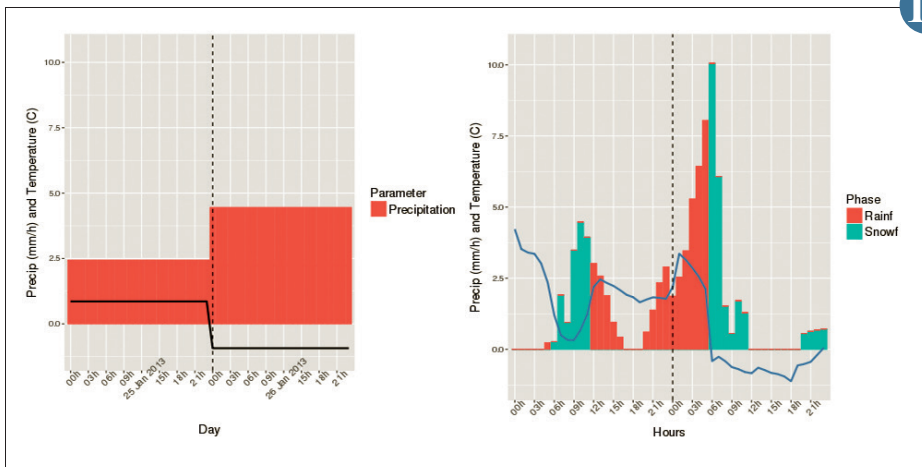
ADAMONT consists on adjusting daily distributions of a set of parameters by a quantile mapping method, with respect to reference distributions (observations or reanalysis). This correction is differentiated according to weather regimes. Corrected forecasts are then disaggregated at a finer time-step (hourly for instance) by means of hourly profiles taken from analogue past situations. This last step ensures inter-parameter consistency at fine time-step. Datasets thus produced for PROSNOW are promising. Downscaled forecasts correctly represent local climate and snowfall, and properly restore the inter-annual variability present in raw seasonal forecast.

13



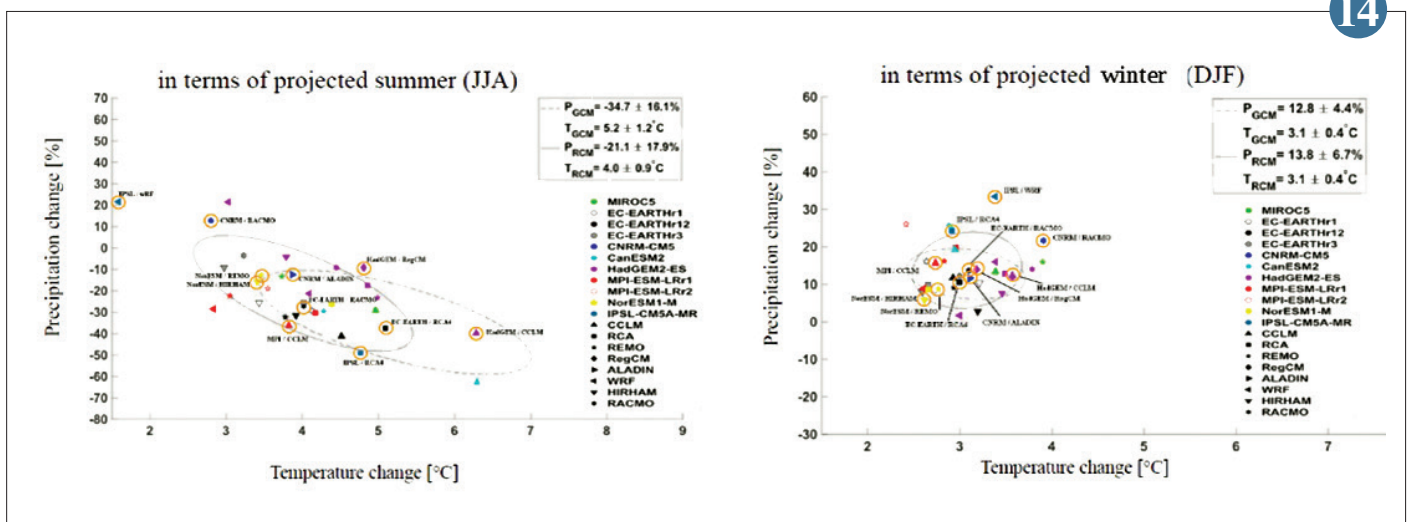
12

Example of evolution of precipitable water on Burkina Faso. In dotted lines are represented the different successive runs, in blue analysis and in red the forecast of 26 August. The peak observed in the week of August 19 was well anticipated and was associated with a revival of rainy activity.



13

Example of forecast downscaled by ADAMONT, for the PROSNOW project. On the left, raw daily temperature and precipitation forecast, on a grid-point of Meteo-France System 6 seasonal forecast model, for one member of its ensemble. On the right, the hourly corrected forecast on a mountain zone, with precipitation spread in rain and snow fall.



14

Diagrams of the bi-varient climate change signal in terms of projected changes in temperature and precipitation (summer = JJA left and winter = DJF right) for 2071-2100 compared to 1981-2010 for the CPR8.5 emission scenario.

The orange circles indicate the RCMs selected for DRIAS. The symbols identify the RCM and the colours of the forcing GCMs.

The dotted line (solid) indicates the probability ellipse for the GCM results (RCM) (confidence interval, covering 68.2% of the data). Mean and standard deviation scores for precipitation (P, %) and temperature (T, °C) for the GCM and RCM ensemble, respectively, are shown in the upper right corner of each figure.

(Source: PRINCIPLES project).

Chemistry, aerosols and air quality

The year 2019 was marked by several intense forest fires around the world. This was the case in Siberia, Amazonia, Indonesia and California, but it was perhaps the fires in Australia, combined with an exceptional heat wave, that made the biggest impression. They emitted around 400 million tonnes of CO₂ into the atmosphere, which is comparable to the human emissions of greenhouse gases from a country like France. The Australian fires also emitted large quantities of other gases such as CO, but also particles that were transported to South America and to the upper troposphere / lower stratosphere (UTLS). However, in this part of the atmosphere, which has an important influence on the Earth's radiation balance and climate, the dynamic, microphysical and chemical processes involving water vapour, ozone, CO and aerosols are complex, strongly coupled, and often poorly represented by models. As shown by two studies presented in this section, progress in physico-chemical modelling (MOCAGE) and the quality of observations (IAGOS, now spanning more than 20 years) are making it possible to improve the understanding and representation of the impact of biomass fires on the CO and ozone composition of the UTLS. These are important steps towards a more comprehensive understanding of the processes involved in this part of the atmosphere.

Other developments completed in 2019 will allow to better anticipate the dispersion of volcanic plumes, which can cause major disruptions to air traffic. It has thus been shown that a better representation of volcanic particle emission sources combined with the assimilation of the optical thicknesses of aerosols measured by Météo-France's ground-based lidars greatly improves the prediction of the evolution of the plume generated by the 2010 eruption in Iceland.

Finally, significant progress has been made in modelling the impact of agricultural spreading on air quality, which for a long time was little or poorly represented by the models. This now makes it possible to provide information to regulate spreading practices, avoiding periods that would lead to a deterioration in air quality dangerous to human health.

1

Ozone climatology in the upper troposphere as seen by IAGOS airborne measurements and by MOCAGE model

The *in situ* measurements gathered aboard commercial aircrafts through the research infrastructure IAGOS, of which Météo-France is one of the partners, are widely used to evaluate atmospheric chemistry models in the upper troposphere and lower stratosphere. Since IAGOS database includes now more than 20 years of data for ozone and more than 15 years for carbon monoxide, it offers the opportunity to evaluate long-term simulations done in the frame of international chemistry-climate inter-comparison exercises, such as CCMI which is contributing to the IPCC reports.

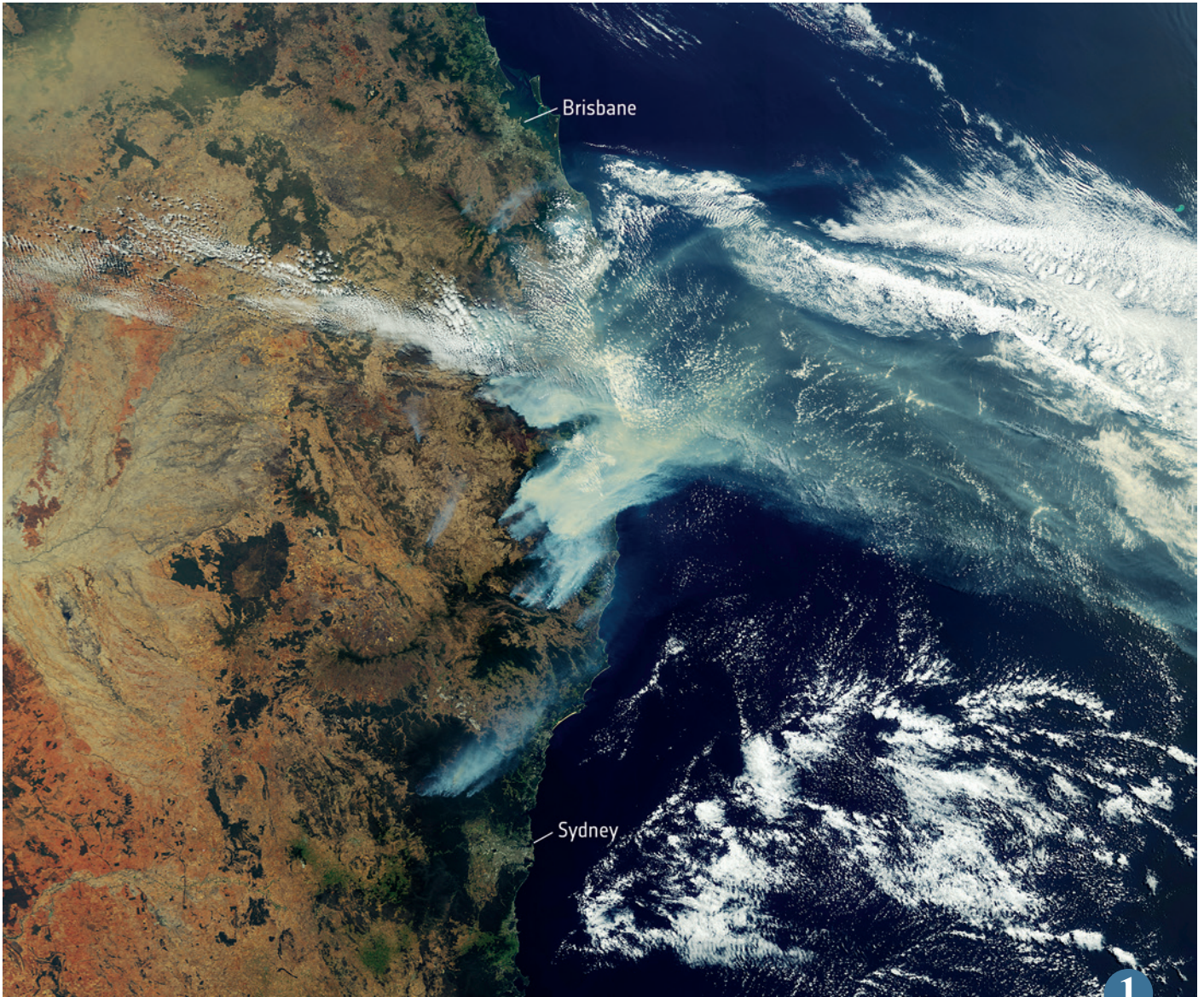
The usual way for model evaluations against airborne data on experiments over relatively short durations is to interpolate the simulations at the measurement locations and times. But to produce climatologies over 20 years in a consistent manner between IAGOS and the model, an original method has been developed. Its general concept is to map IAGOS measurements onto the model grid on a monthly basis since CCMI provides monthly means.

This new method was tested on the MOCAGE simulation run for recent climate conditions in the framework of CCMI. The climatologies

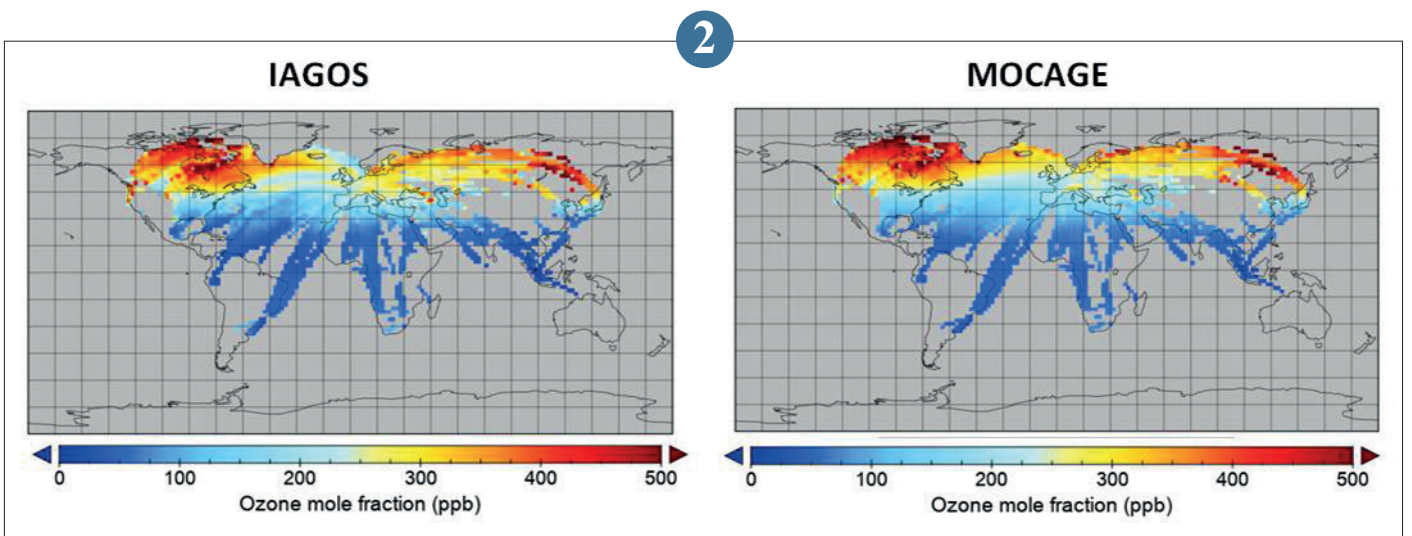
of ozone obtained for the 1994-2013 period are plotted in the figure for model level 24 (~225 hPa, i.e. ~11km in altitude). They show that the CCMI MOCAGE simulation is in very good agreement with IAGOS measurements. The application of this method can be expanded to CCMI simulations from other models than MOCAGE or for simulations of similar type.

2

Climatology maps showing ozone mole fraction averaged over the 1994-2013 period from IAGOS measurements (left panel) and from MOCAGE simulation produced for CCMI (right panel). Note that the MOCAGE climatology is only shown where IAGOS measurements are available to ease the visual comparison.



▲ The multiple bushfires raging across Australia's east coast, captured by the Copernicus Sentinel-3 mission on 13 November 2019, 09:15 local time. Plumes of smoke can be seen drifting east over the Tasman Sea. © Contains modified Copernicus Sentinel data (2019), processed by ESA.

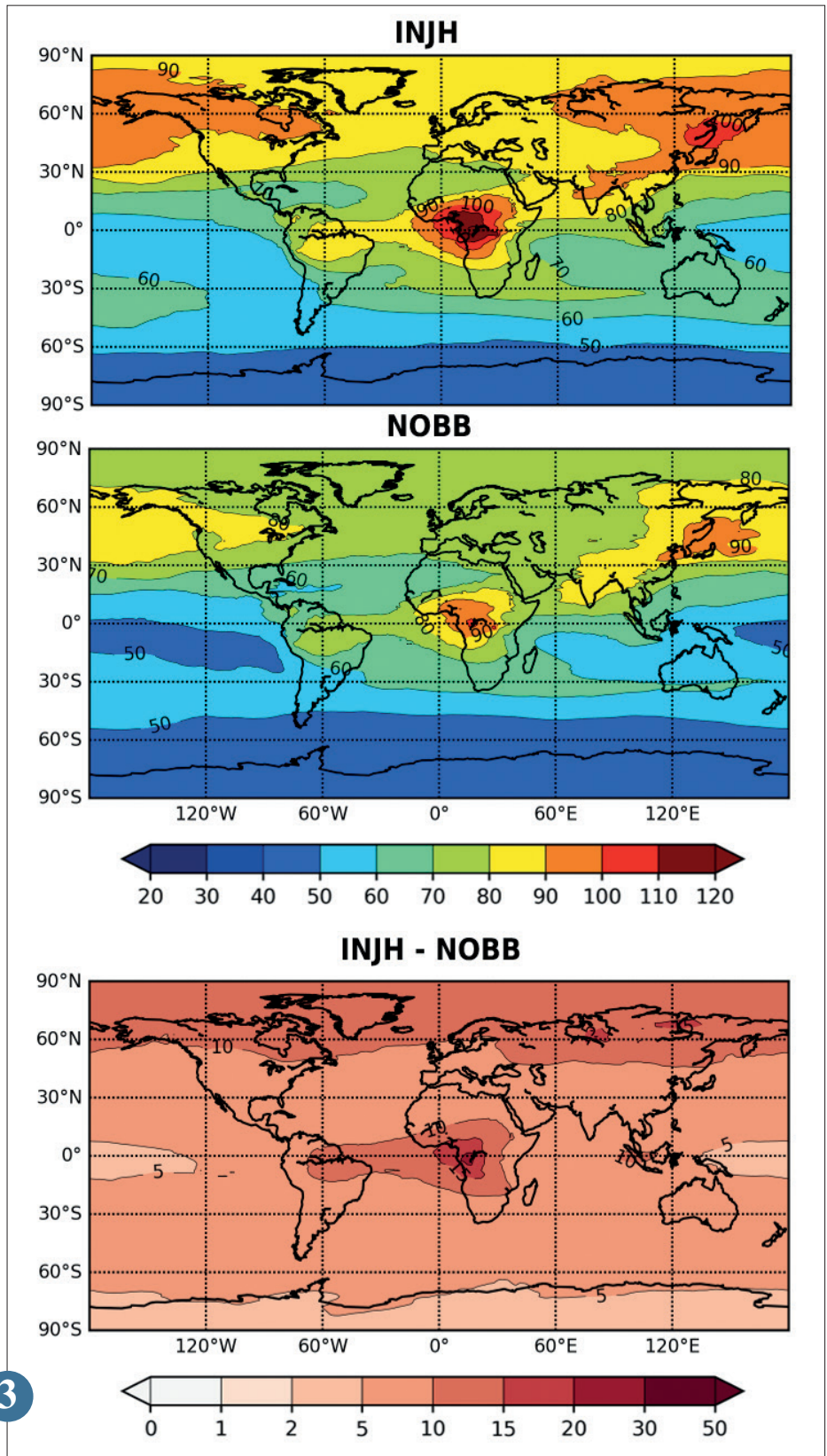


The impact of biomass burning emissions on upper tropospheric air chemical composition

Carbon monoxide (CO) is a key species when studying upper tropospheric air composition, in particular because it is a precursor to ozone at this altitude (8 to 10 km at mid-latitude). One of the main source of CO in the atmosphere are biomass burning emissions, but their representation in global models sometimes remains inaccurate, because of phenomenon such as pyro-convection. Chemistry-transport model MOCAGE is used to assess how biomass burning emissions impact upper tropospheric CO concentrations does. For this purpose a simulation has been carried out for the year of 2013, and it has been validated with CO in-situ measurements from the IAGOS European research infrastructure which places instrument units on commercial aircraft in order to monitor air chemical composition along their flight track. Then, by comparing this simulation to a similar one in which biomass burning emissions were turned off, we can estimate their impact on upper tropospheric CO concentration (figure). Areas impacted the most are above the boreal forests and equatorial Africa, as well as above the amazon forest and equatorial Asia to a lesser extent. Impacts are stronger for the most emitting areas, but also depend on the occurrence of fast vertical transport to the upper troposphere: deep convection in tropical areas; and pyro-convection for boreal wildfires.

This study is a first step towards a more in depth work on upper tropospheric air composition. Chemical production where CO is a precursor will be investigated, especially ozone production, because its radiative impact is at its maximum at this altitude.

3



Map of the 2013 mean upper tropospheric CO (in ppb) as simulated by MOCAGE: with biomass burning emissions activated (INJH, top panel); without biomass burning emissions (NOBB, middle panel); as well as the difference between the two (bottom panel).

Improving the representation of agricultural ammonia emissions: a simple model for estimating fertilization dates from meteorological constraints

Ammonia (NH₃) is a major air pollutant and a precursor of small particles (PM₁₀ and PM_{2.5}) that impacts the environment and human health and must therefore be monitored and predicted. One of the major sources of NH₃ is the use of fertilizers by the agricultural community.

As part of the Amp'Air project, funded by PRIMEQUAL, Météo-France is developing a simple model to predict fertilization dates based on temperature, rainfall and agricultural practices. This model will allow a better representation of the fertilization windows and therefore the temporal variations of NH₃ emissions.

The model first determines whether the weather conditions allow for seeding and spreading activities (too muddy soil, too much wind, frozen ground, etc.). A probability

of seed on a given date is then calculated based on agricultural parameters specific to each seed (wheat, sunflower, etc....). Finally, probable fertilization dates are estimated with regard to seed dates, the evolution of the atmospheric parameters necessary for the plant (i.e. temperature accumulation), and the usual development stages requiring fertilizer application. Figure "a" describes the operating diagram of the model. Figure "b" represents the probability results for maize in

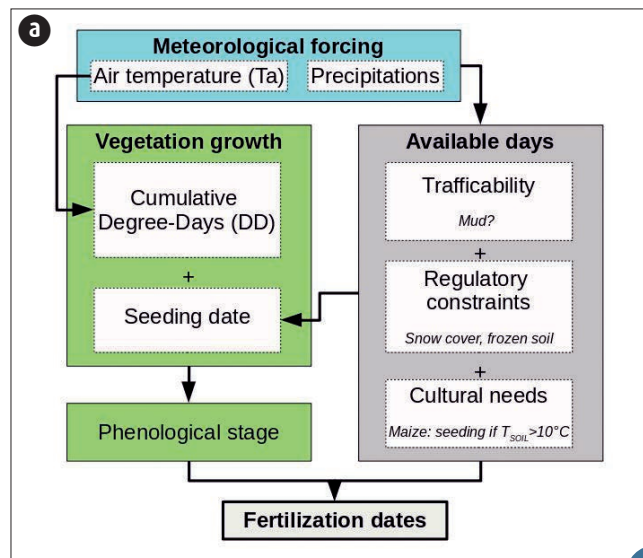
the Normandy region in 2006. The top panel shows the excluded days for activities, in the middle the probable planting and fertilization days and at the bottom the evolution of the temperature sum.

This model will soon be coupled to a model for calculating NH₃ emissions from the fertilizer compounds applied.

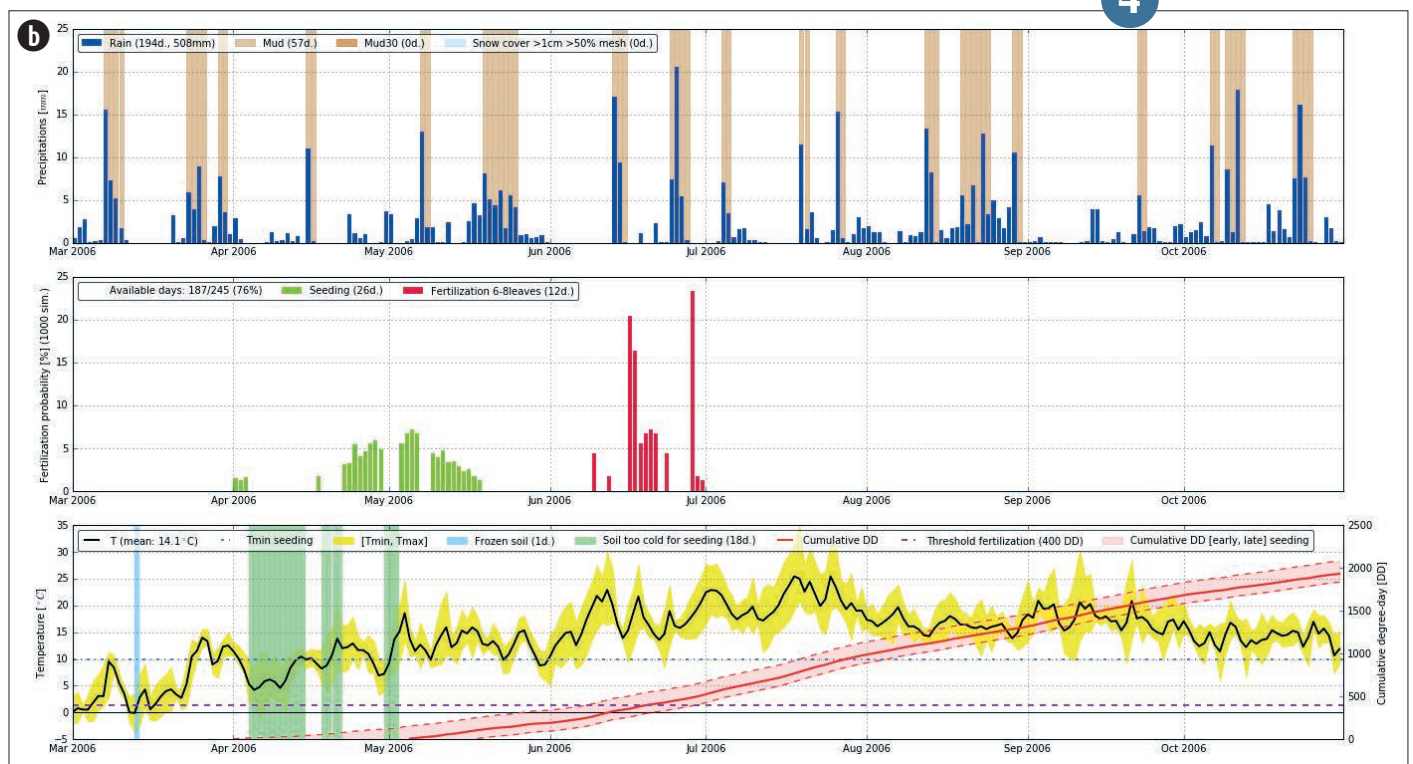
4

(a) Schematic diagram of the model.

(b) Forecast of sowing and fertilization dates for maize in the Normandy region in 2006.



4



Snow

Research conducted at Météo-France on snow in the mountains covers short-term time scales (monitoring and forecasting) as well as long-term (past and future) climate changes in weather and snow conditions. The combination of these time scales, and the work addressing both hazards and impacts (natural risks, tourism, water resources, ecosystems) place the research carried out at the Centre d'Etudes de la Neige (CEN) at the heart of the issues of climate risk analysis and climate change adaptation. From 2017 to 2019, CEN, through its director S. Morin, took part in the drafting of the IPCC Special Report on the Ocean and Cryosphere in a Changing Climate (SROCC). The SROCC report was produced jointly by IPCC Working Group 1, which works on the physical aspects of climate change, and Working Group 2, which studies impacts, vulnerabilities and adaptation. This approach makes it possible to address the issues in an integrated manner. The chapter on mountains deals specifically with the evolution of weather conditions in mountains (temperature, precipitation), the physical evolution of snow, glaciers, mountain permafrost, and the impacts on water resources, natural hazards (avalanches, landslides, floods, phenomena of glacial and periglacial origin), mountain fauna and flora, agriculture, hydropower, tourism, lifestyles and the cultural identity of mountain populations.

For more information: <https://www.ipcc.ch/srocc/>

1

Tomography and motion of dust particles in dry snow

Light-absorbing particles in snow, such as mineral dust or black carbon, are a potent climate forcing agent. Their presence darkens the snow surface and leads to higher solar energy absorption. Several studies have quantified this radiative impact by assuming that these particles were motionless in dry snow.

To evaluate this assumption, we obtained time series of X-ray tomography images of dust-contaminated samples evolving under isothermal conditions at -2°C and under a temperature gradient of about 20 K/m .

We showed that temperature gradient metamorphism impacts the location of the particles with respect to the ice matrix and

their relative vertical position in the snow layer. In the temperature gradient experiment, we observed a progressive embedding of dust particles within the ice matrix (Fig. 1a) and a downward displacement of the dust center of mass by $200\text{ }\mu\text{m}$ on average for 200h (Fig. 1b). The dust motion mainly results from the fall of the dust particles into the pore space (Fig. 1c), while embedded particles only move with the settlement of the ice matrix. The comparison with the isothermal experiment, in which no significant motion was observed, confirms that the main driver of this motion is the presence of intensive water vapor fluxes related to sublimation–deposition mechanisms.

Such data are crucial for our understanding of the interaction of dust with snow and the associated modification of the radiative balance. For typical arctic and sub-arctic conditions, in which strong temperature gradient metamorphism prevails, we estimated that the dust motion could lead to a significant decrease in the solar energy absorbed when the dust is located on the top layer of the snowpack for a long duration.

2

Statistical post-processing of ensemble forecasts of the height of new snow

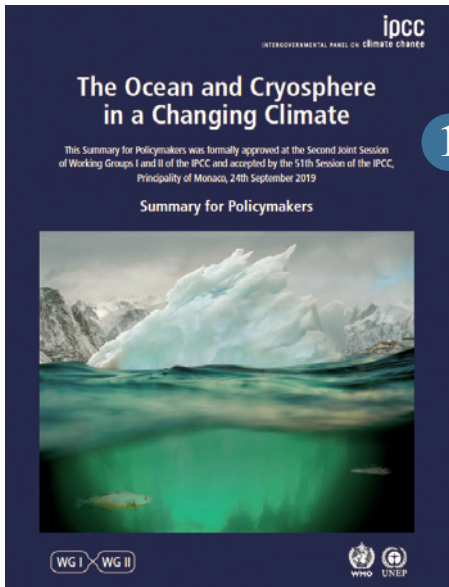
Forecasting the height of new snow (HN) is crucial for avalanche hazard forecasting, roads viability, ski resorts management and tourism attractiveness.

Météo-France operates the PEARP-S2M probabilistic forecasting system including 35 members of the PEARP Numerical Weather Prediction (NWP) system, where the SAFRAN downscaling tool is refining the elevation resolution, and the Crocus snowpack model is representing the main physical processes in the snowpack. It provides better HN forecasts than direct NWP diagnostics but exhibits significant biases and under-dispersion. We applied a statistical post-processing to these ensemble forecasts, inspired by a

method developed by NOAA for precipitation forecasts. Observations come from manual measurements of 24-hour HN in French Alps and Pyrenees. Different training strategies were tested in terms of spatial scale and of training dataset. Significant improvements are obtained compared to the raw forecasts with all training strategies. The results show that the post-processing can be applied at any point of the massifs, not only where observations are available. They also show that using long-term reforecasts for training improves the reliability of severe snowfall but leads to over-dispersion due to the discrepancy in initial perturbations between reforecasts and real time forecasts.

Thus, the development of reliable automatic forecasting products of HN needs long reforecasts as homogeneous as possible with the operational systems. Nevertheless, a first version of post-processed HN forecasts can be provided to the Alpha operational project of Météo-France in mountainous areas as an alternative to the strongly biased automatic forecasts currently available for this variable.

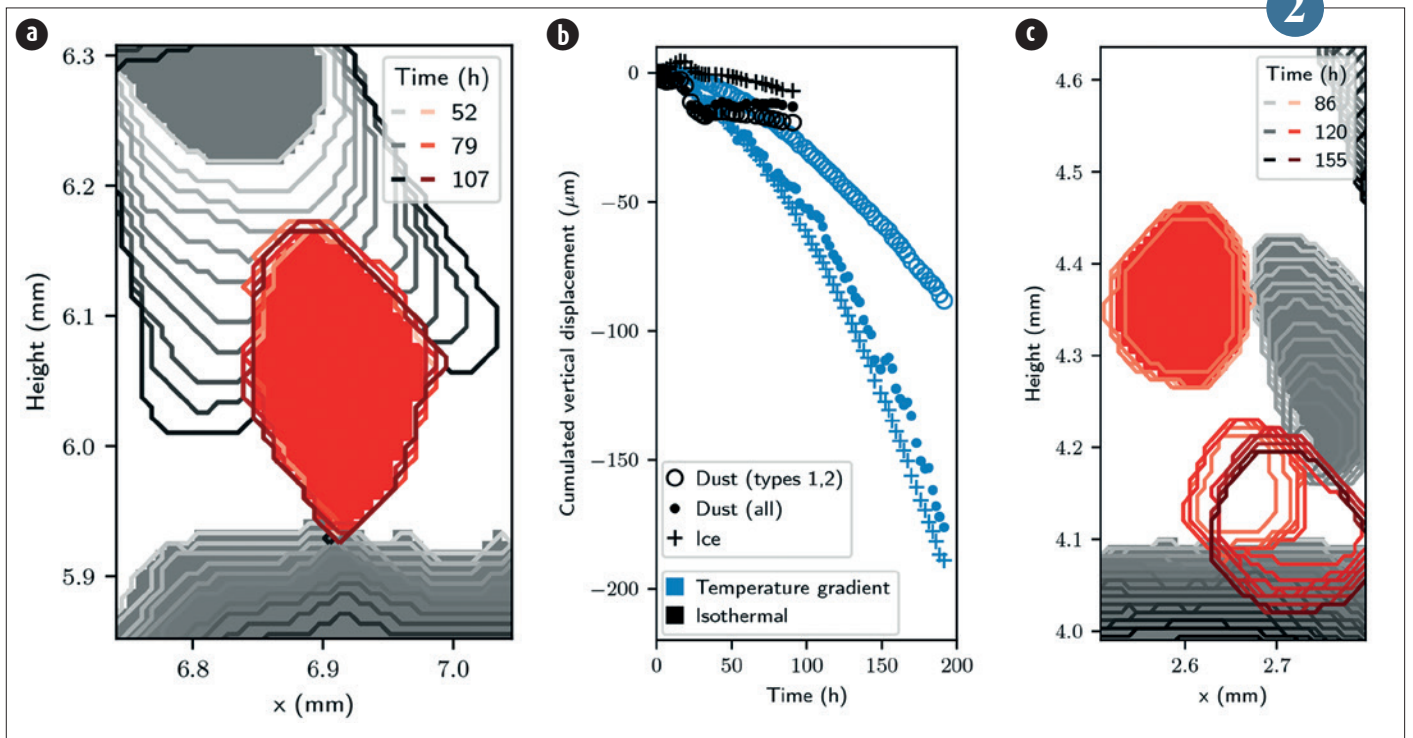
3



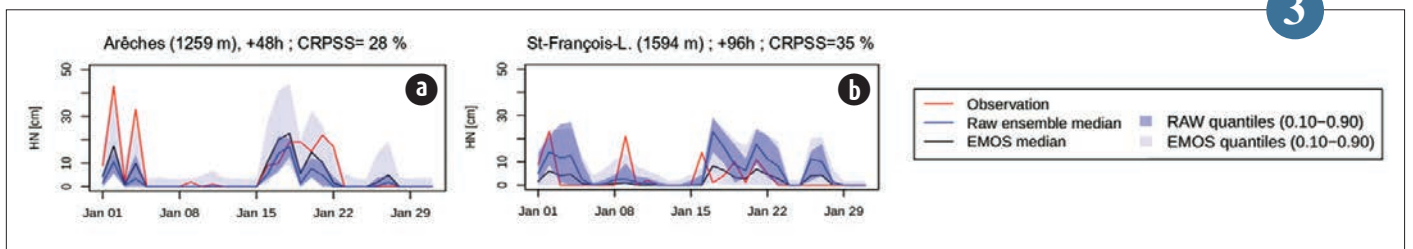
Cover page of the IPCC Special Report on the Ocean and Cryosphere in a Changing Climate (SROCC).

1

(a) Example of the dust progressive inclusion into the ice matrix for the temperature gradient experiment. The initial location of ice is shown in solid gray. The initial location of dust is shown in solid red. Their time evolutions are shown by the different contours; (b) Mean vertical velocity of the ice surface and of dust computed with all dust particles or only those not falling within the pore space (types 1 and 2); (c) Example of a particle falling by loss of contact to ice and then progressive downward movement with the sublimating ice surface.



2



3

Examples of forecasts of the 24h height of new snow during January 2018 (a) for Arèches station with 48 h lead time and (b) for Saint-François-Longchamp station with 96 h lead time. The blue envelope represents the probability distribution of the raw forecasts (indigo line for the median), and the grey envelope the probability distribution obtained from the statistical post-processing (black line for the median). The raw forecasts underestimate snowfall in example (a) and overestimate snowfall in example (b). In both cases, the raw forecasts underestimate forecast uncertainty. Thus, the statistical correction increases (a) or decreases (b) the median and increase the spread in both cases. Observations (red line) are much more often included in the post-processed distribution than in the raw distribution.

Climate projections of snow conditions in ski resorts

Ski tourism is a major sector of mountain regions economy. Snow management, and in particular grooming and artificial snowmaking, has become a routine component of ski resort operations, holding potential for counteracting the detrimental effect of natural snow decline under climate change. Whether snowmaking is a relevant adaptation measure under future climate change is a widely debated issue in mountainous regions, with major socio-economic implications. Work carried out at the Snow Research Center (Météo-France – CNRS, CNRM), in collaboration with INRAE Grenoble, has been carried out over the past years and shows how climate change influences the operating conditions

of ski tourism in the French Alps. A study published in *Scientific Reports* in 2019 has addressed snow reliability in 129 ski resorts, using a dedicated snowpack model explicitly accounting for grooming and snowmaking driven by a large ensemble of adjusted and downscaled regional climate projections, and using a geospatial model of ski resorts organization. A 45% snowmaking fractional coverage, representative of the infrastructures in the early 2020s, is projected to improve snow reliability over grooming-only snow conditions at the scale of the French Alps, both during the reference period 1986–2005 and below 2 °C global warming since pre-industrial. Beyond 3 °C of global warming, snow conditions would

become frequently unreliable and induce higher water requirements. Météo-France has also contributed to the development of a dedicated Copernicus Climate Change Service for European Tourism, including pan-European snow reliability indicators. Work is in progress to transfer knowledge and tools to local and national stakeholders, providing services in support to climate change adaptation strategies, taking into account the local specificities of the ski resorts.

4

Simulating Sentinel-1 observations in mountainous areas, a first step towards their assimilation into a snow model

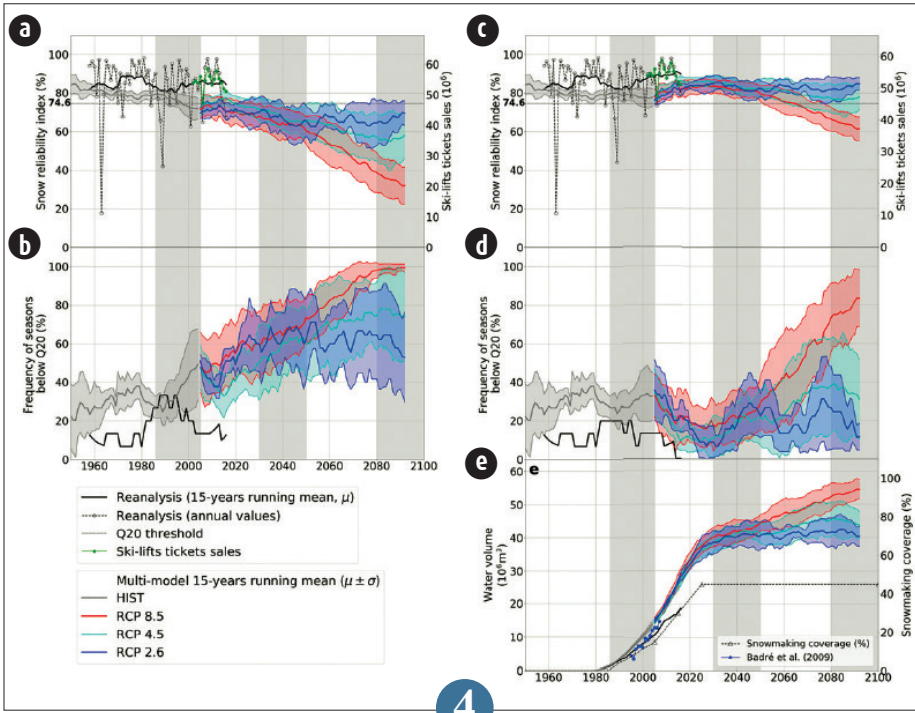
SAR measurements from Sentinel-1 now offer new possibilities to monitor snowpack evolution in space and time. Their use depends on understanding interactions between the surface-snow-atmosphere components and electromagnetic radiations. The assimilation of Sentinel-1 observations in the snow model Crocus would allow for optimal fusion of information from existing models (giving a priori information about soil, snowpack and atmospheric conditions) and observations.

However, effective snow radiative transfer simulations are necessary to achieve this fusion. Simulations of C-band backscatter were performed using the MEMLS3&a model

for radiative transfer in snow, fed by outputs from the ISBA/Crocus snow model. The simulations were carried out over a period of 3 years in a high altitude area. These simulations were evaluated by comparison to 141 scenes of Sentinel-1 observations. We showed that our modelling chain is able to consistently reproduce the SAR signal of bare ground and dry snow. In case of wet snow, a negative bias between observations and simulations was found, particularly during melting periods. The temporal variability of the simulations compares well with that of the observations, which is very encouraging for assimilation (see the accompanying figure).

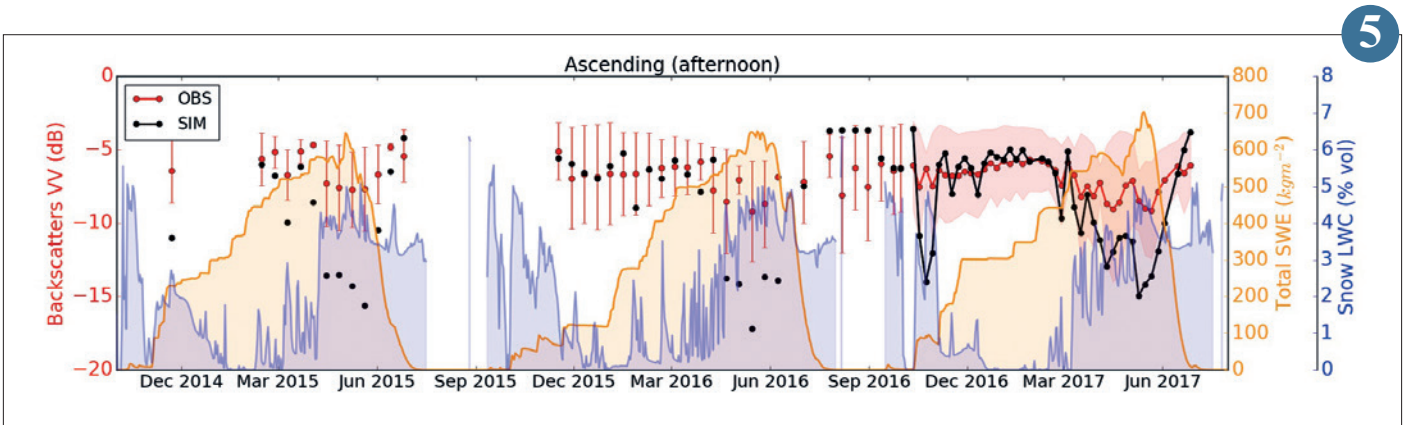
The bias may have several causes and needs to be corrected. This is the first study ever demonstrating the relevance of a model chain for performing SAR backscatter simulations over a complex mountain region, and a first step towards assimilating Sentinel-1 measurements into a snow physical model.

5



4

Figure (from Spandre et al., 2019).
 (a), (c): Simulation of the snow cover reliability (a) and the frequency of challenging seasons (c) without snowmaking, at the scale of the whole Alps, and for several climate scenarios.
 (b), (d): idem, but taking into account the evolution of snowmaking fractional coverage reaching 45% in 2025.
 (e): Estimated volume of snowmaking water requirements at the scale of the whole Alps, corresponding to the snow production calculated for the whole Alps according to the climate scenarios.



5

Time series of observed (red) and simulated (black) VV polarization backscatter coefficients representative of high altitudes (between 2850 and 3150 in the Oisans Mountains) and a snowpack at the end of the day. Snow liquid water content is shown in blue and its water equivalent in orange.

Oceanography

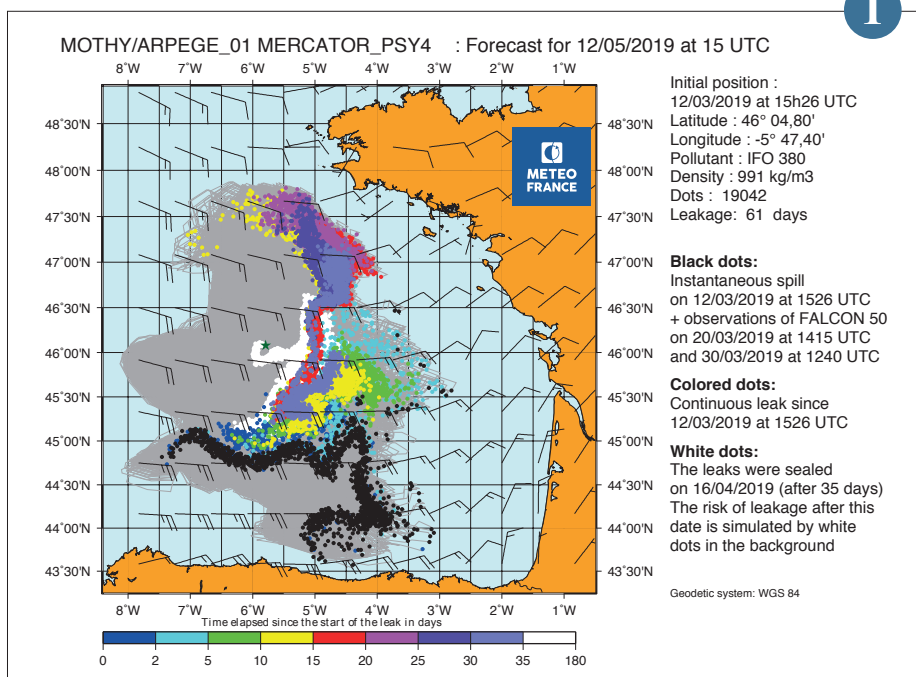
Météo-France researchers advance marine meteorology activities. In close collaboration with the scientific community, they take advantage of progresses in ocean sciences and technologies, especially those focusing on interactions between environments. Marine meteorology provides essential services for human activities, at sea or on the coast: sea states, drifts, coastal phenomena, water properties, in all weathers and at all latitudes. Algorithms and models represent more finely the phenomena, the complex interactions at the interface between air, sea, coast and river - where everything becomes complex... They integrate observations delivered by the most modern space systems: the value of new sensors onboard the Copernicus programme's Sentinels satellites is namely proven by the work presented here. Collaborations with academic laboratories and international collaborations are driving forces behind these endeavours. The stakes are high. The ocean drives the climate. It contributes to major atmospheric risks: Ocean-atmosphere interactions, including waves, determine the characteristics of extreme episodes such as cyclones or Mediterranean events. Ships, maritime installations, coastal works, or simply coastal landscapes in overseas territories as well as in mainland France are subject to the onslaught of water masses. Oceanography, like the other sciences that describe the different compartments of the "Earth system", is part of the obligatory panoply of meteorological services.

Drift at sea for crisis management

As part of its national and international responsibilities, Météo-France operates the MOTHY model for forecasting the drift of oil slicks or floating objects at sea. The system is activated about 20 times a week for actual oil spill or search and rescue operations. The Grande America accident in the Bay of Biscay is the most significant event of 2019. Due to a fire, the Grande America, which carried 365 containers and 2,000 vehicles, sank on 12 March 2019, 350 km off the

French coast, with approximately 2,200 tonnes of bunker fuel on board. An unknown quantity of heavy fuel oil was released into the marine environment on the day the vessel sank, followed by 35 days of continuous leakage before the breaches in the hull were sealed by an underwater robot. From 14 March, the Drift Committee, bringing together experts from Cedre, Météo-France, Ifremer and Shom, is responsible for providing the maritime Prefect with coherent

and relevant information on oil slick drift on a daily basis. The MOTHY model is used daily during the aerial surveillance and recovery at sea period. It provides drift forecasts for oil slicks and containers up to 3 days in deterministic mode and up to 10 days in probabilistic mode. Long-term modelling of residual diffuse pollution is also carried out over several months, in particular to manage continuous leaks from the wreck. Drift forecasts did not indicate any oil arrival at the coast. This allowed the authorities to organise the response at sea without mobilising resources ashore. Indeed, no pollution has been observed on the coasts.



1

1

MOTHY output from a simulated 2 months drift since the accident. It is based on an instantaneous spill scenario on the day of the accident combined with aerial observations (black dots), followed by continuous leaks from the wreck (color dots) for up to 35 days, and potential leaks (white dots) thereafter. The calculations were carried out using the winds of the ARPEGE model of Météo-France and the currents of the global MERCATOR model of the Copernicus Marine Environment Monitoring Service. The position of the wreck is marked by a green star.

Sea state modelling: the specificities of the French Guiana coast

The SEAGUY project, led by Météo-France's DIRAG and funded by the DEAL of French Guiana, aims at taking into account the specificities of French Guiana for a better estimate of coastal hazard and an improvement of high surf watches and warnings. French Guiana's coastline is characterized by complex hydrodynamics and a fast-varying morphology. Mudflats colonized in their supratidal part by mangroves are being strongly eroded by wave action and coastal currents, leading to significant mobility of sedimentary deposits.

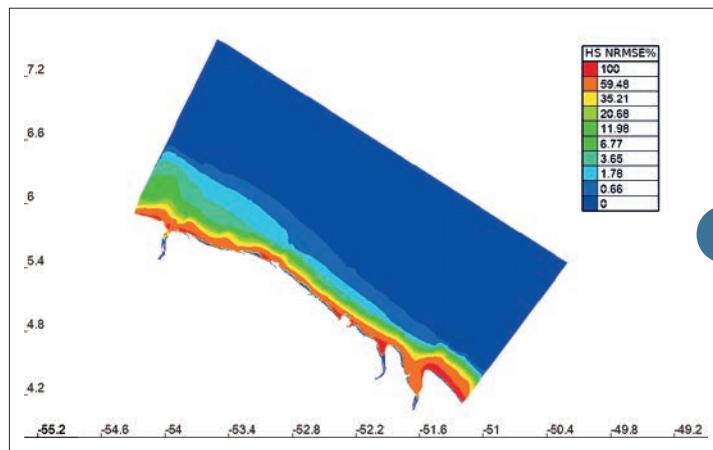
During SEAGUY's phase 1, the modelling strategy was based on Météo-France's operational chain comprising an offshore sea state model (MFWAM) used to force an unstructured coastal domain (WAVEWATCH III). Wave climatology has been obtained to estimate the return periods of extreme events. The impact of ocean currents (provided by MERCATOR) such as the North Brazil Current has been found to be important for the

prediction of sea states along French Guiana's coastline.

In a second phase, studies were carried out on the impacts of mud-bank location and dissipation by bottom friction. Results show that a two-year old bathymetry results in a significant wave height error of up to 1.5m at the coast. Mud-bank migration modifies the distribution of wave energy at the coast through changes in reflection, refraction, diffraction and dissipation by wave breaking, or through friction.

To improve the quality of wave forecasting along the Guyanese coastline, it would be useful to revise the method and frequency of bathymetric surveys (through satellites or video imaging) and / or to couple a morphological model to the wave model, as well as to explicitly consider river outflows.

2



2

▲ Normalized root mean square error of significant wave height for a 2013 hindcast, carried out with uniform sediment of diameter 200µm (medium sand) instead of heterogeneous sediment from Shom data.



3

◀ Barotropic modelled current around Mayotte (that is the vertically averaged current). The isolines represent the strength of current, as does the length of the arrows.

Sea surface height modelling for the lagoon of Mayotte

As part of the HOMONIM project, managed by Météo-France and Shom, with the support of DGPR and DGSCGC, an improved version of the Hycom2D hydrodynamic surge prediction model was installed during the year 2019, covering the southwestern part of the tropical Indian Ocean.

This version involves a down-scale process, enhancing the resolution to 200 metres in the lagoon of Mayotte, and 800 metres around the island « La Réunion ». It allows to reproduce more accurately the tide, especially around Mayotte, where the lagoon and its passes are better represented.

Thus, we can see on the joined illustration the very detailed current field, occurring during a rising tide period around Mayotte. We can notice that the north-east flow is very intense, especially at the big North pass, the Eastern passes and also along the deeper part of the reef in these both exposed areas. The important channelling effect of the incoming flow through the wide and deep North pass is also to be noticed, which then gradually dilutes downstream.

Furthermore, the sea surface wind stress uses in this version of the model a scheme which proved to be the most efficient during hindcast simulations of the Irma hurricane, which crossed in September 2017 the West Indies (generating a two-metre observed storm surge).

Lastly, the sea surface level and current fields around Mayotte which are modelled by this new version, will be used, in the year 2020, to force the wave model, to better simulate sea states in the lagoon of Mayotte.

These changes in surge and wave modelling will permit the forthcoming implementation of an early warnings system for waves and storm surges on the island « La Réunion », to be then extended to Mayotte.

3

Assimilation of new data in the wave models

The availability of observations on the directional properties of ocean waves represents a crucial stake for the improvement of the operational forecast of sea state. In addition, the analysis of the wave climate in coastal areas requires accurate information on the direction of the dominant wave trains. The CFOSAT mission through its SWIM wave scatterometer provides wave spectra describing the energy and direction of the different wave trains with a wavelength validity varying from 70 to 500 meters. The operational chain of the MFWAM wave model has been using the assimilation of these directional observations since 2018, in this case the wave spectra were provided by the Copernicus satellite Sentinel-1 through its synthetic aperture radar (SAR). In the Calibration/Validation phase of the CFOSAT mission, assimilation tests for wave spectra provided by SWIM were developed in order to assess the quality of these data and their impact on operational forecasting of ocean waves around the globe. The latest level 2 data processing developed by CNES provides better quality of SWIM wave spectra with a significant reduction in the speckle noise observed previously (Hauser et al. 2020). The results of the assimilation of these upgraded SWIM spectra show a significant impact on the integrated wave parameters such as the significant wave height and the mean and peak wave periods.

As the SWIM instrument detects increasingly short waves (70 m wavelength), we note the efficiency of assimilation on rapid wave growth in limited fetch (distance of wind action) conditions. We show a remarkable example of a Mediterranean sea event with waves generated by the Mistral and the Tramontane wind regimes. The figure shows the analysis increment induced by assimilation over the mean wave period. There is clearly a very spread impact which can reach 1.5 sec, at the peak of the event. The impact is propagated to the west coasts of Corsica and Sardinia, and reaches the north-east coast of Algeria. This finding opens a promising use of SWIM wave spectra to better understanding the wave physics implemented in models.

4

Improvement of sea surface temperature analyses on European seas at a resolution of 2 km with the DINEOF method using satellite data

Sea surface temperature (SST) plays an important role in ocean-atmosphere exchanges (initialization of Mediterranean convective phenomena, cyclones). Its assimilation at high resolution will lead to improvements in all areas of modelling.

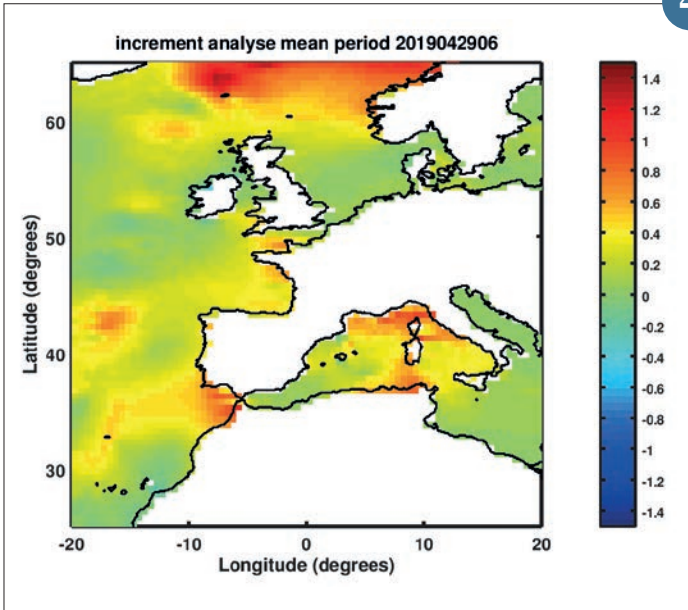
SST is computed using observations from multiple infrared (IR) and microwave (MW) sensors (AVHRR, SLSTR, SEVIRI, VIIRS, MODIS AMSR2...) available on meteorological satellites (METOP, MSG, Sentinel3, NOAA20, AQUA, TERRA, GCOM_W). Despite the good global spatial and temporal satellite coverage, IR sensors are blocked in the presence of clouds and unreliable in the presence of aerosols. MW sensors, insensitive to clouds, are rare and have a very low resolution.

In order to model meteorological and oceanographic phenomena, it is necessary to evaluate SST at all points regardless of clouds. Historically, optimal interpolations are used where the SST of the previous day is assumed; these prove problematic at high resolution, especially when local clouds persist for several days.

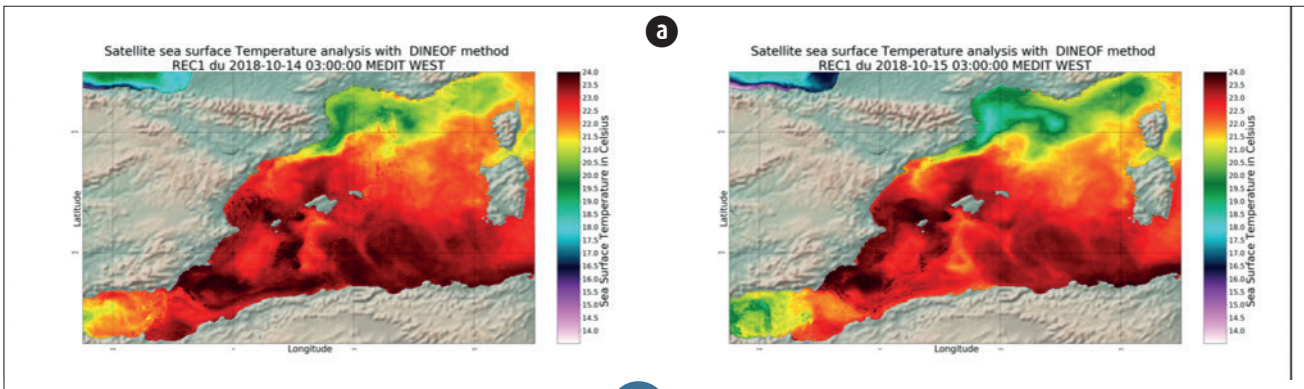
The DINEOF method developed by the University of Liège GHER is used to fill in missing data and has been installed and adapted by CNRM/CEM3 on daily multi satellite L3S data over European seas produced at CEM3 (as part of Copernicus Marine Project) and on experimental trihourly L3S products implemented by CEM3. It is based on empirical orthogonal functions EOF (singular values, cross validation, sophisticated, efficient and robust statistical filters). The obtained and validated daily and trihourly analyses are of much higher quality than an optimal interpolation. They are consistent in assessing the diurnal cycle that is difficult to evaluate (scarcity of buoys). A study of the diurnal cycle in European seas using DINEOF on high frequency SST data from SEVIRI will be carried out.

5

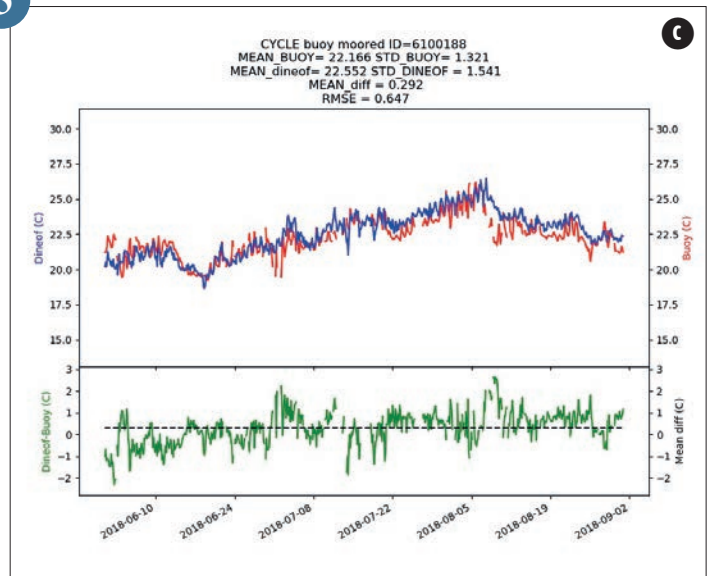
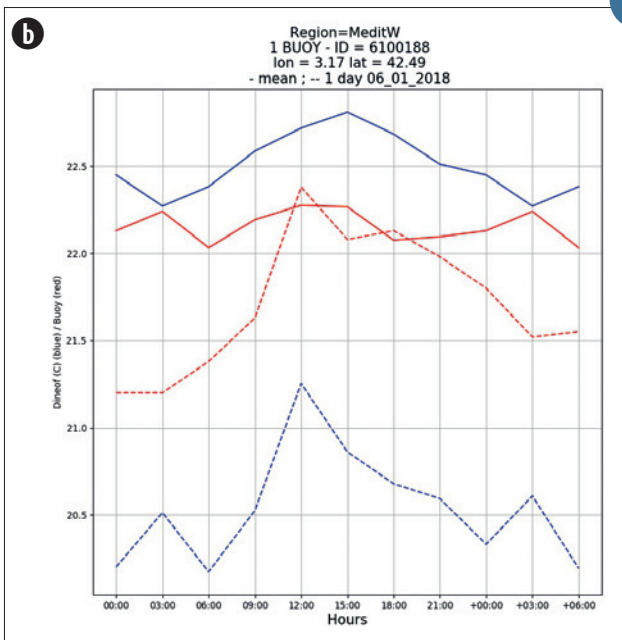
4



Increment of analysis on mean wave period induced by the assimilation of wave spectra and significant wave heights provided by CFOSAT mission during a Mediterranean storm event on 29 April 2019, at 6:00 (UTC).



5



(a) Example of trihourly sea surface temperature satellite analysis using the DINEOF method over the western Mediterranean at a resolution of 2 km. Corresponds to the Mediterranean event of October 15 at 3 a.m. Left on October 14, 2018 at 3 a.m., right on October 15, 2018 at 3 a.m. where we can see the pumping of energy that fed the stationary convection process in the Aude.

(b) Diurnal cycle of a moored buoy (red dotted line) and diurnal cycle of the Dineof analysis (blue dotted line) on June 1 2018. Average diurnal cycle from June 1, 2018 to September 1, 2018 of a moored buoy (red solid line) and Dineof diurnal cycle (blue solid line).

(c) Diurnal cycle of a moored buoy from June 1, 2018 to September 1, 2018 compared to the Dineof analysis cycle (in blue). Difference between Dineof analysis and this moored buoy over this period of 2018 (in green).

Engineering, campaigns and observation products

Observation plays a crucial role in earth sciences. They provide a better understanding of how systems work, evaluate and improve the ability of numerical models to simulate reality, and better define the state of the atmosphere at a given moment, for climatological purposes, to detect particular events, or to initialize numerical forecasts. The contribution of space observation continues to grow with the measurement of wind over the entire globe and the entire depth of the atmosphere, now accessible with the AEOLUS space lidar. The transport of dusts thousands of kilometers away from their source regions is better characterized thanks to geostationary satellites. However, observation from space cannot reach the spatial or temporal resolutions required to characterize the rapid and fine-scale phenomena that are supposed to be represented by numerical models whose resolution is now kilometeric or even hectometric. Solutions are being explored to use opportunity data measured by sensors embedded on connected objects, such as private weather stations, telephones, or cars, or, in a more original way, on animals such as sea turtles. Data processing techniques are developed to produce estimates of the value of meteorological parameters between stations in an observation network, or, using artificial intelligence techniques, parameters not directly observed such as the height of the boundary layer. The development of services that meet unmet or new needs involves the development of models whose quality must be validated on sets of observations, as was the case for forecasting the risk of icing or snow accumulation on overhead power cables.

Observation engineering and products

Suspended dust detection from geostationary meteorological satellite data

The CNRM / CEMS cloud team is developing data processing software for geostationary meteorological satellites (SAFNWC-GEO) permitting the detection of the presence of suspended dust in the troposphere (and thus volcanic dust). The latest version of the software allows the processing of several geostationary satellites such as MSG, Himawari and GOES, providing a global observation of suspended dust (see Figure 1). Detection of dust is performed according to three different algorithms depending on the conditions: day on sea, day on land and night on sea. Currently, there is no detection at night on land.

By day, the suspended dust is detected thanks to the infrared (IR) and visible channels. The detection methods are based on the spatial homogeneity of the visible reflectance and on the fact that in the presence of suspended dusts, the absorption in some channels is greater than in others (ex: IR at $\lambda = 10.8 \mu\text{m}$ and $\lambda = 12 \mu\text{m}$).

By night over sea, the method consists in the use of a thermal test and the Sahara Dust Index (SDI; supplied by ocean team of CNRM / CEMS – SAFOSI). The SDI is based on the differences between radiances measured at $\lambda = 10.8 \mu\text{m}$ and $\lambda = 12 \mu\text{m}$ and the differences between radiances measured at $\lambda = 3.8 \mu\text{m}$ and $\lambda = 8.7 \mu\text{m}$. In general, the thresholds to distinguish between suspended dust and clouds or surfaces are estimated empirically for each satellite with clearly identified suspended dust situations.

Detection of suspended dust with geostationary meteorological satellite data is validated using observations from the lidar (CALIOP) on board the CALIPSO satellite. These two types of data observations are spatially and temporally co-located in the latitude zone from 15° South to 45° North. Lidar provides vertical profiles of the backscattering of atmospheric particles and thus permits the detection of layers of smoke, dust and aerosols (also pollution) as well as clouds of low optical depth. Lidar can observe dust layers with small optical thickness (< 0.25). Since the distinction of suspended dust using geostationary satellites is based mainly on reflectances and thermal contrasts, this method fails for low optical thicknesses where the thermal contrasts are not high enough. Consequently, suspended dust layers with optical thicknesses of less than 0.3 are not considered for validation.

Above sea surfaces, 47% of suspended dust are detected with geostationary satellites during the day against 31% at night when compared to observations from CALIOP lidar. However, only 5% of the events observed by CALIOP lidar are detected with geostationary satellites over continental surfaces in daytime. The number of false alarms is very low for all three algorithms.

Methodologies used to detect suspended dust have been improved in preparation for MTG. Above continental surfaces, by day, detection at the beginning and the end of the day has been improved with the addition of a

threshold depending on the solar angle. On continental surfaces by night, it is difficult to rely solely on the differences in radiances between channels to define this algorithm. Thus, simulations of brightness temperatures with radiative transfer model RTTOV over clear sky have been added to the methodology. This new version of the dust mask will be available in the SAFNWC-GEO software version delivered for MTG during 2022.

1

Automatic detection of boundary layer top with supervised and unsupervised classification

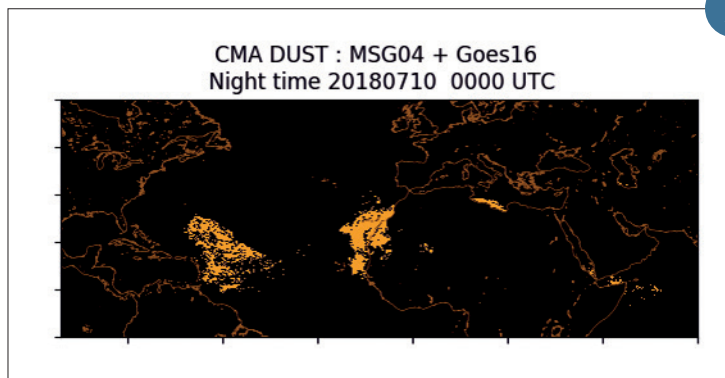
The atmospheric boundary layer height (BLH) is a key parameter in several meteorological applications such as air quality forecasts. A common method to measure BLH is via aerosol lidar, where a strong decrease in the backscatter signal indicates the top of the boundary layer. Two machine learning methods have been tested to derive the BLH from backscatter profiles, the K-means algorithm and the AdaBoost algorithm. The K-means for Atmospheric Boundary Layer (KABL) and AdaBoost for Atmospheric Boundary Layer (ADABL) algorithm codes are open source and under a free licence. In

both cases, the measurement points of the lidar are cast into classes. The HCL is then attributed as the top of the 'boundary layer' class (figure). Both methods are compared to the lidar manufacturer's algorithm and to reference BLHs derived from colocated radiosonde data. The radiosonde data were used as the reference for all methods. A comparison was carried for a two-year period (2017-2018) for two Météo-France operational network sites (Trappes and Brest). A large discrepancy in the results was observed between the two sites. At the Trappes site, KABL and ADABL outperformed

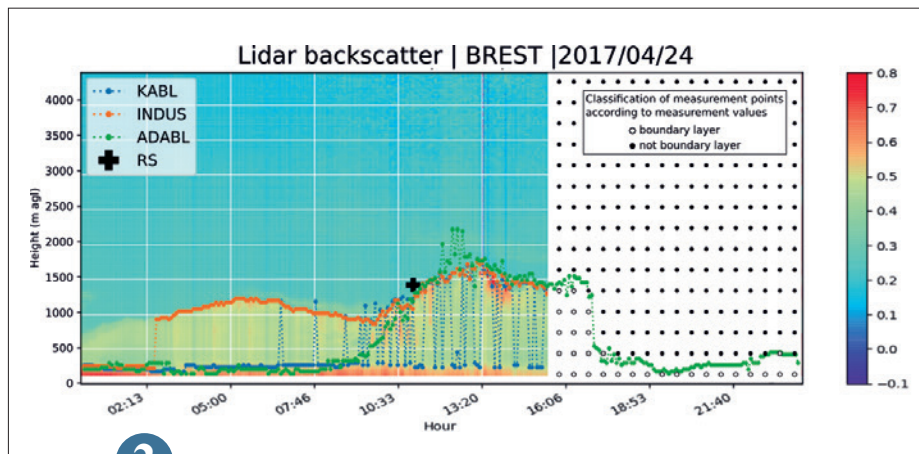
the manufacturer's algorithm, while the performance was clearly reversed at the Brest site. We conclude that ADABL is a promising algorithm but has training issues that need to be resolved, KABL has a lower performance than ADABL but is much more versatile, and the manufacturer algorithm is performing well with little tuning but is not open-source.

2

1



The suspended dusts appear yellow. Observations of MSG4 and GOES 16 at night for the 00h slot with the new algorithm developed for MTG.



2

Example of boundary layer height detection by three algorithms: KABL (blue), ADABL (green) and manufacturer (orange). In background, the shade of color is the backscatter measurement from the lidar (up to 16:00); then (after 16:00) an illustration of the measurement point classification (white for boundary layer, black else). The boundary layer top line follows the border between black and white.

New infra-hourly frequency analyses of basic parameters (temperature, humidity, wind, sea level pressure)

To have a real-time and spatialized analysis providing the observed value at the station point, new basic parameter analyses have been developed: the temperature and humidity at different levels (2, 20, 50, 100 and 250m), the meridian and zonal wind, and the sea level pressure. Initially, these analyses were performed on hourly basis, by correcting the most recent prevision of the model by the observations. The frequency of production is now of 15 minutes and the correction principle remains the same for H.15 analysis. At H.15, the analysis of AROME-PI model of H.00 is used. Before any computation, the observations are controlled by screening

those that are too different from the model. Temperature and humidity at 2m are mapped using a multivariate regression with elevation and model field. The regression residuals are then spatialized by kriging. The final analysis is the sum of spatialized residuals and initial model field. For higher levels, the correction done at 2m is passed on model field by weighting with an exponential factor which decreases with height. For sea level pressure and wind, the difference between observations and model is spatialized using inverse distance weighting (sea level pressure) and ordinary kriging (wind).

In the sea, due to the lack of observations, spatialization cannot be achieved: the raw model field is not modified. For the following quarter hours, the adopted methods for spatialization are the same but the model field is replaced by the previous spatialized analysis.

3

Contribution of personal weather stations to the observation of deep-convection features near the ground

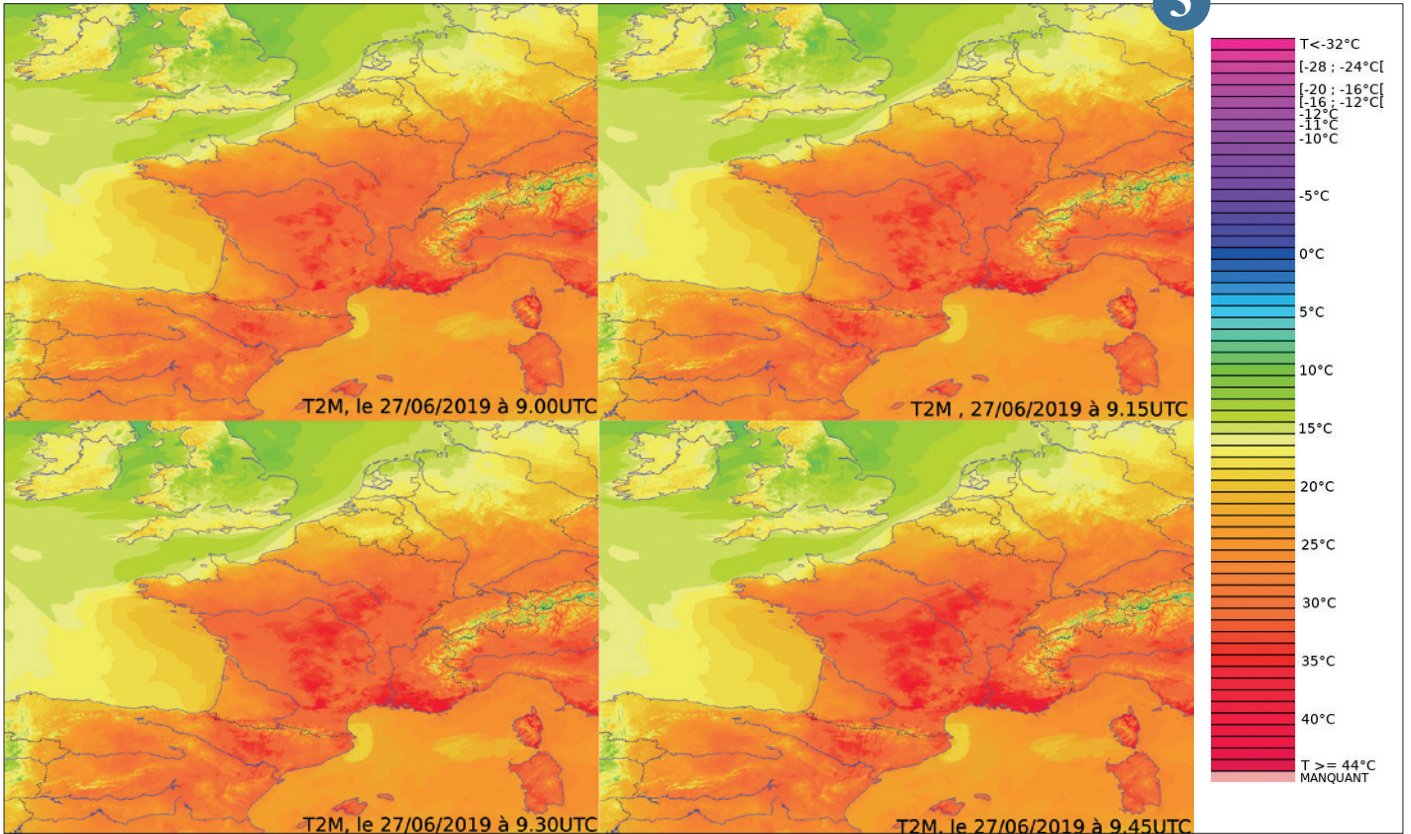
Numerous networks of objects connected to the Internet and equipped with meteorological sensors now observe in real time the first few metres of the atmosphere at high spatial and temporal resolution. The contribution of observations from a network of personal weather stations in addition to observations from the operational network of Météo-France has been evaluated for the characterization of phenomena related to deep convection near the surface. These personal observations, which do not meet the standards set by the WMO, are of variable quality and required the design of an automatic quality control system based on the Météo-France observation

network. Evaluation of the method applied to temperature, relative humidity and mean sea level pressure during four stormy days in 2018 shows that this method improves the quality of personal observations while maintaining a large number of them. Analyses combining personal and Météo-France observations were compared to analyses using only Météo-France observations. Cross validations show that the combined analyses are the closest to the reference observations. In addition, small-scale meteorological variations previously invisible with the Météo-France network alone were detected (see figure).

The use of personal weather stations therefore improves the near-surface observation of phenomena associated with thunderstorms. These results pave the way for the use of these observations to evaluate on a finer scale the numerical simulations of phenomena related to deep convection.

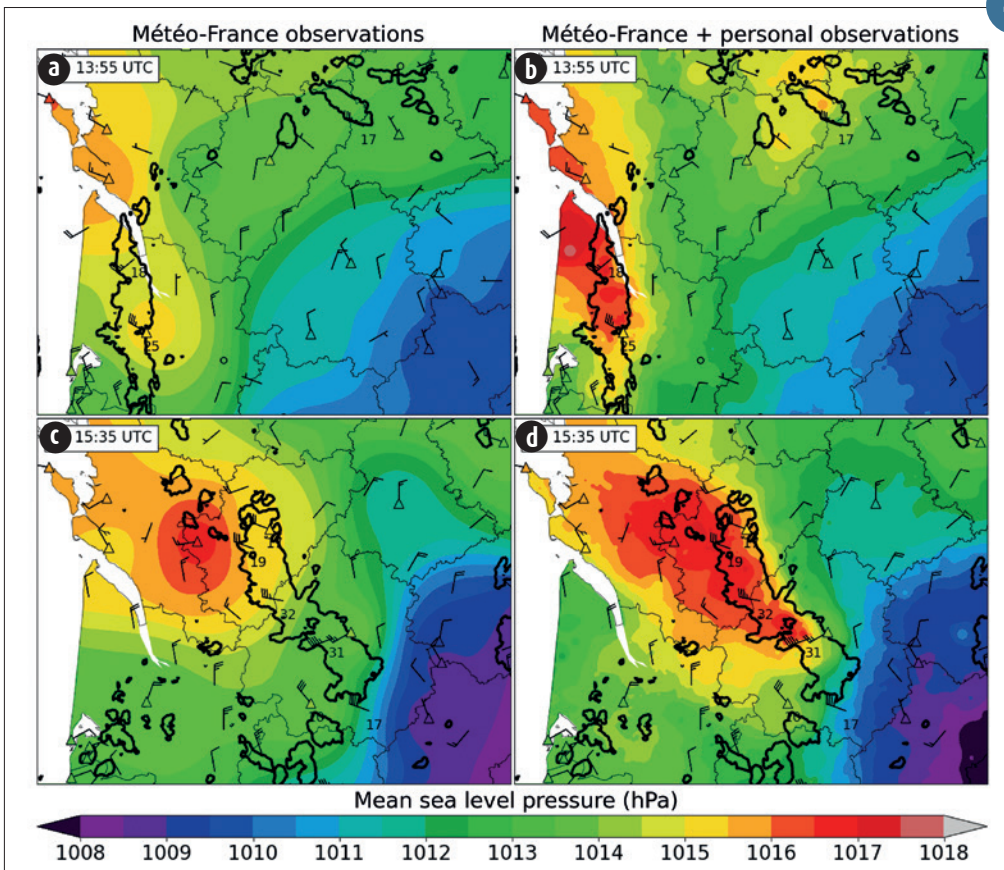
4

3



Example of temperature field at 2m: from 9.00UTC to 9.45UTC, 27 June 2019.

4



Mean sea level pressure analyses built with (a,c) only Météo-France observations and (b,d) combining Météo-France and personal observations on 4 July 2018 at (a,b) 13:55 UTC and (c,d) 15:35 UTC. Radar reflectivities over 40 dBZ indicating the location of thunderstorm convective cores are illustrated with bold black contours. Météo-France mean sea level pressure observations are shown by coloured triangles with black contours. The instantaneous wind gust is shown with bars, and the highest gust during the last 10 min over 17 m s⁻¹ is annotated nearby.

Campaigns

The spaceborne Doppler lidar AEOLUS improves weather forecasts

The AEOLUS satellite of the European Space Agency was launched on August 22, 2018 after a long development period. The flight acceptance phase was completed at the end of January 2019. The exploitation phase then started. The CNRM/GMEI is responsible for maintaining and improving the calibration processor and the Level 2 processor aimed at retrieving the optical properties of aerosols and clouds. The CNRM/GMAP is conducting studies on the impact of wind measurements on global weather forecasting with ARPEGE. This activity benefits from financial support from CNES.

The first monitoring and impact results were presented in September 2019 at an international workshop organized by ESA, which was attended by many meteorological centers making numerical global forecasts (European Center, United Kingdom, Germany, Canada, United States). The results, obtained by these centers, converge: the impact of AEOLUS wind measurements is neutral in the Northern hemisphere where many wind measurements are already available, and significantly positive in the Tropics and in the Southern hemisphere, while these new observations represent only 0.2% of the assimilated data. Work continues to improve the calibration of the instrument, to reduce measurement bias and to increase the positive impact on forecasts. Measurements of the optical properties of clouds and aerosols, the quality of which is more difficult to assess, are also the subject of intense improvement work with a view to their assimilation into air quality models.

The nominal lifetime of the mission will end at the end of 2021. An extension of one to two years is possible. Discussions have started between EUMETSAT and ESA to design a future similar space mission that should be less costly and last longer.

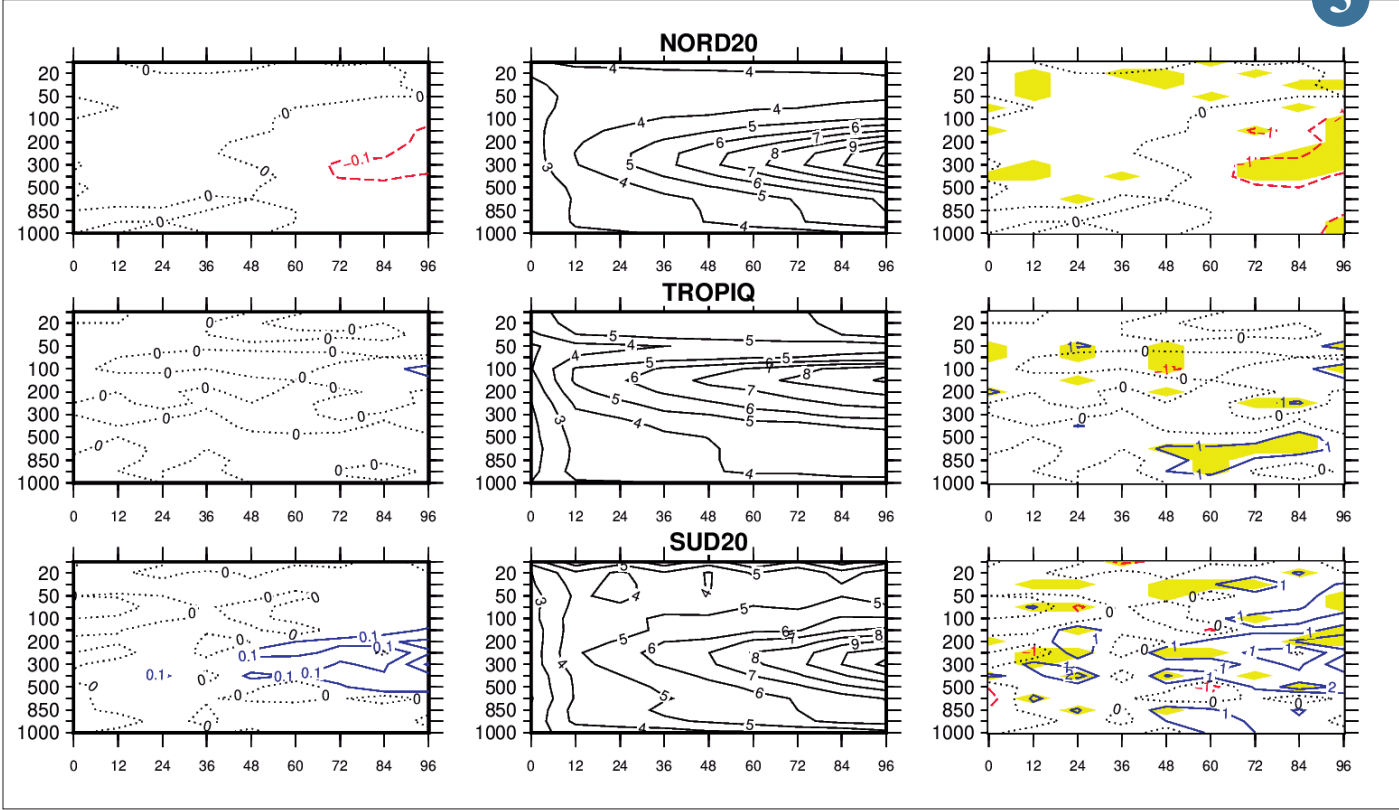
5

First analysis of data collected during the Sea Turtles for Ocean Research and Monitoring (STORM) project

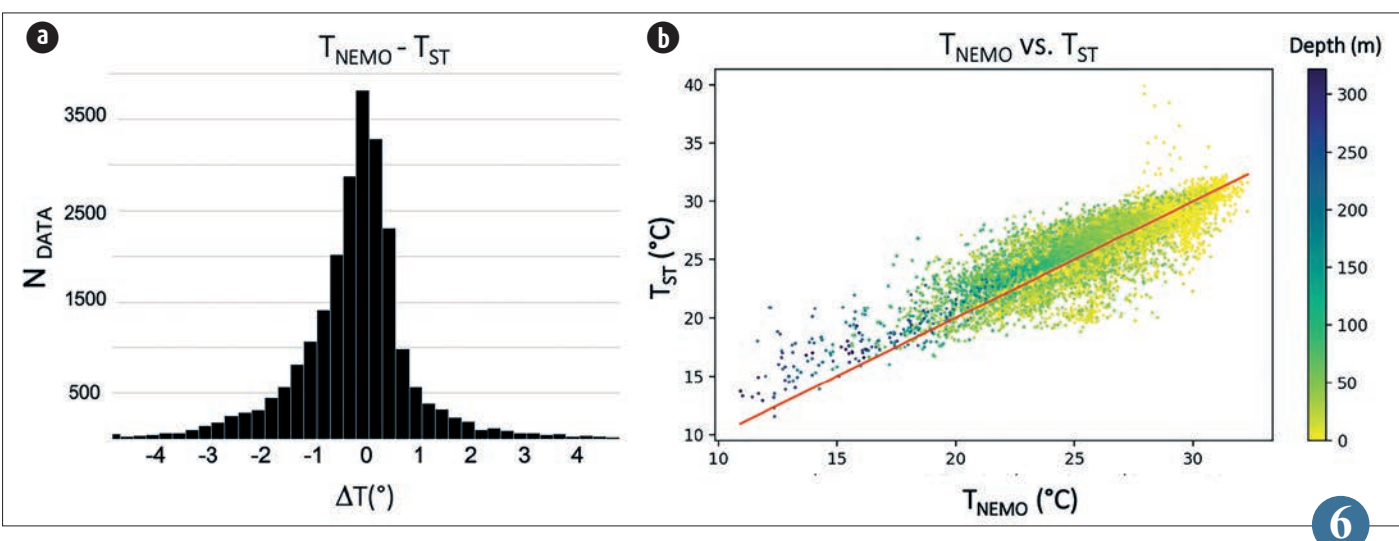
STORM (Sea Turtles for Ocean Research and Monitoring) is a research program aiming at studying the thermodynamic properties of the tropical Indian Ocean at high space-time resolution using sea turtles equipped with environmental sensors. Analysis of the data collected during the first phase of the programme (Jan 2019 - April 2020; 11 turtles and nearly 120,000 triplets of position/depth/temperature data) has demonstrated the value of such an approach, both in the fields of climatology and observation and numerical modelling of the tropical oceans. Comparison of surface and in-depth temperature measurements collected by sea turtles against conventional in-situ (Argo) and satellite (OSTIA, OSI-SAF) observations shows excellent agreement, with a mean bias (standard deviation) of about 0.1° (0.5°). Comparisons against Mercator Ocean operational model Glo12 (Figure 1) also demonstrate the value of

such observations for evaluating and, in the long term, improving ocean forecasts in this region, which is severely under-equipped with conventional ocean sensors. During the next phase of the programme, which will start in November 2020 for 2 years, nearly 80 turtles will be released all over the Indian Ocean (Seychelles, Mozambique, Comoros, Reunion, Madagascar, Tromelin) in collaboration with 7 marine reservations in the region. Collected measurements will notably be assimilated in the Glo12 and NEMO-Indian Ocean models in order to assess the impact of these new measurements on tropical cyclone forecasting.

6



▲ Relative impact on the ARPEGE model forecast of AEOLUS wind measurements in the Northern Hemisphere (top line), the Tropics (middle line) and the Southern Hemisphere (bottom line). This impact was calculated over a one-month period between mid-September and mid-October 2018. For each region, the left column is the variation of the root mean square of the wind forecast error measured with respect to the radiosondes, from 0 to 96 h (abscissa) and as a function of the pressure level (ordinate) with respect to a reference experiment without AEOLUS assimilation. The middle column is the root mean square of the wind forecast, and the right column is the ratio between the left column and the middle column (in percentage). The contour lines in blue mark a reduction in forecast error, those in red a degradation. The yellow background indicates areas where the statistics are considered significant.



▲ Histogram (left panel) and scatterplot (right panel) of differences between temperature data collected by sea turtles (TST) and forecasted by Glo12 (TNEMO) between January 2019 - March 2020 in the West tropical Indian Ocean (20°S-15°N; 40-60°E). Colours in (b) indicate the depth of collected ST measurements / model forecasts between 0 and 320m (colour scale to the right). Adapted from Bousquet et al. (2020; Frontiers in Marine Science).

An experimental campaign for observation of ice and snow accretion on transmission overhead wires

Since 2016, a R&D project has been conducted in Météo-France to improve the anticipation of meteorological risks impacting transmission overhead wires. A forecasting system to simulate snow and ice accretion on overhead wires has been developed. This system, called WIRE (Winter Risks for Energy), consists in using the ensemble forecasts of the AROME model to force snow and ice accretion diagnostic model and thus to elaborate a probabilistic forecast of accretion risk. In order to evaluate the capacity of WIRE to simulate accretion and to improve it, a dedicated experimental campaign was set up in November 2018 on one of the experimental

mountainous sites of the Snow Research Centre of Météo-France located at Col de Porte (1325m, Chartreuse massif). Observations from the first 2018-2019 winter campaign were compared to the results of WIRE model simulations forced by the analyses of the AROME model.

This first experimental winter has shown that the model was able to simulate the majority of accretion events of snow and ice on experimental wires (RTE and ENEDIS wires). In order to go further in the analysis, the measurement campaign was extended to this 2019-2020 winter with an improvement of the experimental set-up (carried out in October 2019).

While a SNCF wire was also added, an additional webcam was implemented. Its resolution is finer and consequently the snow sleeves and more particularly ice sleeves which often have a low thickness will be better documented. This campaign analysis should allow the improvement of the model as well as the evaluation of the forecasting system, which is an essential phase to consider an operational use of this system.

7



(a) Experimental site dedicated to observation of snow and ice accretion events on transmission overhead wires (RTE and ENEDIS electricity transportation wires, SNCF catenary) located at Col de Porte.



(b) Example of a wet snow accretion event (2019, February 1st).

GIRAFE 2 AIRGRAVI observation campaign (measurement of the gravimetric field)

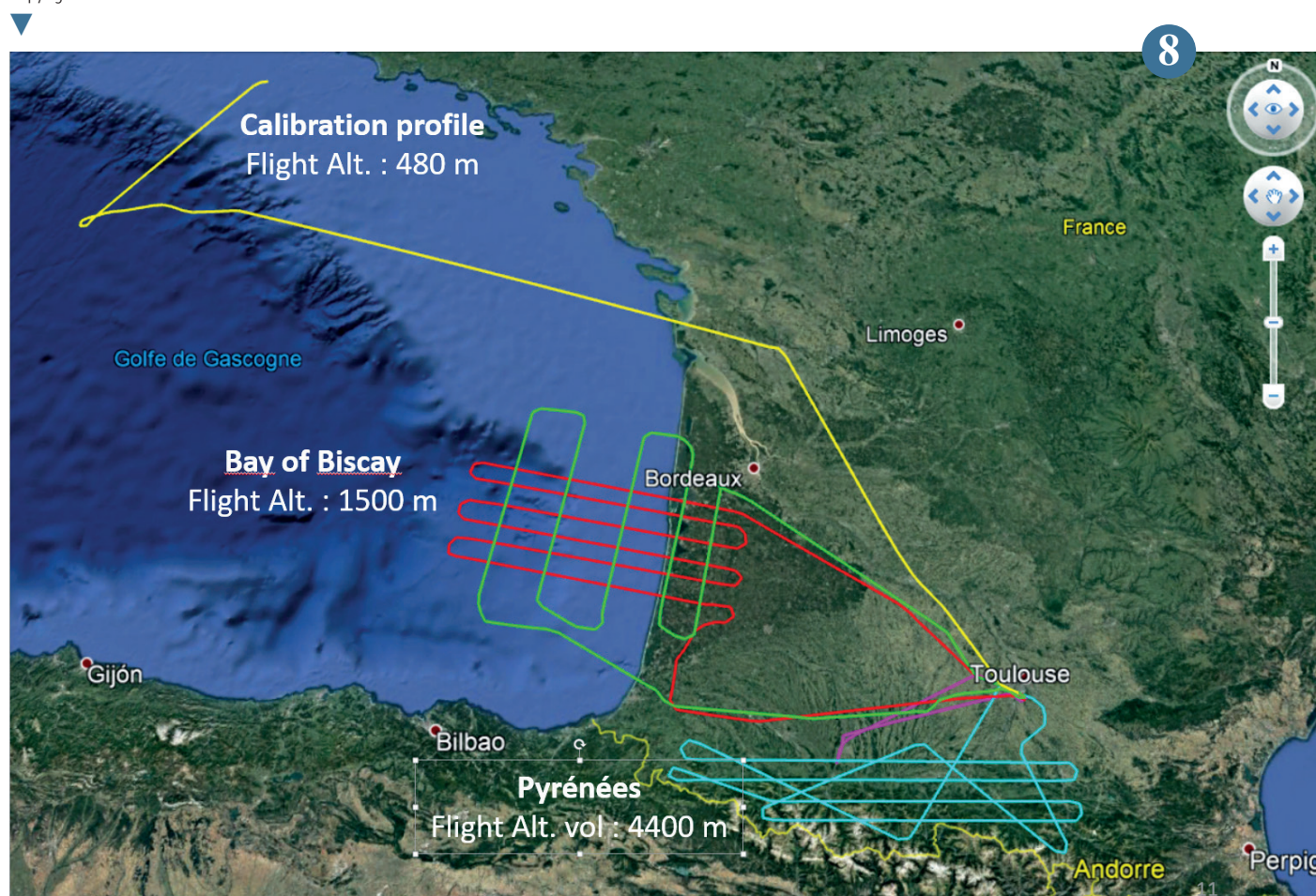
The GIRAFE 2 AIRGRAVI campaign, supported by CNES, seeks to evaluate the potential of an airborne interferometric gravimeter for geodesy, geophysics and oceanography. The new sensor "Gravimètre Interférométrique de Recherche à Atomes Froides Embarqués" (GIRAFE-2), based on an innovative atomic interferometry technology and developed by ONERA, has been designed to carry out absolute gravimetric measurements from a mobile platform. The originality of such an instrument, unique in the world, is to enable the acquisition of absolute measurements in dynamic mode and on regional scales, making it possible to offer a new range of absolute observations on the surface of the globe, particularly in areas that are little or not accessible by current means (mountainous areas or areas with no access roads, shallow coastal areas, etc.), while gaining in accuracy and limiting survey costs.

The ATR 42 operated by the French Instrumental Aircraft Service for Environmental Research SAFIRE (Research Infrastructure CNRS/ Météo-France/CNES) carried the GIRAFE 2 instrument, in addition to other instruments for measuring the relative gravitational field. Based out of Toulouse-Franczal, the ATR 42 thus carried out more than 20 hours of flights in the spring of 2019 to carry out gravimetric surveys in various areas, notably in the Bay of Biscay and over the Pyrenees. Thanks to the expertise of staff from the Geosciences Environnement Toulouse (GET) laboratory, ONERA, SHOM, and also Danish partners (DTU-Space), a large amount of airborne data was collected, supplemented by ground data. The expected outcomes of this project are to strengthen the synergy between instrument designers and potential users to promote the development of devices that respond to scientific issues and to ensure the transfer of

these innovative instruments to the scientific community. The scientific applications of this instrument are potentially of interest to many fields of applications relating to the observation of the Earth, continental surfaces and oceans: geodesy (gravity field, geoid); geology-geophysics (structure of continental margins, mountain ranges or sedimentary basins, inventory of subsoil resources, assessment of natural risks, etc.); oceanography (ocean circulation); but also any future Cal/Val operation for future space gravity/altimetry missions.

8

Trajectories of the instrumented ATR 42 for evaluation of the GIRAFE sensor: an oceanic zone and land-sea transition zone (Bay of Biscay / Landes), a mountainous zone (Pyrenees) and a calibration profile over a reference zone (oceanic slope off Brest).
Copyright: GET-ONERA-SHOM-DTU



Research and aeronautics

In the frame of the SESAR Deployment program, which Météo-France has been highly involved in, collaboration with partnering European meteorological services intensified. Activities towards a routine operational production of harmonized data over a large Europe of observation and forecast of convection, icing and turbulence resulted in production processes being ready for implementation. In parallel, a prototype version for the future SWIM compliant meteorological information exchange system was designed and made available for first tests and trials to be conducted in collaboration with some aviation users.

In 2019 main research activities on hazardous weather impacting aviation operations dealt with short term seamless forecast of precipitations over the 0-3h time frame aiming at better anticipating heavy convective rain over this strategic time slot for air traffic management; with global turbulence forecast enhancement based on a combination of several diagnosis allowing to discriminate turbulence sources; and with high altitude ice crystals detection based on satellite imagery. Météo-France research teams also considered how to assimilate data from remote sensing equipment on board satellite and from Lidar for aerosols in order to improve the numerical analysis of the initial state of volcanic ash clouds, and so, to improve the ash movement and dispersion forecast.

In addition, 2019 was the final stage of the air phase of project TERRISCOPE aiming at the development of a platform for research in airborne remote sensing. A success in aviation serving research in meteorology.

1

Forecasting the dispersion of ash from the Eyjafjallajökull in 2010: benefits of data assimilation

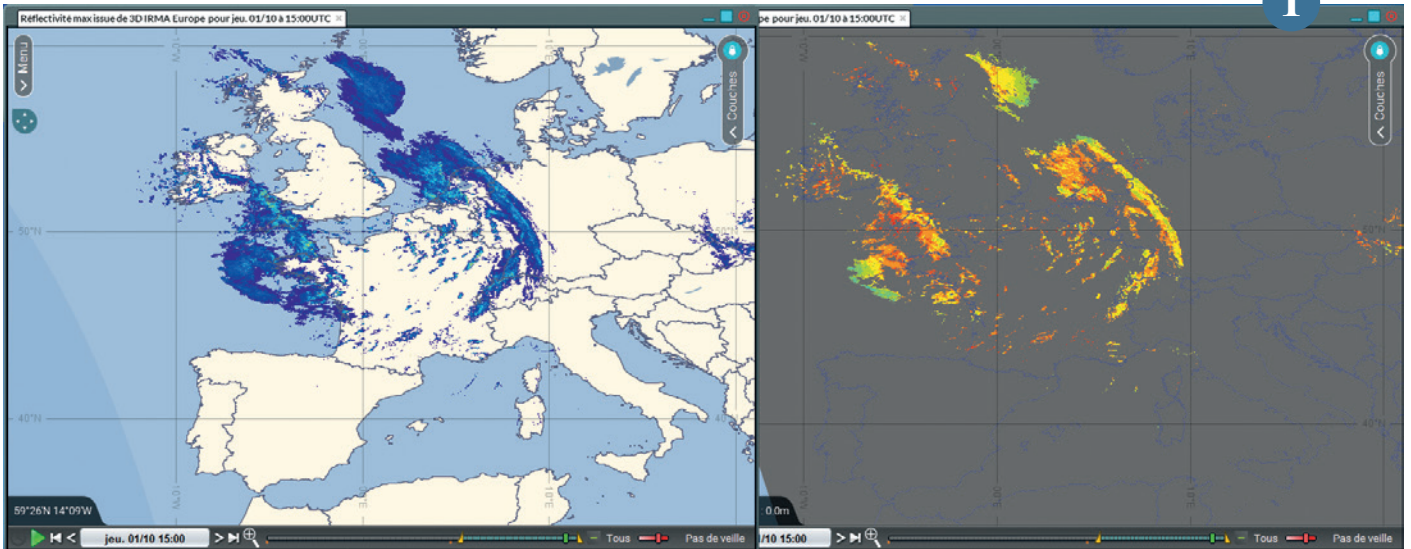
By dispersing ashes over the Atlantic and Europe in April and May 2010, the eruption of the Eyjafjallajökull had a huge impact on air traffic. Following this disaster, it was recognized that better estimates of ash dispersion in the atmosphere were needed to make flight decisions. Since then, Météo-France, in collaboration with research laboratories in Europe, has improved the representation of volcanic emissions in MOCAGE and developed data assimilation. The FPLUME emission module has been implemented in MOCAGE. Unlike the existing

empirical emission law (Mastins, 2009), FPLUME models the physical mechanisms in the emission plume, and therefore proposes more realistic predictions of the mass and vertical distribution of the plume. The resulting maps out of MOCAGE (Figure) with FPLUME show a less spread plume and closer to the plume observed by MSG. The assimilation of MODIS satellite data further improves the horizontal distribution of the plume. On this case study, when the plume arrives in Northern Europe, we were able to show that the assimilation of the data from

two ground-based lidars allows a better vertical representation of ash concentrations. By developing these tools and evaluating them on this major eruption, we get prepared to have the best possible dispersion tools in case of an eruption of equivalent magnitude in the future, in particular by assimilating the data from Météo-France lidars in MOCAGE.

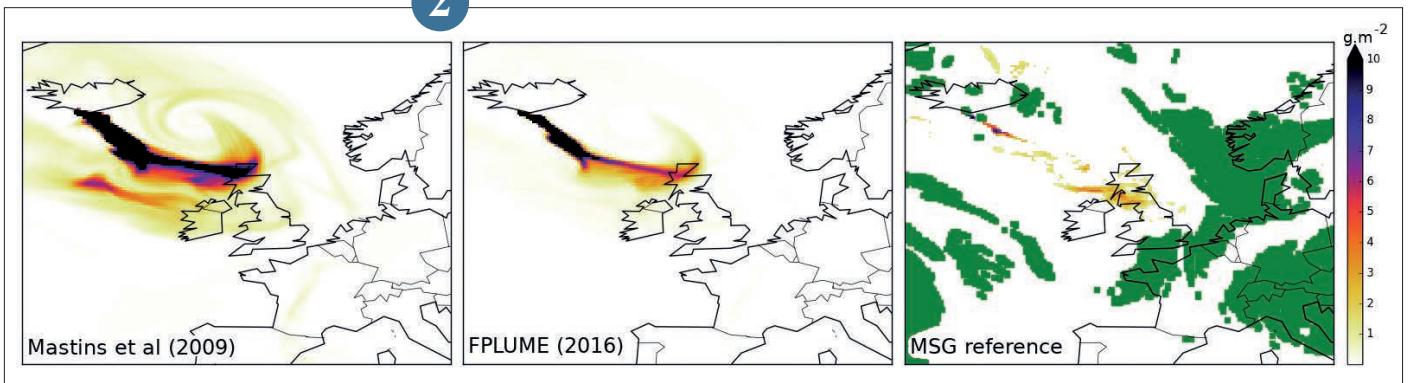
2

1



Very High Resolution Maximum Reflectivity and Echo Top 18dBZ from 3D radar data over Europe - from SESAR Deployment project 2015_067_AF5 for Convection Detection based on 3D Radar mosaic.

2



Total columns of volcanic ash concentrations on May 16, 2010 at 09h UTC, for MOCAGE with Mastins emission (2009) (left), for MOCAGE with FPLUME (middle) and for the reference observed by MSG (right). The green dots on the right figure are points where ash detection by the satellite could not be done (mainly due to the presence of clouds).

TERRISCOPE 2019

A long period of collaboration between Safire (CNRS Research Infrastructure, Météo-France and Cnes) and Onera has just been crowned with success. Indeed, this ambitious "Platform for Research in Airborne Remote Sensing" project has just completed its programme of technical validation flights on Météo-France's ATR42. The TERRISCOPE project, led by Onera, aims to pool very high-tech airborne optical instruments. It is supported by the European Union and the Occitania Region within the framework of ERDF funding, as well as Sofradir, Boreal, M3Systèmes and Leosphere.

From the first week of the flights, the Lidar 3D of Riegl for the first time integrated on a "big plane", the hyperspectral camera FENIX also mounted for the first time on the ATR of SAFIRE and the 2 infrared cameras TELOPS allowed to obtain a sum of data that the teams of Onera of Toulouse exploit from now on. The second week was devoted to the first flight of the Lidar Vent or "LIVE", an instrument using an innovative laser amplifier developed by Onera's Department of Optics and Associated Techniques (DOTA). Here too the results look promising.

A long and meticulous upstream work was necessary not only to prepare the flights and equip the aircraft, but also to obtain the certification of the instruments, most of which were prototypes. The exceptional weather in February contributed to the success of this campaign, which finalises the airborne part of the TERRISCOPE project, but the success of the 13.5 hours of flight accomplished highlights above all the exemplary commitment and coordination of all the participants in this project.

For the future, seven configurations of the ATR are certified and 4 configurations of the Piper Aztec will make it possible to carry out various measurement campaigns with the mutualised instruments of the Onera platform. Thus, the Terriscope platform is a unique means of passive and active airborne remote sensing, making it possible to carry out both scientific research (study of the natural or artificial environment surrounding an anthropogenic activity) and more applied work, particularly in the fields of surveillance, security and defence.

3

A new global turbulence forecast product for aeronautics

Aeronautical turbulence is a major risk for this sector with dozen of millions of dollars for companies, and more than 7000 hours of sick leaves. Turbulence suffered by planes has multiple sources such as CAT which is particularly dangerous because non detectable. Météo-France has developed a new diagnostic of turbulence through a common project between DSM/AERO and DR/CNRM.

This new diagnostic is a combination of predictors following the method developed by NCAR for the GTG product. Each predictor detects different sources of CAT, such as vertical or horizontal wind shear or thermal vertical instability. The choice of the best predictors is made by a learning process using EDR observed by commercial flights over the United States of America. In order to produce a final diagnostic in EDR (OACI recommendation), each predictor computed in numerical model is converted into this unit under the hypothesis that each predictor follows the same law of distribution than the observed EDR.

This new diagnostic has been built on the global numerical model ARPEGE and validated over the first semester of 2019 with objective scores using observed EDR and case studies using reports from pilots. It will be available every 10 Flight Levels with a time step of one hour.

As turbulence causes (jet, convection) are subjected to forecast errors, future works should evaluate the contribution of ensemble forecasts to this diagnostic.

4

Development of a hydrometeors seamless 0-3h forecast

In order to improve the 0-3 hours forecast Météo-France has developed a fusion technique that every 5 minutes calculates the relative weight of radar-based extrapolation fields and high frequency numerical weather model AROME-NWC output. The technique is called PIAF1 and relies on a so-called "sequential aggregation of predictors by exponential weights" method. The resulting linear combination provide the best reflectivity forecast at target forecast ranges. In order to discriminate between the different classes of hydrometeors PIAF-Reflectivity is then combined with wet-bulb temperature profile provided by AROME-NWC when and where extrapolation has the heaviest weight. AROME-NWC hydrometeor output are used if AROME-NWC has the heaviest weight.

This approach, called PIAF-Hydrometeor, allow to provide every 5 minutes a hydrometeor forecast over a large domain including French territory. PIAF-Hydrometeor provides useful information for various sectors, for example airport operations.

Evaluation exhibits good coherency between forecasts and reference (given by HYDRE product that uses dual polarization of radars) for the different type of snow, the drizzle and rainfall. Concerning hail the predictability is reduced (30 minutes).

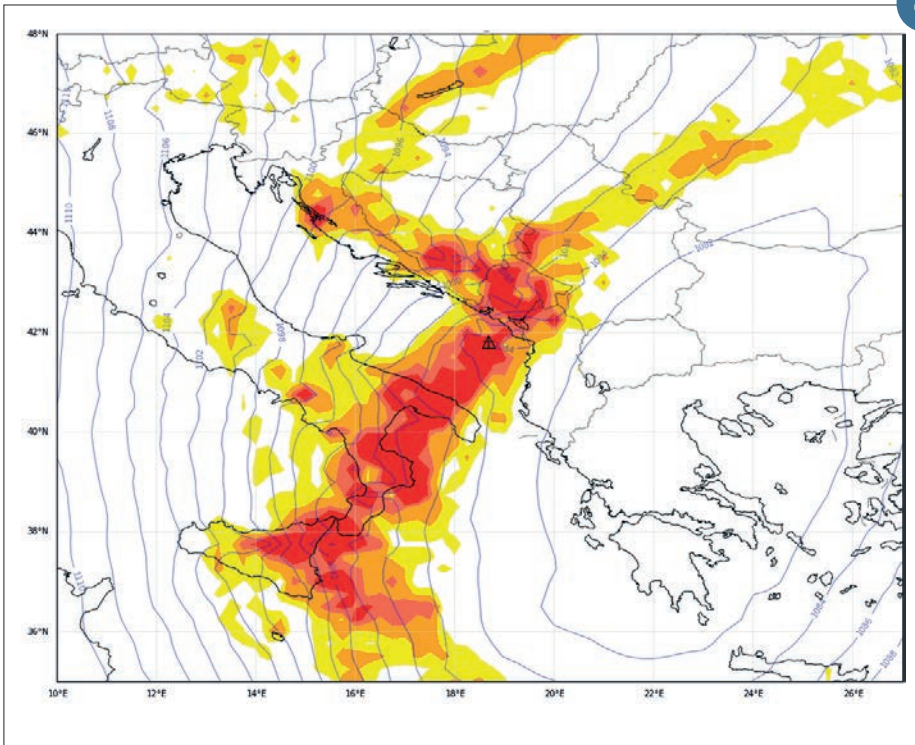
5

3



▲ The Onera DOTA wind lidar team and part of the SAFIRE team at the foot of the ATR42 of Météo-France. Copyright : SAFIRE.

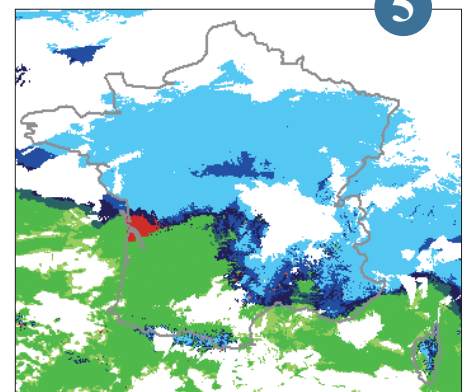
4



PIAF Hydrometeors for 28th February 2018 – 60 minutes forecast for 21:00 UTC. In this example the hydrometeors are drizzle (light green), rainfall (dark green), snow more (dark blue) or less (light blue) wet, freezing rain (red).

▲ EDR diagnostic forecast valid for the 13/02/2019 12h UTC – Maximum for the layer FL370/390 in color shade: red: severe, orange: medium, yellow: light to moderate. Geopotential height in blue lines. Report of severe turbulence indicated with the red triangle.

5



Appendix

2019 Scientific papers list

- Abbatt, J. P., Leaitch, W. R., Aliabadi, A. A., Bertram, A. K., Blanchet, J. P., Boivin-Rioux, A., ... & Chaubey, J. P. (2019). Overview paper: New insights into aerosol and climate in the Arctic. *Atmospheric Chemistry and Physics*, 19(4), 2527-2560.
- Ablain M., L. Zawadzki, R. Jugier, B. Meyssignac, A. Ribes, A. Cazenave, N. Picot (2019) : Uncertainty in Satellite estimate of Global Mean Sea Level changes, trend and acceleration, *Earth System Science Data Discuss*, 1-26.
- Albergel, C., Dutra, E., Bonan, B., Zheng, Y., Munier, S., Balsamo, G., de Rosnay, P., Munoz-Sabater, J. and Calvet, J. C. Monitoring and forecasting the impact of the 2018 summer heatwave on vegetation. *Remote Sensing*, 2019, Vol. 11(5), 520 <https://doi.org/10.3390/rs11050520>
- Ardilouze, C., Batté, L., Decharme, B. and Déqué, M. On the Link between Summer Dry Bias over the U.S. Great Plains and Seasonal Temperature Prediction Skill in a Dynamical Forecast System. *Weather and Forecasting, American Meteorological Society*, 2019, Vol. 34(4), pp. 1161-1172. <https://doi.org/10.1175/waf-d-19-0023.1>
- Ardilouze, C., Batté, L., Déqué, M., van Meijgaard, E. and van den Hurk, B. Investigating the impact of soil moisture on European summer climate in ensemble numerical experiments. *Climate Dynamics*, 2019, Vol. 52(7-8), pp. 4011-4026. <https://doi.org/10.1007/s00382-018-4358-1>
- Auguste, F., G. Réa, R. Paoli, C. Lac, V. Masson, and D. Cariolle, Implementation of an immersed boundary method in the Meso-NH v5.2 model: applications to an idealized urban environment, *Geosci. Model Dev.*, 12, 2607-2633, 2019.
- Barbary, D., Leroux, M. and Bousquet, O. The orographic effect of Reunion Island on tropical cyclone track and intensity. *Atmospheric Science Letters*, 2019, Vol. 20(2), pp. E882. <https://doi.org/10.1002/asl.882>
- Baumet, J., Déqué, M., Krinner, G., Agosta, C. and Alias, A. Effect of prescribed sea surface conditions on the modern and future Antarctic surface climate simulated by the ARPEGE atmosphere general circulation model. *The Cryosphere*, 2019, Vol. 13(11), pp. 3023-3043. <https://doi.org/10.5194/tc-13-3023-2019>
- Bergot, T., and R. Lestringant, On the predictability of radiation fog formation in a mesoscale model: A case study in heterogeneous terrain, *Atmosphere*, 10, 165, 2019.
- Berre, L. Simulation and diagnosis of observation, model and background error contributions in data assimilation cycling. *Quarterly Journal of the Royal Meteorological Society*, 2019, Vol. 145(719), pp. 597-608. <https://doi.org/10.1002/qj.3454>
- Berthet, S., Séférian, R., Bricaud, C., Chevallier, M., Voldoire, A. and Ethé, C. Evaluation of an Online Grid-Coarsening Algorithm in a Global Eddy-Admitting Ocean Biogeochemical Model. *Journal of Advances in Modeling Earth Systems*, 2019, Vol. 11(6), pp. 1759-1783. <https://doi.org/10.1029/2019ms001644>
- Beucher, F, Lafore, J-P, Chapelon, N. Simulation and analysis of the moist vortex associated with the extreme rain event of Ouagadougou in 2009. *Q J R Meteorol Soc.* 2020; 146: 86– 104. <https://doi.org/10.1002/qj.3645>
- Bhowmick, S. A., Cotton, J., Fore, A., Kumar, R., Payan, C., Rodríguez, E., Sharma, A., Stiles, B., Stoffelen, A. and Verhoef, A. An Assessment of the Performance of ISRO's SCATSAT-1 Scatterometer. *Current Science*, 2019, Vol. 117(6), pp. 959. <https://doi.org/10.18520/cs/v117/i6/959-972>
- Bhuiyan, M. A. E., Nikolopoulos E., Anagnostou, E., Albergel, C., Dutra, E., Fink, G., Martinez de la Torre, A., Munier, S. and Polcher, J. : Assessment of Precipitation Error Propagation in Multi-Model Global Water Resources Reanalysis. *Hydrology and Earth System Sciences*, 2019, Vol. 23, pp. 1973-1994 <https://doi.org/10.5194/hess-23-1973-2019>
- Bigeard, G., Arteta, J. and Plu, M. Improving the Representation of Agricultural Ammonia Emissions for a Better Air Quality Forecasting Over France: A Simple Model to Estimate Fertilization Dates from Meteorological Constraints. *IGARSS 2019 - 2019 IEEE International Geoscience and Remote Sensing Symposium*, 2019. <https://doi.org/10.1109/igarss.2019.8900427>
- Bigeard, G., Sic, B., Amraoui, L. E. and Plu, M. Monitoring Volcanic ASH with the Chemistry-Transport Model Mocage: Improvements of Source Term and Assimilation of Observations. *IGARSS 2019 - 2019 IEEE International Geoscience and Remote Sensing Symposium*, 2019. <https://doi.org/10.1109/igarss.2019.8900396>
- Blunden, J. and Arndt, D. S. State of the Climate in 2018. *Bulletin of the American Meteorological Society*, 2019, Vol. 100(9), pp. Si-S306. <https://doi.org/10.1175/2019bamsstateoftheclimate.1>
- Blyverket, J.; Hamer, P.D.; Schneider, P.; Albergel, C.; Lahoz, W.A. Monitoring Soil Moisture Drought over Northern High Latitudes from Space. *Remote Sens.* 2019, 11, 1200.
- Blyverket, J.; Hamer, P.D.; Bertino, L.; Albergel, C.; Fairbairn, D.; Lahoz, W.A. An Evaluation of the EnKF vs. EnOI and the Assimilation of SMAP, SMOS and ESA CCI Soil Moisture Data over the Contiguous US. *Remote Sens.* 2019, 11(5), 478; <https://doi.org/10.3390/rs11050478>
- Borderies, M., Caumont, O., Delanoë, J., Ducrocq, V., Fourrié, N. and Marquet, P. Impact of airborne cloud radar reflectivity data assimilation on kilometre-scale numerical weather prediction analyses and forecasts of heavy precipitation events. *Natural Hazards and Earth System Sciences*, 2019, Vol. 19(4), pp. 907-926. <https://doi.org/10.5194/nhess-19-907-2019>
- Borderies, M., O. Caumont, J. Delanoë, V. Ducrocq et N. Fourrié, 2019 : Assimilation of wind data from airborne Doppler cloud-profiling radar in a kilometre-scale NWP system. *Natural Hazards and Earth System Sciences*, 19(4), 821-835. doi : 10.5194/nhess-19-821-2019
- Bouchard, B., Eeckman, J., Dedieu, J.-P., Delclaux, F., Chevallier, P., Gascoïn, S. and Arnaud, Y. On the Interest of Optical Remote Sensing for Seasonal Snowmelt Parameterization, Applied to the Everest Region (Nepal). *Remote Sensing*, 2019, Vol. 11(22), pp. 2598. <https://doi.org/10.3390/rs11222598>
- Bourras, D., Cambra, R., Marié, L., Bouin, M. N., Baggio, L., Branger, H., ... & Maes, C., 2019 : Air-sea turbulent fluxes from a wave-following platform during six experiments at sea. *Journal of Geophysical Research: Oceans*, DOI: 10.1029/2018JC014803,124 (6), 4290-4321.
- Bousquet, O., Barbary, D., Bielli, S., Kebir, S., Raynaud, L., Malardel, S. and Faure, G. An evaluation of tropical cyclone forecast in the Southwest Indian Ocean basin with AROME? Indian Ocean convection? permitting numerical weather predicting system. *Atmospheric Science Letters*, 2019, pp. E950. <https://doi.org/10.1002/asl2.950>
- Bovalo, C., Barthe, C. and Pinty, J. Examining relationships between cloud-resolving model parameters and total flash rates to generate lightning density maps. *Quarterly Journal of the Royal Meteorological Society*, 2019, Vol. 145(720), pp. 1250-1266. <https://doi.org/10.1002/qj.3494>
- Brient, F., Roehrig, R. and Voldoire, A. Evaluating Marine Stratocumulus Clouds in the CNRM-CM6-1 Model Using Short-Term Hindcasts. *Journal of Advances in Modeling Earth Systems*, 2019, Vol. 11(1), pp. 127-148. <https://doi.org/10.1029/2018ms001461>
- Brient F., Couvreur F, Villefranque N, Rio C, Honnert R, 2019: Object-oriented identification of coherent structures in large-eddy simulations: importance of downdrafts in stratocumulus. *Geophysical Research Letters*, 46, 1-11, <https://doi.org/10.1029/2018GL081499>
- Bénard, P. Numerical investigation of Rossby waves for nonlinear shallow-water equations on the sphere. *Quarterly Journal of the Royal Meteorological Society*, 2019. <https://doi.org/10.1002/qj.3504>

- Bénaud, P. and Grinton, M. R. Circumventing the pole problem of reduced lat-lon grids with local schemes. Part I: Analysis and model formulation. *Quarterly Journal of the Royal Meteorological Society*, 2019. <https://doi.org/10.1002/qj.3509>
- Calmer R., G.C. Roberts., K.J. Sanchez, J. Sciare, K. Sellegri, D. Picard, M. Vrekoussis and M. Pidridas. Aerosol–cloud closure study on cloud optical properties using remotely piloted aircraft measurements during a BACCHUS field campaign in Cyprus. *Atmos. Chem. Phys.*, 2019. <https://doi.org/10.5194/acp-19-13989-2019>
- Calonne, N., Milliancourt, L., Burr, A., Philip, A., Martin, C. L., Flin, F. and Geindreau, C. Thermal Conductivity of Snow, Firn, and Porous Ice From 3-D Image-Based Computations. *Geophysical Research*, 2019, Vol. 46(22), pp. 13079-13089. <https://doi.org/10.1029/2019gl085228>
- Calvet J-C, de Rosnay P and Penny SG (2019), "Editorial for the Special Issue "Assimilation of Remote Sensing Data into Earth System Models"", *Remote Sensing*, sep, 2019. Vol. 11(18), pp. 2177. MDPI AG.
- Caron, J.-F., Michel, Y., Montmerle, T. and Arbogast, É. Improving Background Error Covariances in a 3D Ensemble-Variational Data Assimilation System for Regional NWP. *Monthly Weather Review*, 2019, Vol. 147(1), pp. 135-151. <https://doi.org/10.1175/mwr-d-18-0248.1>
- Carrer, D.; Ceamanos, X.; Moparthy, S.; Vincent, C.; C. Freitas, S.; Trigo, I.F. Satellite Retrieval of Downwelling Shortwave Surface Flux and Diffuse Fraction under All Sky Conditions in the Framework of the LSA SAF Program (Part 1: Methodology). *Remote Sens.* 2019, 11, 2532.
- Carrer, D.; Moparthy, S.; Vincent, C.; Ceamanos, X.; C. Freitas, S.; Trigo, I.F. Satellite Retrieval of Downwelling Shortwave Surface Flux and Diffuse Fraction under All Sky Conditions in the Framework of the LSA SAF Program (Part 2: Evaluation). *Remote Sens.* 2019, 11, 2630.
- Carréric, A., Dewitte, B., Cai, W., Capotondi, A., Takahashi, K., Yeh, S.-W., Wang, G. and Guémas, V. Change in strong Eastern Pacific El Niño events dynamics in the warming climate. *Climate Dynamics*, 2019, Vol. 54(1-2), pp. 901-918. <https://doi.org/10.1007/s00382-019-05036-0>
- Ceamanos, X., Moparthy, S., Carrer, D. and Seidel, F. C. Assessing the Potential of Geostationary Satellites for Aerosol Remote Sensing Based on Critical Surface Albedo. *Remote Sensing*, 2019, Vol. 11(24), pp. 2958. <https://doi.org/10.3390/rs11242958>
- Chang, K.-L., Cooper, O. R., West, J. J., Serre, M. L., Schultz, M. G., Lin, M., Maréchal, V., Josse, B., Deushi, M., Sudo, K., Liu, J. and Keller, C. A. A new method (M3Fusion v1) for combining observations and multiple model output for an improved estimate of the global surface ozone distribution. *Geoscientific Model Development*, 2019, Vol. 12(3), pp. 955-978. <https://doi.org/10.5194/gmd-12-955-2019>
- Chauvin, F., Pilon, R., Palany, P. and Belmadani, A. Future changes in Atlantic hurricanes with the rotated-stretched ARPEGE-Climat at very high resolution. *Climate Dynamics*, 2019. <https://doi.org/10.1007/s00382-019-05040-4>
- Ching J, Aliaga D, Mills G, Masson V, See L, Neophytou M, Middel A, Baklanov A, Ren C, Ng E, Fung J, Wong M, Huang Y, Martilli A, Brousse O, Stewart I, Zhang X, Shehata A, Miao S, Wang X, Wang W, Yamagata Y, Duarte D, Li Y, Feddema J, Bechtel B, Hidalgo J, Roustan Y, Kim Y, Simon H, Kropp T, Bruse M, Lindberg F, Grimmond S, Demazure M, Chen F, Li C, Gonzales-Cruz J, Bornstein B, He Q, Tzu-Ping, Hanna A, Erell E, Tapper N, Mall R and Niyogi D (2019), "Pathway using WUDAPT's DigitalSynthetic City tool towards generating urban canopy parameters for multi-scale urban atmospheric modeling", *Urban Climate*, jun, 2019. Vol. 28, pp. 100459.
- Cimini, D., Hocking, J., Angelis, F. D., Cersosimo, A., Paola, F. D., Gallucci, D., Gentile, S., Geraldini, E., Larosa, S., Nilo, S., Romano, F., Ricciardelli, E., Ripepi, E., Viggiano, M., Luini, L., Riva, C., Marzano, F. S., Martinet, P., Song, Y., Ahn, M. H. and Rosenkranz, P. RTTOV-gb v1.0 - updates on sensors, absorption models, uncertainty, and availability. *Geoscientific Model Development*, 2019, Vol. 12(5), pp. 1833-1845. <https://doi.org/10.5194/gmd-12-1833-2019>
- Colin, M., Sherwood, S., Geoffroy, O., Bony, S. and Fuchs, D. Identifying the Sources of Convective Memory in Cloud-Resolving Simulations. *Journal of the Atmospheric Sciences*, 2019, Vol. 76(3), pp. 947-962. <https://doi.org/10.1175/jas-d-18-0036.1>
- Colombo, R., Garzonio, R., Mauro, B. D., Dumont, M., Tuzet, F., Cogliati, S., Pozzi, G., Maltese, A. and Cremonese, E. Introducing thermal inertia for monitoring snowmelt processes with remote sensing. *Geophysical Research Letters*, 2019, Vol. 46, pp. 4308-4319. <https://doi.org/10.1029/2019GL082193>
- Conte, L., Szopa, S., Séférian, R. and Bopp, L. The oceanic cycle of carbon monoxide and its emissions to the atmosphere. *Biogeosciences*, 2019, Vol. 16(4), pp. 881-902. <https://doi.org/10.5194/bg-16-881-2019>
- Cornforth R, Parker DJ, Diop-Kane M, Fink AH, Lafore J-P, Laing A, Afiesimama E, Caughey J, Diongue-Niang A, Kassimou A, Lamb P, Lamptey B, Mumba Z, Nnodu I, Omotosho J, Palmer S, ParrishP, Razafindrakoto L-G, Thiaw W, Thorncroft C and Tompkins A (2019), "The First Forecasters' Handbook for West Africa", *Bulletin of the American Meteorological Society*, nov, 2019. Vol. 100(11), pp. 2343-2351.
- Corona-Lozada, M., Morin, S. and Choler, P. Drought offsets the positive effect of summer heat waves on the canopy greenness of mountain grasslands. *Agricultural and Forest Meteorology*, 2019, Vol. 276-277, pp. 107617. <https://doi.org/10.1016/j.agrformet.2019.107617>
- Daniel M, Lemonsu A, Déqué M, Somot S, Alias A, Masson V (2019) Benefits of explicit urban parameterization in regional climate modelling to study climate and city interactions. *Climate Dynamics*, 52(5-6):2745-2764.
- Darmaraki, S., Somot, S., Sevault, F. and Nabat, P. Past Variability of Mediterranean Sea Marine Heatwaves. *Geophysical Research Letters*, 2019, Vol. 46(16), pp. 9813-9823. <https://doi.org/10.1029/2019GL082933>
- Darmaraki, S., Somot, S., Sevault, F., Nabat, P., Narvaez, W. D. C., Cavicchia, L., Djurdjevic, V., Li, L., Sannino, G. and Sein, D. V. Future evolution of Marine Heatwaves in the Mediterranean Sea. *Climate Dynamics*, 2019, Vol. 53(3-4), pp. 1371-1392. <https://doi.org/10.1007/s00382-019-04661-z>
- DeVries, T., Quéré, C. L., Andrews, O., Berthet, S., Hauck, J., Ilyina, T., Landschützer, P., Lenton, A., Lima, I. D., Nowicki, M., Schwinger, J. and Séférian, R. Decadal trends in the ocean carbon sink. *Proceedings of the National Academy of Sciences*, 2019, pp. 201900371. <https://doi.org/10.1073/pnas.1900371116>
- Decharme, B., Delire, C., Minvielle, M., Colin, J., Vergnes, J.-P., Alias, A., Saint-Martin, D., Séférian, R., Sénéci, S. and Voldoire, A. Recent Changes in the ISBA-CTRIP Land Surface System for Use in the CNRM-CM6 Climate Model and in Global Off-Line Hydrological Applications. *Journal of Advances in Modeling Earth Systems*, 2019, Vol. 11(5), pp. 1207-1252. <https://doi.org/10.1029/2018ms001545>
- Deroubaix, A., Menut, L., Flamant, C., Brito, J., Denjean, C., Dreiling, V., Fink, A., Jambert, C., Kalthoff, N., Knippertz, P., Ladkin, R., Mailler, S., Maranay, M., Pacífico, F., Pignat, B., Siour, G. and Turquet, S. Diurnal cycle of coastal anthropogenic pollutant transport over southern West Africa during the DACCIIWA campaign. *Atmospheric Chemistry and Physics*, 2019, Vol. 19(1), pp. 473-497. <https://doi.org/10.5194/acp-19-473-2019>
- Descheemaeker, M., Plu, M., Maréchal, V., Claeysman, M., Olivier, F., Aoun, Y., Blanc, P., Wald, L., Guth, J., Sic, B., Vidot, J., Piacentini, A. and Josse, B. Monitoring aerosols over Europe: an assessment of the potential benefit of assimilating the VIS04 measurements from the future MTG/FCI geostationary imager. *Atmospheric Measurement Techniques*, 2019, Vol. 12(2), pp. 1251-1275. <https://doi.org/10.5194/amt-12-1251-2019>
- Di Mauro, B., Garzonio, R., Rossini, M., Filipa, G., Pogliotti, P., Galvagno, M., di Cella, U. M., Migliavacca, M., Baccolo, G., Clemenza, M., Delmonte, B., Maggi, V., Dumont, M., Tuzet, F., Lafaysse, M., Morin, S., Cremonese, E. and Colombo, R. Saharan dust events in the European Alps: role in snowmelt and geochemical characterization. *The Cryosphere*, 2019, Vol. 13, pp. 1147-1164. <https://doi.org/10.5194/tc-13-1147-2019>
- Dion, I.-A., Ricaud, P., Haynes, P., Carminati, F. and Dauhut, T. Ice injected into the tropopause by deep convection – Part 1: In the austral convective tropics. *Atmospheric Chemistry and Physics*, 2019, Vol. 19(9), pp. 6459-6479. <https://doi.org/10.5194/acp-19-6459-2019>
- Dixon R. D., P. Peyrillé and F. Guichard, 2019: Sahelian precipitation change induced by SST increase: the contrasting roles of regional and larger-scale drivers. *Geophys. Res. Lett.*, 46, 11378-11387. doi:10.1029/2019GL084872
- Doerenbecher, A. and Mahfouf, J.-F. Impact of additional AMDAR data in the AROME-France model during May 2017. *Advances in Science and Research*, 2019, Vol. 16, pp. 215-222. <https://doi.org/10.5194/asr-16-215-2019>
- Domine, F., Picard, G., Morin, S., Barrere, M., Madore, J.-B. and Langlois, A. Major issues in simulating some Arctic snowpack properties using current detailed snow physics models: Consequences for the thermal regime and water budget of permafrost. *Journal of Advances in Modeling Earth Systems*, 2019, Vol. 11, pp. 34-44. <https://doi.org/10.1029/2018MS001445>
- Douville H., A. Ribes (2019) Breakdown of NAO reproducibility into internal versus externally forced components : a pilot study, *Climate Dynamics*, 52 (1-2), 29-48, doi:10.1007/s00382-018-4141-3.

- Drugé, T., Nabat, P., Mallet, M. and Somot, S. Model simulation of ammonium and nitrate aerosols distribution in the Euro-Mediterranean region and their radiative and climatic effects over 1979–2016. *Atmospheric Chemistry and Physics*, 2019, Vol. 19(6), pp. 3707–3731. <https://doi.org/10.5194/acp-19-3707-2019>
- Dunic, N., Vilibic, I., Sepic, J., Mihanovic, H., Sevault, F., Somot, S., Waldman, R., Nabat, P., Arsouze, T., Pennel, R., Jordà, G. and Precali, R. Performance of multi-decadal ocean simulations in the Adriatic Sea. *Ocean Modelling*, 2019, Vol. 134, pp. 84–109. <https://doi.org/10.1016/j.ocemod.2019.01.006>
- Duflot, V., Tulet, P., Flores, O., Barthe, C., Colomb, A., Deguillaume, L., Vaïtilingom, M., Perring, A., Huffman, A., Hernandez, M. T., Sellegri, K., Robinson, E., O'Connor, D. J., Gomez, O. M., Burnet, F., Bourriane, T., Strasberg, D., Rocco, M., Bertram, A. K., Chazette, P., Totems, J., Fournel, J., Stamenoff, P., Metzger, J.-M., Chabasset, M., Rousseau, C., Bourriane, E., Sancelme, M., Delort, A.-M., Wegener, R. E., Chou, C., and Elizondo, P. Preliminary results from the FARCE 2015 campaign: multidisciplinary study of the forest–gas–aerosol–cloud system on the tropical island of La Réunion. *Atmos. Chem. Phys.*, 19, 10591–10618, <https://doi.org/10.5194/acp-19-10591-2019>, 2019
- Duruiseau, F., Chambon, P., Wattrelot, E., Barreyat, M. and Mahfouf, J.-F. Assimilating cloudy and rainy microwave observations from SAPHIR on board Megha Tropiques within the ARPEGE global model. *Quarterly Journal of the Royal Meteorological Society*, 2019, Vol. 145(719), pp. 620–641. <https://doi.org/10.1002/qj.3456>
- Eeckman J, Nepal S, Chevallier P, Camensuli G, Delclaux F, Boone A and Rouw AD (2019), "Comparing the ISBA and J2000 approaches for surface flows modelling at the local scale in the Everestregion", *Journal of Hydrology*, feb, 2019. Vol. 569, pp. 705–719. Elsevier BV.
- Ehsan Bhuiyan, M. A., Nikolopoulos, E. I., Anagnostou, E. N., Polcher, J., Albergel, C., Dutra, E., Fink, G., Martínez-de la Torre, A., and Munier, S.: Assessment of precipitation error propagation in multi-model global water resource reanalysis. *Hydrol. Earth Syst. Sci.*, 23, 1973–1994, <https://doi.org/10.5194/hess-23-1973-2019>, 2019
- El Hajj, M.; Baghdadi, N.; Wigneron, J.-P.; Zribi, M.; Albergel, C.; Calvet, J.-C.; Fayad, I. First Vegetation Optical Depth Mapping from Sentinel-1 C-band SAR Data over Crop Fields. *Remote Sens.* 2019, 11(23), 2769; <https://doi.org/10.3390/rs11232769>
- Evin, G., Hingray, B., Blanchet, J., Eckert, N., Morin, S. and Verfaillie, D. Partitioning uncertainty components of an incomplete ensemble of climate projections using data augmentation. *Journal of Climate*, 2019, Vol. 32, pp. 2423–2440. <https://doi.org/10.1175/JCLI-D-18-0606.1>
- Farouk, I., Fourrié, N. and Guidard, V. Homogeneity criteria from AVHRR information within IASI pixels in a numerical weather prediction context. *Atmospheric Measurement Techniques*, 2019, Vol. 12(6), pp. 3001–3017. <https://doi.org/10.5194/amt-12-3001-2019>
- Federico, S., R. C. Torcasio, E. Avolio, O. Caumont, M. Montopoli, L. Baldini, G. Vulpiani et S. Dietrich, 2019 : The impact of lightning and radar data assimilation on the performance of very short term rainfall forecast for two case studies in Italy. *Natural Hazards and Earth System Sciences*, 19(8), 1839–1864. doi : 10.5194/nhess-19-1839-2019
- Flores-Rojas J, Pereira-Filho A, Karam H, Vemado F, Masson V and Silva-Vidal F (2019), "Modeling the Effects of Explicit Urban Canopy Representation on the Development of Thunderstorms above a Tropical Mega City", *Atmosphere*, jun, 2019. Vol. 10(7), pp. 356
- Formenti, P., D'Anna, B., Flamant, C., Mallet, M., Piketh, S. J., Schepanski, K., Waquet, F., Auriol, F., Brogniez, G., Burnet, F., Chaboureau, J.-P., Chauvigné, A., Chazette, P., Denjean, C., Desboeufs, K., Doussin, J.-F., Elguindi, N., Feuerstein, S., Gaetani, M., Giorio, C., Klopfer, D., Mallet, M. D., Nabat, P., Monod, A., Solmon, F., Namwoonde, A., Chikwilliwa, C., Mushi, R., Welton, E. J. and Holben, B. The Aerosols, Radiation and Clouds in southern Africa (AEROCLO-SA) field campaign in Namibia: overview, illustrative observations and way forward. *Bulletin of the American Meteorological Society*, 2019. <https://doi.org/10.1175/bams-d-17-0278.1>
- Fourrié, N., M. Nuret, P. Brousseau, O. Caumont, A. Doerenbecher, E. Wattrelot, P. Moll, H. Bénichou, D. Puech, O. Bock, P. Bossier, P. Chazette, C. Flamant, P. Di Girolamo, E. Richard et F. Saïd, 2019: The AROME-WMED reanalyses of the first special observation period of the hydro-logical cycle in the mediterranean experiment (HyMeX). *Geoscientific Model Development*, 12(7), 2657–2678. <https://doi.org/10.5194/gmd-12-2657-2019>
- Friedlingstein, P., Jones, M. W., O'Sullivan, M., Andrew, R. M., Hauck, J., Peters, G. P., Peters, W., Pongratz, J., Sitch, S., Quéré, C. L., Bakker, D. C. E., Canadell, J. G., Ciais, P., Jackson, R. B., Anthoni, P., Barbero, L., Bastos, A., Bastrikov, V., Becker, M., Bopp, L., Buitenhuis, E., Chandra, N., Chevallier, F., Chini, L. P., Currie, K. I., Feely, R. A., Gehlen, M., Gilfillan, D., Gkritzalis, T., Goll, D. S., Gruber, N., Gutekunst, S., Harris, I., Haverd, V., Houghton, R. A., Hurtt, G., Ilyina, T., Jain, A. K., Joetzjer, E., Kaplan, J. O., Kato, E., Goldewijk, K. K., Korsbakken, J. I., Landschützer, P., Lausset, S. K., Lefèvre, N., Lenton, A., Lienert, S., Lombardozi, D., Marland, G., McGuire, P. C., Melton, J. R., Metz, N., Munro, D. R., Nabel, J. E. M. S., Nakaoka, S.-I., Neill, C., Omar, A. M., Ono, T., Peregon, A., Pierrot, D., Poulter, B., Rehder, G., Resplandy, L., Robertson, E., Rödenbeck, C., Séférian, R., Schwinger, J., Smith, N., Tans, P. P., Tian, H., Tilbrook, B., Tubiello, F. N., van der Werf, G. R., Wiltshire, A. J. and Zaehle, S. Global Carbon Budget 2019. *Earth System Science Data*, 2019, Vol. 11(4), pp. 1783–1838. <https://doi.org/10.5194/essd-11-1783-2019>
- Fumière, Q., Déqué, M., Nuissier, O., Somot, S., Alias, A., Caillaud, C., Laurantin, O. and Seity, Y. Extreme rainfall in Mediterranean France during the fall: added value of the CNRM-AROME Convection-Permitting Regional Climate Model. *Clim. Dyn.*, 1–15, 2019. <https://doi.org/10.1007/s00382-019-04898-8>
- Geoffroy, O. and Saint-Martin, D. Equilibrium- and transient-state dependencies of climate sensitivity: are they important for climate projections? *Journal of Climate*, 2019. <https://doi.org/10.1175/jcli-d-19-0248.1>
- Giffard, P., Llovel, W., Jouanno, J., Morvan, G. and Decharme, B. Contribution of the Amazon River Discharge to Regional Sea Level in the Tropical Atlantic Ocean. *Water*, 2019, Vol. 11(11), pp. 2348. <https://doi.org/10.3390/w11112348>
- Glinton, M. R. and Bénard, P. Circumventing the pole problem of reduced lat-lon grids with local schemes. Part II: Validation experiments. *Quarterly Journal of the Royal Meteorological Society*, 2019. <https://doi.org/10.1002/qj.3495>
- Gonzalez, S., Bech, J., Udina, M., Codina, B., Paci, A. and Trapero, L. Decoupling between Precipitation Processes and Mountain Wave Induced Circulations Observed with a Vertically Pointing K-Band Doppler Radar. *Remote Sensing*, 2019, Vol. 11(9), pp. 1034. <https://doi.org/10.3390/rs11091034>
- Goret, M., Masson, V., Schoetter, R. and Moine, M.-P. Inclusion of a CO2 flux modelling in an urban canopy layer model and evaluation over an old European city centre. *Atmospheric Environment*, 2019, Vol. 3, (100042), pp. 1–21 <https://doi.org/10.1016/j.aeaoa.2019.100042>
- Granados-Muñoz, M. J., Sicard, M., Román, R., Benavent-Oltra, J. A., Barragán, R., Brogniez, G., Denjean, C., Mallet, M., Formenti, P., Torres, B. and Alados-Arboledas, L. Impact of mineral dust on shortwave and longwave radiation: evaluation of different vertically resolved parameterizations in 1-D radiative transfer computations. *Atmospheric Chemistry and Physics*, 2019, Vol. 19(1), pp. 523–542. <https://doi.org/10.5194/acp-19-523-2019>
- Guillet, O., Weaver, A. T., Vasseur, X., Michel, Y., Gratton, S. and Gürol, S. Modelling spatially correlated observation errors in variational data assimilation using a diffusion operator on an unstructured mesh. *Quarterly Journal of the Royal Meteorological Society*, 2019. <https://doi.org/10.1002/qj.3537>
- Guyomarc'h, G., Bellot, H., Vionnet, V., Naaim-Bouvet, F., Deliot, Y., Fontaine, F., Pugliese, P., Nishimura, K., Durand, Y. and Naaim, M. A meteorological and blowing snow data set (2000–2016) from a high-elevation alpine site (Col du Lac Blanc, France, 2720m a.s.l.). *Earth System Science Data*, 2019, Vol. 11, pp. 57–69. <https://doi.org/10.5194/essd-11-57-2019>
- Hagenmuller, P., Flin, F., Dumont, M., Tuzet, F., Peinke, I., Lapalus, P., Dufour, A., Roule, J., Pézard, L., Voisin, D., Ando, E., Rolland du Roscoat, S. and Charrier, P. Motion of dust particles in dry snow under temperature gradient metamorphism. *The Cryosphere*, 2019, Vol. 13, pp. 2345–2359. <https://doi.org/10.5194/tc-13-2345-2019>
- Hajj ME, Baghdadi N, Wigneron J-P, Zribi M, Albergel C, Calvet J-C and Fayad I (2019), "First Vegetation Optical Depth Mapping from Sentinel-1 C-band SAR Data over Crop Fields", *Remote Sensing*, nov, 2019. Vol. 11(23), pp. 2769
- Haslett, S. L., Taylor, J. W., Evans, M., Morris, E., Vogel, B., Dajuma, A., Brito, J., Batenburg, A. M., Borrmann, S., Schneider, J., Schulz, C., Denjean, C., Bourriane, T., Knippertz, P., Dupuy, R., Schwarzenböck, A., Sauer, D., Flamant, C., Dorsey, J., Crawford, I. and Coe, H. Remote biomass burning dominates southern West African air pollution during the monsoon. *Atmospheric Chemistry and Physics*, 2019, Vol. 19(24), pp. 15217–15234. <https://doi.org/10.5194/acp-19-15217-2019>
- Hermozo, L., L. Eymard, F. Karbou, B. Picard, M. Pardé, A 1D-Var approach to retrieve clear sky wet tropospheric correction from current and future altimetry missions, *Journal of Atmospheric and Oceanic Technology*, <https://doi.org/10.1175/JTECH-D-17-0133.1>, 2019
- Hidalgo J, Lemonsu A, Masson V (2019) Between progress and obstacles on urban climate interdisciplinary studies and knowledge transfer to society. *Annals of the New York Academy of Sciences*, 1436(1):5–18

- Hidalgo, J., Dumas, G., Masson, V., Petit, G., Bechtel, B., Bocher, E., Foley, M., Schoetter, R. and Mills, G. Comparison between local climate zones maps derived from administrative datasets and satellite observations. *Urban Climate*, 2019, Vol. 27, pp. 64-89 <https://doi.org/10.1016/j.uclim.2018.10.004>
- Hogan RJ, Fielding MD, Barker HW, Villefranque N and Schäfer SAK (2019), "Entrapment: An Important Mechanism to Explain the Shortwave 3D Radiative Effect of Clouds", *Journal of the Atmospheric Sciences.*, jul, 2019. Vol. 2019(1), pp. 48-66
- Hourdin F, Jam A, Rio C, Couvreur F, Sandu I, Lefebvre M.P., Brient F., Idelkadi A, 2019: Unified parameterization of convective boundary layer transport and clouds with the thermal plume model, *Journal of Advances in Modeling Earth Systems*, 11, 9, 2910-2933, <https://doi.org/10.1029/2019MS001666>
- Huijnen, V., Pozzer, A., Arteta, J., Brasseur, G., Bouarar, I., Chabrilat, S., Christophe, Y., Dombia, T., Flemming, J., Guth, J., Josse, B., Karydis, V. A., Maréchal, V. and Pelletier, S. Quantifying uncertainties due to chemistry modelling – evaluation of tropospheric composition simulations in the CAMS model (cycle 43R1). *Geoscientific Model Development*, 2019, Vol. 12(4), pp. 1725-1752. <https://doi.org/10.5194/gmd-12-1725-2019>
- Illingworth, A. J., Cimini, D., Haefele, A., Haefelin, M., Hervo, M., Kotthaus, S., U. L., Martinet, P., Mattis, I., O'Connor, E. J. and Potthast, R. How can Existing Ground-Based Profiling Instruments Improve European Weather Forecasts?, *BAMS*, 2019. *Bull. Amer. Meteor. Soc.*, 2019. <https://doi.org/10.1175/BAMS-D-17-0231.1>
- Jones, C. D., Frölicher, T. L., Koven, C., MacDougall, A. H., Matthews, H. D., Zickfeld, K., Rogelj, J., Tokarska, K. B., Gillett, N. P., Ilyina, T., Meinshausen, M., Mengis, N., Séférian, R., Eby, M. and Burger, F. A. The Zero Emissions Commitment Model Intercomparison Project (ZECMIP) contribution to C4MIP: quantifying committed climate changes following zero carbon emissions. *Geoscientific Model Development*, 2019, Vol. 12(10), pp. 4375-4385. <https://doi.org/10.5194/gmd-12-4375-2019>
- Kim, R. S., Durand, M., Li, D., Baldo, E., Margulis, S. A., Dumont, M. and Morin, S. Estimating alpine snow depth by combining multifrequency passive radiance observations with ensemble snowpack modeling. *Remote Sensing of Environment*, 2019, Vol. 226, pp. 1-15. <https://doi.org/10.1016/j.rse.2019.03.016>
- Kokhanovsky A., Lamare M., Danne O., Brockmann C., Dumont M., Picard G., Arnaud L., Favier V., Jourdain B., Le Meur E., Di Mauro B., Aoki T., Niwano M., Rozanov V., Korkin S., Kipfstuhl S., Freitag J., Hoerhold M., Zühr A., Vladimirova D., Faber A., Steen-Larsen H.-C., Wahl S., Andersen J., Vandecrux B., Van As D., Mankoff K., Kern M., Zege E. and Box J. Retrieval of Snow Properties from the Sentinel-3 Ocean and Land Colour Instrument. *Remote Sensing*, 2019, Vol. 11, pp. 2280. <https://doi.org/10.3390/rs11192280>
- Køltzow, M., Casati, B., Bazile, E., Haiden, T. and Valkonen, T. A NWP model inter-comparison of surface weather parameters in the European Arctic during the Year of Polar Prediction Special Observing Period Northern Hemisphere 1. *Weather and Forecasting*, 2019. <https://doi.org/10.1175/waf-d-19-0003.1>
- Kwok, Y.T., Schoetter, R., Lau, K.K.L., Hidalgo, J., Ren, C., Pigeon, G. and Masson, V. How well does the Local Climate Zone scheme discern the thermal environment of Toulouse (France) ? An analysis using numerical simulation data. *International Journal of Climatology*, 2019, Vol. 39(14), pp. 5292-5315, <https://doi.org/10.1002/joc.6140>
- Lamy, K., Portafaix, T., Josse, B., Brogniez, C., Godin-Beekmann, S., Bencherif, H., Revell, L., Akiyoshi, H., Bekki, S., Hegglin, M. I., Jöckel, P., Kirner, O., Liley, B., Marecal, V., Morgenstern, O., Stenke, A., Zeng, G., Abraham, N. L., Archibald, A. T., Butchart, N., Chipperfield, M. P., Genova, G. D., Deushi, M., Dhomse, S. S., Hu, R.-M., Kinnison, D., Kotkamp, M., McKenzie, R., Michou, M., O'Connor, F. M., Oman, L. D., Pitari, G., Plummer, D. A., Pyle, J. A., Rozanov, E., Saint-Martin, D., Sudo, K., Tanaka, T. Y., Visioni, D. and Yoshida, K. Clear-sky ultraviolet radiation modelling using output from the Chemistry Climate Model Initiative. *Atmospheric Chemistry and Physics*, 2019, Vol. 19(15), pp. 10087-10110. <https://doi.org/10.5194/acp-19-10087-2019>
- LeBastard, T., O. Caumont, N. Gaussiat et F. Karbou, 2019 : Combined use of volume radar observations and high-resolution numerical weather predictions to estimate precipitation at the ground: methodology and proof of concept. *Atmospheric Measurement Techniques*, 12(10), 5669-5684. doi : 10.5194/amt-12-5669-2019
- Le Cozannet, G., Bulteau, T., Castelle, B., Ranasinghe, R., Wöppelmann, G., Rohmer, J., Bernon, N., Idier, D., Louisor, J. and Salas-y-Méllia, D. (2019). Quantifying uncertainties of sandy shoreline change projections as sea level rises. *Scientific Reports*. 9. 10.1038/s41598-018-37017-4
- Leger, J., Lafore, J.-P., Piriou, J.-M. and Guérémy, J.-F. A Simple Model of Convective Drafts Accounting for the Perturbation Pressure Term. *Journal of the Atmospheric Sciences*, 2019, Vol. 76(10), pp. 3129-3149. <https://doi.org/10.1175/jas-d-18-0281.1>
- Lejeune, Y., Dumont, M., Panel, J.-M., Lafaysse, M., Lapalus, P., Gac, E. L., Lesaffre, B. and Morin, S. 57 years (1960–2017) of snow and meteorological observations from a mid-altitude mountain site (Col de Porte, France, 1325m of altitude). *Earth System Science Data*, 2019, Vol. 11, pp. 71-88. <https://doi.org/10.5194/essd-11-71-2019>
- Lemonsu A, Amossé A, Gaudio N, Haouès-Jouve S, Hidalgo J, Le Bras J, Legain D, Marchandise S (2019) Comparison of microclimate measurements and perceptions as part of a global evaluation of environmental quality at neighbourhood scale. *International Journal of Biometeorology*, 10.1007/s00484-019-01686-1, in-line first
- Le Roy B, Lemonsu A, Koukou-Arnaud R, Brion D, Masson V (2019) Long time series spatialized data for urban climatological studies : a case study of Paris, France. *International Journal of Climatology*, <https://doi.org/10.1002/joc.6414>
- Leroux, M.-D., Davidson, N. E., Hankinson, C. M., Reeder, M. J., Wain, A. G. and Xinmei, H. Environmental Interactions During the Extreme Rain Event associated with ex-Tropical Cyclone Oswald (2013). *Journal of Southern Hemisphere Earth Systems Science*, 2019, Vol. 69(1), pp. 216. <https://doi.org/10.1071/ES19016>
- Libois, Q., Lévesque-Desrosiers, F., Lambert-Girard, S., Thibault, S., & Domine, F. (2019). Optical porosimetry of weakly absorbing porous materials. *Optics express*, 27(16), 22983-22993
- Lievens, H., Demuzere, M., Marshall, H.-P., Reichle, R. H., Brucker, L., Brangers, I., de Rosnay, P., Dumont, M., Giroto, M., Immerzeel, W. W., Jonas, T., Kim, E. J., Koch, I., Marty, C., Saloranta, T., Schöber, J. and De Lannoy, G. J. M. Snow depth variability in the Northern Hemisphere mountains observed from space. *Nature Communications*, 2019, Vol. 10, pp. 4629. <https://doi.org/10.1038/s41467-019-12566-y>
- Lovat A, Vincendon B and Ducrocq V (2019), "Assessing the impact of resolution and soil datasets on flash-flood modelling", *Hydrology and Earth System Sciences.*, apr, 2019. Vol. 23(3), pp. 1801-1818
- Malardel, S. and Bechtold, P. The coupling of deep convection with the resolved flow via the divergence of mass flux in the IFS. *Quarterly Journal of the Royal Meteorological Society*, 2019, Vol. 145(722), pp. 1832-1845. <https://doi.org/10.1002/qj.3528>
- Mallet, M., Nabat, P., Zuidema, P., Redemann, J., Sayer, A. M., Stengel, M., Schmidt, S., Cochrane, S., Burton, S., Ferrare, R., Meyer, K., Saide, P., Jethva, H., Torres, O., Wood, R., Martin, D. S., Roehrig, R., Hsu, C. and Formenti, P. Simulation of the transport, vertical distribution, optical properties and radiative impact of smoke aerosols with the ALADIN regional climate model during the ORACLES-2016 and LASIC experiments. *Atmospheric Chemistry and Physics*, 2019, Vol. 19(7), pp. 4963-4990. <https://doi.org/10.5194/acp-19-4963-2019>
- Masson, T., M. D. Mura, M. Dumont and J. Chanussot, Snow Cover Estimation From Image Time Series Based on Spectral Unmixing, *IEEE Geoscience and Remote Sensing Letters*, 16(3), 337-341, <https://dx.doi.org/10.1109/LGRS.2018.2873836>, 2019
- Masson V, Heldens W, Bocher E, Bonhomme M, Bucher B, Burmeister C, de Munck C, Esch T, Hidalgo J, Kanani-Sühring F, Kwok Y.-T, Lemonsu A, Lévy J-P, Maronga B, Pavlik D, Petit G, See L, Schoetter R, Tornay N, Votsis A, Zeidler J (2019) City-descriptive input data for urban climate models : Model requirements, data sources and challenges. *Urban Climate*, 31, <https://doi.org/10.1016/j.uclim.2019.100536>.
- Mattioli, V., Accadia, C., Prigent, C., Crewell, S., Geer, A., Eriksson, P., Fox, S., Pardo, J. R., Mlawer, E. J., Cadeddu, M., Bremer, M., Breuck, C. D., Smette, A., Cimini, D., Turner, E., Mech, M., Marzano, F. S., Brunel, P., Vidot, J., Bennartz, R., Wehr, T., Michele, S. D. and John, V. O. Atmospheric Gas Absorption Knowledge in the Submillimeter: Modeling, Field Measurements, and Uncertainty Quantification. *Bulletin of the American Meteorological Society*, 2019, Vol. 100(12), pp. ES291-ES295. <https://doi.org/10.1175/bams-d-19-0074.1>
- Mazoyer, M., Burnet, F., Denjean, C., Roberts, G. C., Haefelin, M., Dupont, J.-C. and Elias, T. Experimental study of the aerosol impact on fog microphysics. *Atmospheric Chemistry and Physics*, 2019, Vol. 19(7), pp. 4323-4344. <https://doi.org/10.5194/acp-19-4323-2019>
- McCoy, D. T., Field, P. R., Elsaesser, G. S., Bodas-Salcedo, A., Kahn, B. H., Zelinka, M. D., Kodama, C., Mauritsen, T., Vanniere, B., Roberts, M., Vidale, P. L., Saint-Martin, D., Voldoire, A., Haarsma, R., Hill, A., Shipway, B. and Wilkinson, J. Cloud feedbacks in extratropical cyclones: insight from long-term satellite data and high-resolution global simulations. *Atmospheric Chemistry and Physics*, 2019, Vol. 19(2), pp. 1147-1172. <https://doi.org/10.5194/acp-19-1147-2019>

- Mercier, F., Michel, Y., Montmerle, T., Jolivet, P. and Gürol, S. Speeding up the ensemble data assimilation system of the limited-area model of Météo-France using a block Krylov algorithm. *Quarterly Journal of the Royal Meteorological Society*, 2019, Vol. 145(720), pp. 910-929. <https://doi.org/10.1002/qj.3428>
- Mhedhbi Z, Masson V, Hidalgo J and Haouès-Jouve S (2019), "Collection of refined architectural parameters by crowdsourcing using Facebook social network: Case of Greater Tunis", *Urban Climate*, sep, 2019. Vol. 29, pp. 100499
- Minnett, P., Alvera-Azcárate, A., Chin, T., Corlett, G., Gentemann, C., Karagali, I., Li, X., Marsouin, A., Marullo, S., Maturi, E., Santoleri, R., Picart, S. S., Steele, M. and Vazquez-Cuervo, J. Half a century of satellite remote sensing of sea-surface temperature. *Remote Sensing of Environment*, 2019, Vol. 233, pp. 111366. <https://doi.org/10.1016/j.rse.2019.111366>
- Moparthy, S.; Carrer, D.; Ceamanos, X. Can We Detect the Brownness or Greenness of the Congo Rainforest Using Satellite-Derived Surface Albedo? A Study on the Role of Aerosol Uncertainties. *Sustainability* 2019, 11, 1410
- Morel, X., Decharme, B., Delire, C., Krinner, G., Lund, M., Hansen, B. U. and Mastepanov, M. A New Process-Based Soil Methane Scheme: Evaluation Over Arctic Field Sites With the ISBA Land Surface Model. *Journal of Advances in Modeling Earth Systems*, 2019, Vol. 11(1), pp. 293-326. <https://doi.org/10.1029/2018ms001329>
- Moullec, F., Barrier, N., Drira, S., Guilhaumon, F., Marsaleix, P., Somot, S., Ulses, C., Velez, L. and Shin, Y.-J. An End-to-End Model Reveals Losers and Winners in a Warming Mediterranean Sea. *Frontiers in Marine Science*, 2019, Vol. 6. <https://doi.org/10.3389/fmars.2019.00345>
- Ménard, C. B., Essery, R., Barr, A., Bartlett, P., Derry, J., Dumont, M., Fierz, C., Kim, H., Kontu, A., Lejeune, Y., Marks, D., Niwano, M., Raleigh, M., Wang, L. and Wever, N. Meteorological and evaluation datasets for snow modelling at 10 reference sites: description of in situ and bias-corrected reanalysis data. *Earth System Science Data*, 2019, Vol. 11, pp. 865-880. <https://doi.org/10.5194/essd-11-865-2019>
- Müller, A., Deconinck, W., Kühnlein, C., Mengaldo, G., Lange, M., Wedi, N., Bauer, P., Smolarkiewicz, P. K., Diamantakis, M., Lock, S.-J., Hamrud, M., Saarinen, S., Mozdzyński, G., Thiemert, D., Ginton, M., Bénard, P., Voitus, F., Colavolpe, C., Marguinaud, P., Zheng, Y., Bever, J. V., Degrauwe, D., Smet, G., Termonia, P., Nielsen, K. P., Sassi, B. H., Poulsen, J. W., Berg, P., Osuna, C., Fuhrer, O., Clement, V., Baldauf, M., Gillard, M., Szmelter, J., O'Brien, E., McKinstry, A., Robinson, O., Shukla, P., Lysaght, M., Kulczewski, M., Ciznicki, M., Pia, tek, W., Ciesielski, S., Blazewicz, M., Kurowski, K., Procyk, M., Szychala, P., Bosak, B., Piotrowski, Z., Wyszogrodzki, A., Raffin, E., Mazauric, C., Guilbert, D., Douriez, L., Vigouroux, X., Gray, A., Messmer, P., Macfaden, A. J. and New, N. The ESCAPE project: Energy-efficient Scalable Algorithms for Weather Prediction at Exascale. *Geoscientific Model Development Discussions*, 2019, pp. 1-50. <https://doi.org/10.5194/gmd-2018-304>
- Muñoz-Sabater, J., Lawrence, H., Albergel, C., Rosnay, P., Isaksen, I., Mecklenburg, S., Kerr, Y. and Drusch, M. Assimilation of SMOS brightness temperatures in the ECMWF Integrated Forecasting System. *Quarterly Journal of the Royal Meteorological Society*, 2019, Vol. 145(723), pp. 2524-2548. <https://doi.org/10.1002/qj.3577>
- Nahmani S., O. Bock and F. Guichard, 2019: Sensitivity of GPS tropospheric estimates to mesoscale convective systems in West Africa. *Atmos. Chem. Phys.*, 19, 9541–9561. doi:10.5194/acp-19-9541-2019
- Nicolet, G., Eckert, N., Morin, S. and Blanchet, J. Inférence et modélisation de la dépendance spatiale des extrêmes neigeux dans les Alpes françaises par processus max-stables La Houille Blanche, 2019(5-6), pp. 150-158. <https://doi.org/10.1051/lhb/2019047>
- Nousu, J.-P., Lafaysse, M., Vernay, M., Bellier, J., Evin, G. and Joly, B. Statistical post-processing of ensemble forecasts of the height of new snow. *Nonlinear Processes of Geophysics*, 2019, Vol. 26, pp. 339-357. <https://doi.org/10.5194/npg-26-339-2019>
- O'Carroll, A. G., Armstrong, E. M., Beggs, H. M., Bouali, M., Casey, K. S., Corlett, G. K., Dash, P., Donlon, C. J., Gentemann, C. L., Høyer, J. L., Ignatov, A., Kabobah, K., Kachi, M., Kurihara, Y., Karagali, I., Maturi, E., Merchant, C. J., Marullo, S., Minnett, P. J., Pennybacker, M., Ramakrishnan, B., Ramsankaran, R., Santoleri, R., Sunder, S., Picart, S. S., Vázquez-Cuervo, J. and Wimmer, W. Observational Needs of Sea Surface Temperature. *Frontiers in Marine Science*, 2019, Vol. 6. <https://doi.org/10.3389/fmars.2019.00420>
- Peings, Y., J. Cattiaux and G. Magnusdottir (2019), The polar stratosphere as an arbiter of the projected tropical versus polar tug-of-war, *Geophysical Research Letters*, 46 (15), 9261–9270. doi:10.1029/2019GL082463
- Peinke, I., P. Hagenmuller, G. Chambon, J. Roulle, Investigation of snow sintering at microstructural scale from micro-penetration tests, *Cold Reg. Sci. Technol.*, 162, 43-55, <https://doi.org/10.1016/j.coldregions.2019.03.018>, 2019
- Pellet, V., Aires, F., Munier, S., Fernández Prieto, D., Jordá, G., Dorigo, W. A., Polcher, J., and Brocca, L.: Integrating multiple satellite observations into a coherent dataset to monitor the full water cycle – application to the Mediterranean region, *Hydrol. Earth Syst. Sci.*, 23, 465–491, <https://doi.org/10.5194/hess-23-465-2019>, 2019
- Plazzotta, M., Séférian, R. and Douville, H. Impact of Solar Radiation Modification on Allowable CO₂ Emissions: What Can We Learn From Multimodel Simulations? *Earth's Future*, *American Geophysical Union (AGU)*, 2019, Vol. 7(6), pp. 664-676. <https://doi.org/10.1029/2019ef001165>
- Prodhomme, C., Voldoire, A., Exarchou, E., Deppenmeier, A.-L., García-Serrano, J. and Guemas, V. How Does the Seasonal Cycle Control Equatorial Atlantic Interannual Variability? *Geophysical Research Letters*, 2019, Vol. 46(2), pp. 916-922. <https://doi.org/10.1029/2018GL080837>
- Quast, R.; Albergel, C.; Calvet, J.-C.; Wagner, W. A Generic First-Order Radiative Transfer Modelling Approach for the Inversion of Soil and Vegetation Parameters from Scatterometer Observations. *Remote Sens.* 2019, 11(3), 285; <https://doi.org/10.3390/rs11030285>
- Rahaman, H., Srinivasu, U., Panickal, S., Durgadoo, J., Griffies, S., Ravichandran, M., Bozec, A., Cherchi, A., Voldoire, A., Sidorenko, D. ..., Chassignet, E., Danabasoglu, G., Tsujino, H., Getzlaff, K., Ilicak, M., Bentsen, M., Long, M., Fogli, P., Farneti, R., Danilov, S., Marsland, S., Valcke, S., Yeager, S. and Wang, Q. An assessment of the Indian Ocean mean state and seasonal cycle in a suite of interannual CORE-II simulations. *Ocean Modelling*, 2019, Vol. 145, pp. 101503. <https://doi.org/10.1016/j.ocemod.2019.101503>
- Raynaud, L., Pechin, I., Arbogast, P., Rottner, L. and Destouches, M. Object-based verification metrics applied to the evaluation and weighting of convective-scale precipitation forecasts. *Quarterly Journal of the Royal Meteorological Society*, 2019. <https://doi.org/10.1002/qj.3540>
- Réchou, A., Flores, O., Jumaux, G., Dufloy, V., Bousquet, O., Poupeville, C. and Bonnardot, F. Spatio-temporal variability of rainfall in a high tropical island: Patterns and large-scale drivers in Réunion Island. *Quarterly Journal of the Royal Meteorological Society*, 2019, Vol. 145(720), pp. 893-909. <https://doi.org/10.1002/qj.3485>
- Redelsperger, J. L., Bouin, M. N., Pianezze, J., Garnier, V., & Marié, L., 2019 : Impact of a sharp, small-scale SST front on the marine atmospheric boundary layer on the Iroise Sea: Analysis from a hectometric simulation. *Quarterly Journal of the Royal Meteorological Society*, DOI: 10.1002/qj.3650,145 (725), 3692-3714
- Redon E, Lemonsu A, Masson V (2019) An urban trees parameterization for modelling microclimatic variables and thermal comfort conditions at street level with the Town Energy Balance model (TEB-SURFEX v8.0). *Geoscientific Model Development*, <https://www.geosci-model-dev-discuss.net/gmd-2019-77/>
- Rémy, S., Kipling, Z., Flemming, J., Boucher, O., Nabat, P., Michou, M., Bozzo, A., Ades, M., Huijnen, V., Benedetti, A., Engelen, R., Peuch, V.-H. and Morcrette, J.-J. Description and evaluation of the tropospheric aerosol scheme in the European Centre for Medium-Range Weather Forecasts (ECMWF) Integrated Forecasting System (IFS-AER, cycle 45R1). *Geoscientific Model Development*, 2019, Vol. 12(11), pp. 4627-4659. <https://doi.org/10.5194/gmd-12-4627-2019>
- Ribes A., S. Thao, R. Vautard, B. Dubuisson, S. Somot, J. Colin, S. Planton, J.-M. Soubeyroux (2018) : Observed increase of extreme daily rainfall in the French Mediterranean, *Climate Dynamics*, 52(1-2), 1095-1114, doi:10.1007/s00382-018-4179-2
- Richon, C., Dutay, J.-C., Bopp, L., Vu, B. L., Orr, J. C., Somot, S. and Dulac, F. Biogeochemical response of the Mediterranean Sea to the transient SRES-A2 climate change scenario. *Biogeosciences*, 2019, Vol. 16(1), pp. 135-165. <https://doi.org/10.5194/bg-16-135-2019>
- Rigal A., J.-M. Azaïs, A. Ribes (2019) : Estimating daily climatological normals in a changing climate, soumis à *Climate Dynamics*, 53(1-2), 275-286, doi:10.1007/s00382-018-4584-6
- Risi C, Galewsky J, Reverdin G and Briert F (2019), "Controls on the water vapor isotopic composition near the surface of tropical oceans and role of boundary layer mixing processes", *Atmospheric Chemistry and Physics*, oct, 2019. Vol. 19(19), pp. 12235-12260
- Rodríguez-Fernández, N.; de Rosnay, P.; Albergel, C.; Richaume, P.; Aires, F.; Prigent, C.; Kerr, Y. SMOS Neural Network Soil Moisture Data Assimilation in a Land Surface Model and Atmospheric Impact. *Remote Sens.* 2019, 11, 1334

- Rogelj, J., Forster, P. M., Kriegler, E., Smith, C. J. and Séférian, R. Estimating and tracking the remaining carbon budget for stringent climate targets. *Nature*, 2019, Vol. 571(7765), pp. 335-342. <https://doi.org/10.1038/s41586-019-1368-z>
- Roode, S. R., Frederikse, T., Siebesma, A. P., Ackerman, A. S., Chylik, J., Field, P. R., Fricke, J., Gryscha, M., Hill, A., Honnert, R., Krueger, S. K., Lac, C., Lesage, A. T. and Tomassini, L. Turbulent Transport in the Gray Zone: A Large Eddy Model Intercomparison Study of the CONSTRAIN Cold Air Outbreak Case. *Journal of Advances in Modeling Earth Systems*, 2019, Vol. 11(3), pp. 597-623. <https://doi.org/10.1029/2018ms001443>
- Rottner, L., Arbogast, P., Destouches, M., Hamidi, Y. and Raynaud, L. The similarity-based method: a new object detection method for deterministic and ensemble weather forecasts. *Advances in Science and Research*, 2019, Vol. 16, pp. 209-213. <https://doi.org/10.5194/asr-16-209-2019>
- Sahlaoui, Z., Mordane, S., Wattrelot, E. and Mahfouf, J.-F. Improving heavy rainfall forecasts by assimilating surface precipitation in the convective scale model AROME: A case study of the Mediterranean event of November 4, 2017. *Meteorological Applications*, 2019. <https://doi.org/10.1002/met.1860>
- Saint-Martin, D., Geoffroy, O., Watson, L., Douville, H., Bellon, G., Voltaire, A., Cattiaux, J., Decharme, B. and Ribes, A. Fast-Forward to Perturbed Equilibrium Climate. *Geophysical Research Letters*, 2019, Vol. 46(15), pp. 8969-8975. <https://doi.org/10.1029/2019gl083031>
- Saltikoff, E., Haase, G., Delobbe, L., Gaussiat, N., Martet, M., Idziorek, D., Leijnse, H., Novák, P., Lukach, M. and Stephan, K. OPERA the Radar Project. *Atmosphere*, 2019, Vol. 10(6), pp. 320. <https://doi.org/10.3390/atmos10060320>
- Sassi, M. Z., Fourrié, N., Guidard, V. and Birman, C. Use of Infrared Satellite Observations for the Surface Temperature Retrieval over Land in a NWP Context. *Remote Sensing*, MDPI AG, 2019, Vol. 11(20), pp. 2371. <https://doi.org/10.3390/rs11202371>
- Sauvage C, Brossier CL, Bouin M-N and Ducrocq V (2019), "Characterization of the air-sea exchanges mechanisms during a Mediterranean heavy precipitation event using realistic sea state modelling", *Atmospheric Chemistry and Physics*, sep, 2019
- Séférian, R., Nabat, P., Michou, M., Saint-Martin, D., Voltaire, A., Colin, J., Decharme, B., Delire, C., Berthet, S., Chevallier, M., Sénési, S., Franchistéguy, L., Vial, J., Mallet, M., Joetzjer, E., Geoffroy, O., Guérémy, J.-F., Moine, M.-P., Msadek, R., Ribes, A., Rocher, M., Roehrig, R., y-Mélia, D. S., Sanchez, E., Terray, L., Valcke, S., Waldman, R., Aumont, O., Bopp, L., Deshayes, J., Éthé, C. and Madec, G. Evaluation of CNRM Earth System Model, CNRM-ESM2-1: Role of Earth System Processes in Present-Day and Future Climate. *Journal of Advances in Modeling Earth Systems*, 2019, Vol. 11(12), pp. 4182-4227. <https://doi.org/10.1029/2019ms001791>
- Shamambo, D.C.; Bonan, B.; Calvet, J.-C.; Albergel, C.; Hahn, S. Interpretation of ASCAT Radar Scatterometer Observations Over Land: A Case Study Over Southwestern France. *Remote Sens.* 2019, 11(23), 2842; <https://doi.org/10.3390/rs1123284>
- Spandre, P., François, H., Verfaillie, D., Lafaysse, M., Déqué, M., Eckert, N., George, E. and Morin, S. Climate controls on snow reliability in French Alps ski resorts. *Scientific Reports*, 2019, Vol. 9, pp. 8043. <https://doi.org/10.1038/s41598-019-44068-8>
- Spandre, P., François, H., Verfaillie, D., Pons, M., Vernay, M., Lafaysse, M., George, E. and Morin, S. Winter tourism under climate change in the Pyrenees and the French Alps: relevance of snowmaking as a technical adaptation. *The Cryosphere*, 2019, Vol. 13, pp. 1325-1347. <https://doi.org/10.5194/tc-13-1325-2019>
- Specq, D., Bellon, G., Peltier, A., Lefèvre, J. and Menkes, C. Influence of Subseasonal Variability on the Diurnal Cycle of Precipitation on a Mountainous Island: The Case of New Caledonia. *Monthly Weather Review*, American Meteorological Society, 2019, Vol. 148(1), pp. 333-351. <https://doi.org/10.1175/mwr-d-19-0177.1>
- Strauss, C., D. Ricard, C. Lac, and A. Verrelle, Evaluation of turbulence parameterizations in convective clouds and their environment based on a large-eddy simulation, *Quart. J. Roy. Meteor. Soc.*, 145, 3195-3217, 2019
- Tall M., C. Albergel, B. Bonan, Y. Zheng, F. Guichard, M. S. Dramé, A.T. Gaye, L. O. Sintondji, F. C. Hountondji, P. M. Nikiema and J.-C. Calvet, 2019: Towards a Long-Term Reanalysis of Land Surface Variables over Western Africa: LDAS-Monde Applied over Burkina Faso from 2001 to 2018. *Remote Sens.*, 11(6), 735. doi: 10.3390/rs11060735
- Taylor J. W., Haslett S. L., Bower K., Flynn M., Crawford I., Dorsey J., Choularton T., Connolly P. J., Hahn V., Voigt C., Sauer D., Dupuy R., Brito J., Schwarzenboeck A., Bourriane T., Denjean C., Rosenberg P., Flamant C., Lee J. D., Vaughan A. R., Hill P. G., Brooks B., Catoire V., Knippertz P. and Coe, H. Aerosol influences on low-level clouds in the West African monsoon. *Atmos. Chem. Phys.*, 2019. <https://doi.org/10.5194/acp-19-8503-2019>
- Teich, M., Giunta, A. D., Hagenmuller, P., Bebi, P., Schneebeli, M. and Jenkins, M. J. Effects of bark beetle attacks on forest snowpack and avalanche formation – Implications for protection forest management. *Forest Ecology and Management*, 2019, Vol. 438, pp. 186-203. <https://doi.org/10.1016/j.foreco.2019.01.052>
- Timmermans, R., Segers, A., Curier, L., Abida, R., Attié, J.-L., Amraoui, L. E., Eskes, H., de Haan, J., Kujanpää, J., Lahoz, W., Nijhuis, A. O., Quesada-Ruiz, S., Ricaud, P., Veeffkind, P. and Schaap, M. Impact of synthetic space-borne NO2 observations from the Sentinel-4 and Sentinel-5P missions on tropospheric NO2 analyses. *Atmospheric Chemistry and Physics*, 2019, Vol. 19(19), pp. 12811-12833. <https://doi.org/10.5194/acp-19-12811-2019>
- Tokarska K., G. Hegerl, A. Schurer, A. Ribes, J. Fasullo (2019) Quantifying human contributions to past and future ocean warming and thermohaline sea level rise. *Environmental Research Letters*, 14 (7), 074020, doi:10.1088/1748-9326/ab23c1
- Trimmel H, Weihs P, Faroux S, Formayer H, Hamer P, Hasel K, Laimighofer J, Leidingger D, Masson V, Nadeem I, Oswald SM, Revesz M and Schoetter R (2019), "Thermal conditions during heat waves of a mid-European metropolis under consideration of climate change, urban development scenarios and resilience measures for the mid-21st century", *Meteorologische Zeitschrift.*, jan, 2019. Schweizerbart
- Tuzet, F., Dumont, M., Arnaud, L., Voisin, D., Lamare, M., Larue, F., Revuelto, J. and Picard, G. Influence of light-absorbing particles on snow spectral irradiance Profiles. *The Cryosphere*, 2019, Vol. 13, pp. 2169-2187. <https://doi.org/10.5194/tc-13-2169-2019>
- van Dalum, C. T., van de Berg, W. J., Libois, Q., Picard, G., and van den Broeke, M. R.: A module to convert spectral to narrowband snow albedo for use in climate models: SNOWBAL v1.2, *Geosci. Model Dev.*, 12, 5157–5175, <https://doi.org/10.5194/gmd-12-5157-2019>, 2019
- Vereecken, H., Weihermüller, L., Assouline, S., Šim nek, J., Verhoef, A., Herbst, M., Archer, N., Mohanty, B., Montzka, C., Vanderborght, J., Balsamo, G., Bechtold, M., Boone, A., Chaddburn, S., Cuntz, M., Decharme, B., Ducharme, A., Ek, M., Garrigues, S., Goergen, K., Ingwersen, J., Kollet, S., Lawrence, D. M., Li, Q., Or, D., Swenson, S., de Vrese, P., Walko, R., Wu, Y. and Xue, Y. Infiltration from the Pedon to Global Grid Scales: An Overview and Outlook for Land Surface Modeling. *Vadose Zone Journal*, Soil Science Society of America, 2019, Vol. 18(1), pp. 0. <https://doi.org/10.2136/vzj2018.10.0191>
- Veysiere, G., Karbou, F., Morin, S., Lafaysse, M. and Vionnet, V. Evaluation of Sub-Kilometric Numerical Simulations of C-Band Radar Backscatter over the French Alps against Sentinel-1 Observations. *Remote Sensing*, 2019, Vol. 11, pp. 8. <https://doi.org/10.3390/rs11010008>
- Villefranche N, Fournier R, Couvreur F, Blanco S, Eymet V, Forest V, Tregan J.M., 2019: A path-tracing Monte Carlo Library for 3-D radiative transfer in highly resolved cloudy atmospheres, *Journal of Advances in Modeling Earth Systems*, 11, 8, 2449–2473. <https://doi.org/10.1029/2018MS001602>
- Vionnet, V., Six, D., Auger, L., Dumont, M., Lafaysse, M., Quéno, L., Réveillet, M., Dombrowski-Etchevers, I., Thibert, E. and Vincent, C. Sub-kilometer precipitation datasets for snowpack and glacier modeling in alpine terrain. *Frontiers in Earth Science : Cryospheric Sciences*, 2019, Vol. 7, pp. 182. <https://doi.org/10.3389/feart.2019.00182>
- T. Vischel, G. Panthou, P. Peyrillé, R. Roehrig, G. Quantin, T. Lebel, C. Wilcox, F. Beucher, M. Budiarti, Chapter 4- Precipitation Extremes in the West African Sahel: Recent Evolution and Physical Mechanisms, Editor(s): V. Venugopal, Jai Sukhatme, Raghu Murtugudde, Rémy Roca, *Tropical Extremes*, 2019, Pages 95-138, ISBN 9780128092484, <https://doi.org/10.1016/B978-0-12-809248-4.00004-2>
- Voltaire, A., Exarchou, E., Sanchez-Gomez, E., Demissie, T., Deppenmeier, A.-L., Frauen, C., Goubanova, K., Hazeleger, W., Keenlyside, N., Koseki, S., Prodhomme, C., Shonk, J., Toniazzo, T. and Traoré, A.-K. Role of wind stress in driving SST biases in the Tropical Atlantic. *Climate Dynamics*, 2019. <https://doi.org/10.1007/s00382-019-04717-0>
- Voltaire, A., Saint-Martin, D., Sénési, S., Decharme, B., Alias, A., Chevallier, M., Colin, J., Guérémy, J.-F., Michou, M., Moine, M.-P., Nabat, P., Roehrig, R., y Méliá, D. S., Séférian, R., Valcke, S., Beau, I., Belamari, S., Berthet, S., Cassou, C., Cattiaux, J., Deshayes, J., Douville, H., Ethé, C., Franchistéguy, L., Geoffroy, O., Lévy, C., Madec, G., Meurdesoif, Y., Msadek, R., Ribes, A., Sanchez-Gomez, E., Terray, L. and Waldman, R. Evaluation of CMIP6 DECK Experiments With CNRM-CM6-1. *Journal of Advances in Modeling Earth Systems*, 2019, Vol. 11(7), pp. 2177-2213. <https://doi.org/10.1029/2019MS001683>

- Xian, P., Reid, J. S., Hyer, E. J., Sampson, C. R., Rubin, J. I., Ades, M., Asencio, N., Basart, S., Benedetti, A., Bhattacharjee, P. S., Brooks, M. E., Colarco, P. R., da Silva, A. M., Eck, T. F., Guth, J., Jorba, O., Kouznetsov, R., Kipling, Z., Sofiev, M., Garcia-Pando, C. P., Pradhan, Y., Tanaka, T., Wang, J., Westphal, D. L., Yumimoto, K. and Zhang, J. Current state of the global operational aerosol multi-model ensemble: An update from the International Cooperative for Aerosol Prediction (ICAP). *Quarterly Journal of the Royal Meteorological Society*, 2019, Vol. 145(S1), pp. 176-209. <https://doi.org/10.1002/qj.3497>
- Xu, Y. Estimates of changes in surface wind and temperature extremes in southwestern Norway using dynamical downscaling method under future climate. *Weather and Climate Extremes*, 2019, Vol. 26, pp. 100234. <https://doi.org/10.1016/j.wace.2019.100234>
- Yamaguchi, S., Ishizaka, M., Motoyoshi, H., Nakai, S., Vionnet, V., Aoki, T., Yamashita, K., Hashimoto, A. and Hachikubo, A. Measurement of specific surface area of fresh solid precipitation particles in heavy snowfall regions of Japan. *The Cryosphere*, 2019, Vol. 13(10), pp. 2713-2732. <https://doi.org/10.5194/tc-13-2713-2019>
- Yiou, P., J. Cattiaux, L. Corre, D. Faranda, N. Kadyrov, A. Jézéquel, S. Mittelberger, P. Naveau, A. Ribes, Y. Robin, S. Thao, G.J. van Oldenborgh, R. Vautard, M. Vrac (2020) Analyses of the European summer heatwave of 2018, *BAMS*, 101 (1), S35–S40
- Zhang, W., M. Brandt, J. Penuelas, F. Guichard, X. Tong, F. Tian and R. Fensholt, 2019: Ecosystem structural changes controlled by altered rainfall climatology in tropical savannas. *Nature Communications*, 10, 671. doi:10.1038/s41467-019-08602-6
- Zhang S, Meurey C and Calvet J-C (2019), "Identification of soil-cooling rains in southern France from soil temperature and soil moisture observations", *Atmospheric Chemistry and Physics*, apr, 2019. Vol. 19(7), pp. 5005-5020
- Zhao, Y., Saunio, M., Bousquet, P., Lin, X., Berchet, A., Hegglin, M. I., Canadell, J. G., Jackson, R. B., Hauglustaine, D. A., Szopa, S., Stavert, A. R., Abraham, N. L., Archibald, A. T., Bekki, S., Deushi, M., Jöckel, P., Josse, B., Kinnison, D., Kirner, O., Maréchal, V., O'Connor, F. M., Plummer, D. A., Revell, L. E., Rozanov, E., Stenke, A., Strode, S., Tilmes, S., Dlugokencky, E. J. and Zheng, B. Inter-model comparison of global hydroxyl radical (OH) distributions and their impact on atmospheric methane over the 2000-2016 period. *Atmospheric Chemistry and Physics*, 2019, Vol. 19(21), pp. 13701-13723. <https://doi.org/10.5194/acp-19-13701-2019>
- Zheng Y, Albergel C, Munier S, Bonan B and Calvet J-C (2019), "An Offline Framework for High-dimensional Ensemble Kalman Filters to Reduce the Time-to-solution", *GMDA Bulletin*, jun, 2019

2019 Scientific papers list (outside DR)

- Barbary, D, Leroux, M-D, Bousquet, O. The orographic effect of Reunion Island on tropical cyclone track and intensity. *Atmos Sci Lett*. 2019; 20:e882.<https://doi.org/10.1002/asl.882>.
- Beaufort, A.; Gibier, F. & Palany, P. (2019), 'Assessment and correction of three satellite rainfall estimate products for improving flood prevention in French Guiana', *International Journal of Remote Sensing* 40(1), 171-196. doi: 10.1080/01431161.2018.1511934
- Bonnardot, F, Quetelard, H, Jumaux, G, Leroux, M-D, Bessafi, M. Probabilistic forecasts of tropical cyclone tracks and intensities in the southwest Indian Ocean basin. *Q. J. R. Meteorol. Soc.*, 145, 675– 686. <https://doi.org/10.1002/qj.3459>
- Centurioni, L. R., J. D. Turton, R. Lumpkin, L. Braasch, G. Brassington, Y. Chao, E. Charpentier, Z. Chen, G. Corlett, K. Dohan, C. Donlon, C. Gallage, V. Hormann, A. Ignatov, B. Ingleby, R. Jensen, B. A Kelly-Gerreyn, I. M Koszalka, X. Lin, E. Lindstrom, N. Maximenko, C. J Merchant, P. Minnett, A. G. O'Carroll, T. Paluszkiwicz, P. Poli, P. Poulain, G. Reverdin, X. Sun, V. Swail, S. Thurston, L. Wu, L. Yu, B. Wang, and D. Zhang, 2019: Global in situ Observations of Essential Climate and Ocean Variables at the Air-Sea Interface. *Frontiers in Marine Science*, doi:10.3389/fmars.2019.00419.
- Colomb, A., T. Kriat, and M. Leroux, 2019: On the Rapid Weakening of Very Intense Tropical Cyclone Hellen (2014). *Mon. Wea. Rev.*, 147, 2717–2737, <https://doi.org/10.1175/MWR-D-18-0309.1>
- Foltz, G. R., P. Brandt, I. Richter, B. Rodriguez-Fonseca, F. Hernandez, M. Dengler, R. R. Rodrigues, J. Oliver Schmidt, L. Yu, N. Lefevre, L. Cotrim Da Cunha, M. James McPhaden, M. Cunha de Araujo Filho, J. Karstensen, J. Hahn, M. Martín-Rey, C. M. Patricola, P. Poli, P. Zuidema, R. Hummels, R. C. Perez, V. Hatje, J. Luebbecke, I. Polo, R. Lumpkin, B. Bourlès, F. E. Asuquo, P. Lehodey, A. Conchon, P. Chang, P. Dandin, C. Schmid, A. J Sutton, H. Giordani, Y. Xue, S. Illig, T. Losada, S. Grodsky, F. Gasparin, T. Lee, E. Mohino, P. Nobre, R. Wanninkhof, N. S. Keenlyside, V. Garçon, E. Sanchez-Gomez, H. C. Nnamchi, M. Drevillon, A. Storto, E. Remy, A. Lazar, S. Speich, M. Pereira Goes, T. Dorrington, W. E. Johns, J. N. Moum, C. Robinson, C. Perruche, R. Buss de Souza, A. Gaye, J. Lopez-Parages, P.-A. Monerie, P. Castellanos, N. U. Benson, M. N. Hounkonnou, and J. Trotte Duha, 2019: The Tropical Atlantic Observing System. *Frontiers in Marine Science*, doi:10.3389/fmars.2019.00206.
- Gommenginger, Christine; et al ; 2019 SEASTAR: A mission to study ocean submesoscale dynamics and small-scale atmosphere-ocean processes in coastal, shelf and polar seas. *Frontiers in Marine Science*, 6. <https://doi.org/10.3389/fmars.2019.00457>
- Haggerty, J., Defer, E., de Laat, A., Bedka, K., Moisselin, J.-M. Potts, R., Delanoë, J., Parol, F., Grandin, A., 2019, Detecting Clouds Associated with Jet Engine Ice Crystal Icing, <https://journals.ametsoc.org/doi/pdf/10.1175/BAMS-D-17-0252.1>
- Le Bastard, T., Caumont, O., Gaussiat, N., & Karbou, F. (2019). Combined use of volume radar observations and high-resolution numerical weather predictions to estimate precipitation at the ground: Methodology and proof of concept. *Atmospheric Measurement Techniques*, 12(10), 5669-5684.
- Le Menn, M., P. Poli, A. David, J. Sagot, M. Lucas, A. O'Carroll, M. Belbeoch, and K. Herklotz, 2019: Development of surface drifting buoys for fiducial reference measurements of sea-surface temperature. *Frontiers in Marine Science*, doi:10.3389/fmars.2019.00578.
- Leroux, M.-D., M. C. Nguyen-Hankinson, N. E. Davidson, J. Callaghan, K. Tory, A. Wain and X. Huang, 2019 : Environmental interactions during the extreme rain event associated with ex-tropical cyclone Oswald (2013), *Journal of Southern Hemisphere Earth Systems Science*, 69, 216–238, <https://doi.org/10.1017/ES19016>
- Le Traon, P. Y., Reppucci, A., Alvarez Fanjul, E., Aouf, L., Behrens, A., Belmonte, M., ... & Benkiran, M. (2019). From observation to information and users: the Copernicus Marine Service perspective. *Frontiers in Marine Sciences*, 6, 234, <https://doi.org/10.3389/fmars.2019.00234>.
- Moltmann, T., H.-M. Zhang, J. D. Turton, G. Nolan, C. C. Gouldman, L. Griesbauer, Z. Willis, A. Muñoz Piniella, E. Charpentier, P. Poli, E. Francis Burger, R. Lumpkin, C. Meinig, K. M. O'Brien, A. J Sutton, D. Zhang, and Y. Zhang, 2019: A Global Ocean Observing System (GOOS), delivered through enhanced collaboration across regions, communities, and new technologies. *Frontiers in Marine Science*, doi:10.3389/fmars.2019.00291.
- Penny, S. G., Akella, S., Balmaseda, M. A., Browne, P., Carton, J. A., Chevallier, M., ... & Hogan, P. (2019). Observational Needs for improving Ocean and Coupled Reanalysis, S2S Prediction, and Decadal Prediction. *Frontiers in Marine Science*, 6, 391.
- Pinardi, N., J. Stander, D. Legler, K. O'Brien, T. Boyer, T. Cuff, H. Garcia, E. Freeman, C. Sun, L. Gates, Z. Gong, A. Iona, Y. Xinyang, P. Bahurel, M. Belbouch, S. Belov, S. Lynne Brunner, E. Francis Burger, T. Carval, D. Chang-Seng, E. Charpentier, G. Coppini, A. S. Fischer, C. Gallage, J. Hermes, E. Heslop, S. Grimes, K. Louise Hill, K. James Horsburgh, S. Mancini, N. Moodie, M. Ouellet, P. Poli, P. Pissierssens, R. Proctor, N. Smith, V. Swail, and J. D. Turton, 2019: The Joint IOC (of UNESCO) and WMO Collaborative Effort for Met-Ocean Services. *Frontiers in Marine Science*, doi:10.3389/fmars.2019.00410.
- Poli, P., M. Lucas, A. O'Carroll, M. Le Menn, A. David, G. K. Corlett, P. Blouch, D. Meldrum, C. J. Merchant, M. Belbeoch, and K. Herklotz, 2019: The Copernicus Surface Velocity Platform drifter with Barometer and Reference Sensor for Temperature (SVP-BRST): genesis, design, and initial results. *Ocean Science*, 15, 199-214, doi:10.5194/os-15-199-2019.
- Rey, T.; Leone, F.; Candela, T.; Belmadani, A.; Palany, P.; Krien, Y.; Cécé, R.; Gherardi, M.; Péroche, M. & Zahibo, N. (2019), 'Coastal processes and influence on damage to urban structures during Hurricane Irma (St-Martin & St-Barthélemy, French West Indies)', *Journal of Marine Science and Engineering* 7(215). doi:10.3390/jmse7070215.

Smith, G. C., Allard, R., Babin, M., Bertino, L., Chevallier, M., Corlett, G. K., ... & Hebert, D. (2019). Polar Ocean Observations: A Critical Gap in the Observing System and Its Effect on Environmental Predictions From Hours to a Season. *Frontiers in Marine Science*, 6, 429.

Smith, S. R., G. Alory, A. Andersson, W. Asher, A. Baker, D. I. Berry, K. Drushka, D. Figurskey, E. Freeman, P. Holthus, T. Jickells, H. Kleta, E. C. Kent, N. Kolodziejczyk, M. Kramp, Z. Loh, P. Poli, U. Schuster, E. Steventon, S. Swart, O. Tarasova, L. Petit De La Villéon, and N. Vinogradova Shiffer, 2019: Ship-Based Contributions to Global Ocean, Weather, and Climate Observing Systems. *Frontiers in Marine Science*, doi:10.3389/fmars.2019.00434.

Stein, J. and F. Stoop, 2019: Neighborhood-Based Contingency Tables Including Errors Compensation. *Mon. Wea. Rev.*, 147, 329-344, <https://doi.org/10.1175/MWR-D-17-0288.1>

Storto, A., Alvera-Azcárate, A., Balmaseda, M. A., Barth, A., Chevallier, M., Counillon, F., ... & Garric, G. (2019). Ocean reanalyses: Recent advances and unsolved challenges. *Frontiers in Marine Science*, 6, 418.

Taillardat, M., Fougères, A. L., Naveau, P., & Mestre, O. (2019). Forest-based and semiparametric methods for the postprocessing of rainfall ensemble forecasting. *Weather and Forecasting*, 34(3), 617-634.

Étienne Vignon(1), Olivier Traullé(2), and Alexis Berne(1). ·8 April 2019. On the fine vertical structure of the low troposphere over the coastal margins of East Antarctica. *Atmospheric Chemistry and Physics* 19(7):4659-4683 (1) Environmental Remote Sensing Laboratory (LTE), École Polytechnique Fédérale de Lausanne (EPFL), Lausanne, Switzerland (2) DSO/DOA, Météo-France, Toulouse, France Étienne Vignon (etienne.vignon@epfl.ch)

Vincendon B., Edouard S., Ducrocq V. (2019). De l'incertitude dans un système de prévision d'ensemble des crues rapides méditerranéennes. *LHB*, 3-4 (2019) 22-30. DOI : 10.1051/lhb/2019051.

Jouglà, R., Hidalgo, J., Pouponneau, B., 2019 : Identification des situations météorologiques locales pour une cinquantaine de villes françaises. *La Météorologie*, 106, 59-68 (<http://documents.irevues.inist.fr/handle/2042/70370>)

Peltier H., Dabin W., Dars C., Demaret F., Doremus G., VanCanneyt O., Laran S., Mendez-Fernandez P., Spitz J., Authier M., Daniel P., Ridoux V., 2019: Can modelling the drift of bycaught dolphin stranded carcasses help identify involved fisheries? An exploratory study, *Global Ecology and Conservation*, November 2019. <https://doi.org/10.1016/j.gecco.2019.e00843>

PHD defended in 2019

Ardilouze, C. Impact de l'humidité du sol sur la prévisibilité du climat estival aux moyennes latitudes. Université de Toulouse, 2019

Coopmann, Olivier. Vers une meilleure assimilation des observations satellitaires infrarouges par le couplage des modèles météorologique et chimique. Université de Toulouse, 2019

Darmarakı, S. Canicules océaniques en Méditerranée : détection, variabilité passée et évolution future. Université de Toulouse, 2019

Dion, I.-A. Glace injectée dans la Tropopause Tropicale par Convection Profonde. Université de Toulouse, 2019

Drugé, T. Contribution des aérosols aux scénarios climatiques en Méditerranée pour le 21ème siècle à l'échelle régionale. Université de Toulouse, 2019

Ducongé, L., Etude du cycle de vie du brouillard durant la campagne LANFEX : impact de la dynamique en terrain vallonné et des processus microphysiques, Ph.D. thesis, Université de Toulouse, 2019

Fumière, Q. Impact du changement climatique sur les précipitations du Sud-Est de la France : apport des modèles résolvant la convection profonde. Université de Toulouse, 2019

Goret, M., Etude des interactions entre le climat urbain et le CO₂ : modélisation des flux de CO₂ et application à l'échelle d'une ville, Ph.D. thesis, Université de Toulouse, 2019

Guillet O., Modélisation des corrélations spatiales d'erreurs d'observation en assimilation de données variationnelle. Etude sur des maillages non structurés. INPT, Toulouse, 2019

Joulin, Pierre-Antoine. Modélisation à fine échelle des interactions entre parcs éoliens et météorologie locale. PhD, Océan, atmosphère, climat, Institut National Polytechnique de Toulouse, 2019. <https://oatao.univ-toulouse.fr/25551/>

Le Bastard, Tony. Utilisation des données radar volumiques et d'un modèle de PNT à haute résolution pour une meilleure estimation quantitative des précipitations en plaine et sur les massifs montagneux. INPT, Toulouse, 2019

Lovat, Alexane. Prévision à très courte échéance des crues rapides méditerranéennes. INPT, Toulouse, 2019

Mede, T., Étude numérique du comportement mécanique de la neige: une perspective microstructurale, Université Grenoble Alpes, 2019

Peinke I., Étude à micro-échelle du test de pénétration dans la neige. Université de Toulouse, 2019

Ponzano, Matteo. Prévisibilité des épisodes méditerranéens de pluies intenses à l'aide d'un jeu de données de 30 ans de prévisions rétrospectives. Université de Toulouse, 2019

Sauvage, César. Prévision couplée océan-atmosphère des épisodes méditerranéens : Impact d'une meilleure prise en compte des débits des fleuves et de l'état de mer. Université de Toulouse, 2019.

Vasconcelos, A. Mécanismes contrôlant les anomalies de température de surface de la mer et précipitation au cours des deux années contrastées 2010 et 2012 dans l'océan atlantique tropical. Université de Toulouse, 2019

Veyssière, G. Apport des mesures du radar à synthèse d'ouverture de Sentinel-1 pour l'étude des propriétés du manteau neigeux, Institut Polytechnique de Toulouse, 2019

Villefranche, N., Les effets radiatifs des nuages de couche limite : de leur simulation explicite à leur paramétrisation, Ph.D. thesis, Université de Toulouse, 2019

« Habilitations à diriger des recherches » defended in 2019

Séférián, Roland. Cycle du carbone global - Variabilité, Rétroactions et Couplages aux interfaces.

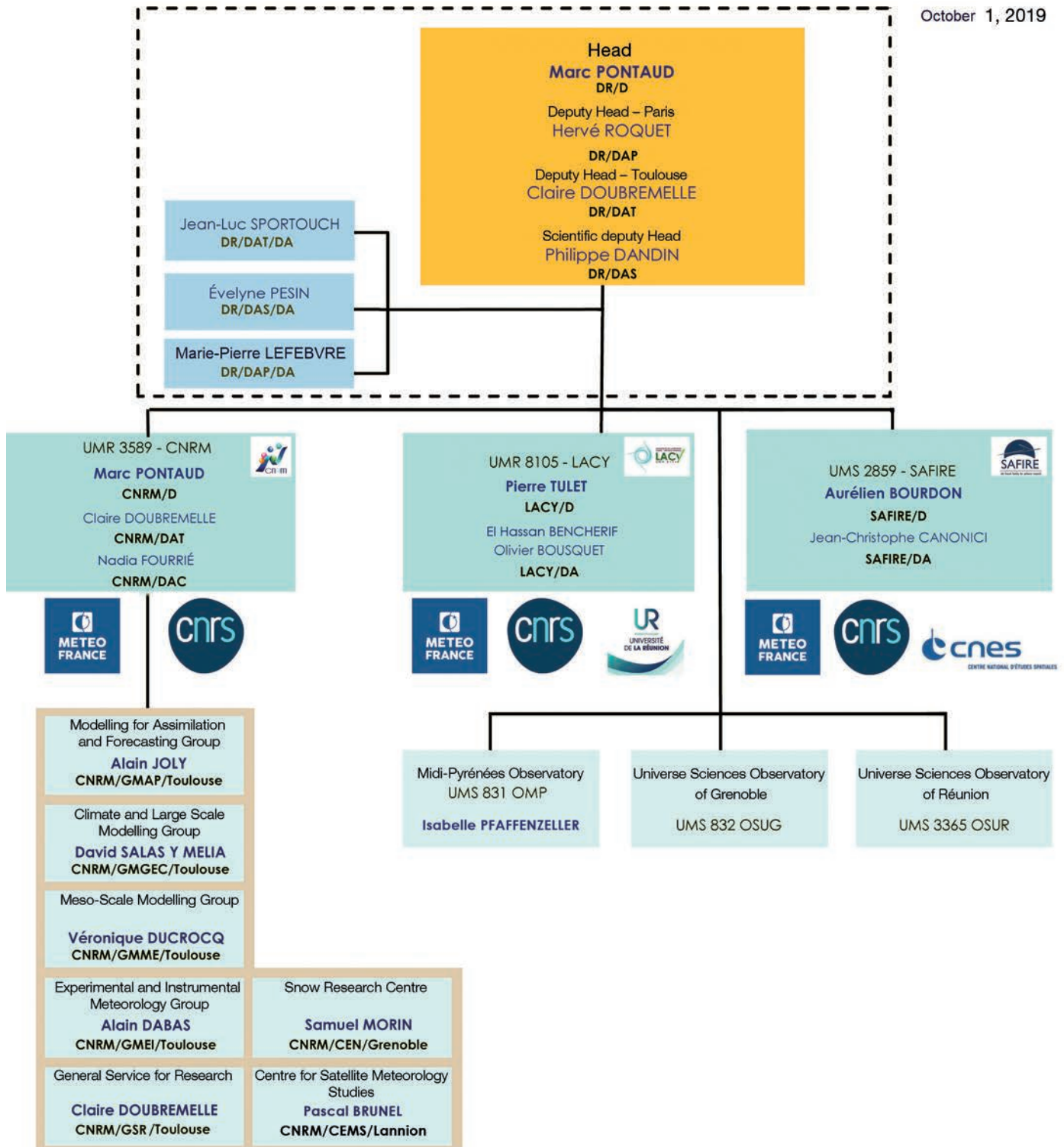
Glossary

ACTRIS-FR	Infrastructure de recherche distribuée, en support des recherches sur le climat et la qualité de l'air.	DGSCGC	Direction générale de la Sécurité Civile et de la Gestion de Crise
ADAMONT	Méthode de descente d'échelle sur les zones de montagne	DINEOF	Data Interpolating Empirical Orthogonal Functions
ADBL	AdaBoost for Atmospheric Boundary Layer	DIRAG	Direction Inter-Régionale Antilles Guyane
ADEME	Agence de l'Environnement et de la Maîtrise de l'Energie	DSM	Direction des Services Météorologiques
ADM	Atmospheric Dynamics Mission	ECMWF	European Centre for Medium-range Weather Forecasts
ADM-Aeolus	Atmospheric Dynamics Mission - Éole	EDR	Eddy Dissipation Rate
AEMET	Agencia Estatal de Meteorología (Espagne)	ENM	Ecole Nationale de la Météorologie
AEOLUS	Atmospheric Explorer Observations with a Lidar UV System	ENSO	El Nino Southern Oscillation
AERIS	Données et services pour l'atmosphère	EOF	Fonction Orthogonale Empirique
ALADIN	Aire Limitée Adaptation Dynamique et développement InterNational	ERA	European Re-Analysis
ALLENVI	ALLiance nationale de recherche pour l'ENVironnement	ESA	European Space Agency
ALPHA	Algorithmes et modèLes pour la Production Homogène globale	EUMETSAT	Organisation européenne pour l'exploitation de satellites météorologiques
AMSR	Advanced Microwave Scanning Radiometer	EXPLORER	Projections climatiques et impacts sur l'agriculture
ANR	Agence Nationale de la Recherche	FEDER	Fonds Européen de Développement Régional
AROME	Application de la Recherche à l'Opérationnel à Méso-Échelle	FORUM	Far-infrared Outgoing Radiation Understanding and Monitoring
AROME-OM	AROME – Outre Mer	GCM	Modèle de circulation Générale
AROME-PI	Configuration AROME Prévision Immédiate	GELATO	Global Experimental Leads and ice for Atmosphere and Ocean
ARPAE-SIMC	Agenzia regionale per la prevenzione, l'ambiente e l'energia - Servizio Idro Meteo Clima	GET	laboratoire de Géosciences Environnement Toulouse
ARPEGE	Action de Recherche Petite Échelle Grande Échelle	GHER	GeoHydrodynamic and Environmental Research
ASCAT	Advanced SCATterometer	GIEC	Groupe Intergouvernemental d'experts sur l'Evolution du Climat
AVHRR	Advanced Very High Resolution Radiometer	GIRAFE	capteur Gravimétrique Interférométrique de Recherche à Atomes Froids Embarqué
BSRN	Baseline Surface Radiation Network	GMAP	Groupe de Modélisation et d'Assimilation pour la Prévision
C3S	Copernicus Climate Change Service	GMEI	Groupe de Météorologie Expérimentale et Instrumentale
CALIOP	Cloud-Aerosol Lidar with Orthogonal Polarization	GOES	Satellites météorologiques géostationnaires américains
CALIPSO	Cloud-Aerosol Lidar and Infrared Pathfinder Satellite Observations	GOES 16/17	Satellites météorologiques géostationnaires américains
CAT	Clear Air Turbulence, Turbulence en Air Clair	GTG	Graphical Turbulence Guidance
CCMI	Chemistry-Climate Model Initiative	HAMSTRAD	H2O Antarctica Microwave Stratospheric and Tropospheric Radiometer
Cedre	Centre de documentation, de recherche et d'expérimentations sur les pollutions accidentelles des eaux	HCERES	Haut Conseil de l'évaluation de la recherche et de l'enseignement supérieur
CEMS	Centre d'Etude en Météorologie Satellitaire	HCL	Hauteur de Couche Limite
CEN	Centre d'Etudes de la Neige	HIRLAM	High Resolution Limited Area Model
CEPMET	Centre Européen pour les Prévisions Météorologiques à Moyen Terme	HOMONIM	Historique Observation MOdélisation des Niveaux Marins
CFOSAT	Chinèse-French SATellite	HYCOM	HYbrid Coordinate Ocean Model
CLIMERI-France	Infrastructure nationale de modélisation du système climatique de la Terre	HyMeX	Hydrological cYcle in the Mediterranean EXperiment
CMCC	Centre euro-Méditerranéen sur le Changement Climatique (Italie)	IAGOS	In-service Aircraft for Global Observing System
CMIP	Coupled Model Intercomparaison Project	IASI	Interféromètre Atmosphérique de Sondage Infrarouge
CMIP6	6 ^e phase du Coupled Model Intercomparaison Project	IFPEN	Institut Français du Pétrole Energies Nouvelles
CMRS	Centre Météorologique Régional Spécialisé	Ifremer	Institut Français de Recherche pour l'Exploitation de la MER
CNES	Centre National d'Études Spatiales	IFS	Integrated Forecasting System
CNRM	Centre National de Recherches Météorologiques	INRA	Institut National de la Recherche Agronomique
CNRM-CM6	Version 6 du Modèle de Climat du CNRM	INRAE	Institut National de Recherche pour l'Agriculture, l'alimentation et l'Environnement
CNRM-ES	Modèle Système Terre incluant le cycle du carbone	IPCC	Intergovernmental Panel on Climate Change (Groupe d'experts intergouvernemental sur l'évolution du climat)
CNRS	Centre National de Recherches Scientifiques	IR	Infra Rouge
CO	Monoxyde de Carbone	ISBA	Interaction Sol-Biosphère-Atmosphère
COMEPHORE	Fusion des données radar et des pluviomètres disponibles	IWV	Quantité de vapeur d'eau intégrée
COMSI	COMité Scientifique	KABL	(K-means for Atmospheric Boundary Layer
COPAL	COMmunity heavy-PAYload Long endurance instrumented aircraft for tropospheric research in environmental and geo-sciences	KALIDEOS-Alpes	Dispositif du CNES visant à promouvoir et à démontrer l'usage de la donnée spatiale
COPERNICUS	European Earth observation system http://www.copernicus.eu/pages-principales/services/climate-change/	LACY	Laboratoire de l'Atmosphère et des Cyclones – UMR 8105
CORDEX	COordinated Regional climate Downscaling EXperiment	LANFEX	Local and Nonlocal Fog Experiment
CREWS	Climate Risk and Early Warning Systems	LAURE	Loi sur l'Air et l'Utilisation Rationnelle de l'Energie
CROCUS	Modèle de simulation numérique du manteau neigeux développé par Météo-France.	LBLRTM	modèle de transfert radiatif raie-par-raie
CTrip	CNRM-Total Routing Integrated Pathway	LEFE	programme national « Les Enveloppes Fluides et l'Environnement »
DCSC	Direction de la Climatologie et des Services Climatiques	LIDAR	light detection and ranging
DEAL	Direction de l'Environnement, de l'Aménagement et du Logement	LIMA	Liquid Ice Multiple Aerosols
DESR	Direction de l'Enseignement Supérieur et de la Recherche	LISA	Lidar SATellite
DGPR	Direction Générale de la Prévention des Risques	LMI	Lifetime Maximum Intensity
		LWP	Eau liquide intégrée

MEDSCOPE	Mediterranean Services Chain based On climate Predictions	RCP8.5	8.5 W/m ² Representative Concentration Pathway corresponding to a 8.5 W/m ² radiative forcing at the end of the 21 st century compared to preindustrial climate
Megha-Tropiques	Satellite franco-indien dédié à l'étude du cycle de l'eau et des échanges d'énergie dans la zone tropicale	ReNov'Risk	Recherche intégrée et innovante sur les risques naturels : Impact Météorologique et Océanographique des Cyclones Tropicaux sur les territoires du Sud-Ouest de l'Océan Indien
MERCATOR-OCEAN	Société Civile Française d'océanographie opérationnelle	ROC	Relative Operating Characteristic curve
MERIT-DEM	Multi-Error-Removed Improved-Terrain	RTTOV	Radiative Transfer for TOVS
MESO-NH	Modèle à MESO-échelle Non Hydrostatistique	S2S	Sub-seasonal to Seasonal
METAR	MEteorological Aerodrome Report	SAF NWC	Satellite Application Facility on support to Nowcasting
METOP	MEteorological Operational Polar satellites	SAF OSI	Satellite Application Facility for Ocean and Sea Ice
METOP – SG	MEteorological Operational Polar satellites – Seconde Génération	SAFIRE	Service des Avions Français Instrumentés pour la Recherche en Environnement
MFWAM	Météo-France WAve Model	SAFRAN	Système d'Analyse Fournissant des Renseignements Atmosphériques pour la Neige
MISTRALS	Mediterranean Integrated STudies at Regional And Local Scales	SAR	Synthetic Aperture Radar
MJO	Madden-Julian Oscillation	SDI	Sahara Dust Index
MOCAGE	MODélisation de la Chimie Atmosphérique de Grande Echelle (modélisation)	SESAR	Single European Sky ATM Research
MODCOU	MODèle hydrologique COUplé surface-souterrain.	SEVIRI	Spinning Enhanced Visible and Infra-Red Imager
MODIS	MODerate-resolution Imaging Spectro-radiometer (instrument)	Shom	Service Hydrographique et Océanographique de la Marine
MoMa	Méthodes Mathématiques pour le couplage modèles et données dans les systèmes non-linéaires stochastiques à grand nombre de degrés de liberté	SLSTR	Sea and Land Surface Temperature Radiometer
MOTHY	Modèle Océanique de Transport d'HYdrocarbure	SOOI	Sud-Ouest Océan Indien
MSG	Météosat Seconde Génération	SROCC	Rapport Spécial sur l'Océan et la Cryosphère dans un Climat Changeant
MTES	Ministère de la Transition Ecologique et Solidaire	SURFEX	code de SURFace EXternalisé
MTG	Météosat Troisième Génération	SWI	Soil Wetness Index
MW	Micro Ondes	SWIM	Surface Wave Investigation and Monitoring
NCAR	National Center for Atmospheric Research	TAF	Terminal Aerodrome Forecast
NEMO	Nucleus for European Modelling of Ocean	TEB	Town Energy Balance
NH₃	formule de l'ammoniac	TEMSI	TEMps Significatif
NOAA	National Ocean and Atmosphere Administration	THEIA	Pôle de données et de services surfaces continentales
NWCSAF	Satellite Application Facility for Nowcasting	TRIP	Total Runoff Integrating Pathways
OACI	Organisation de l'Aviation Civile Internationale	TRL	Technology Readiness Level
OMM	Organisation Météorologique Mondiale	TSM	Températures de Surface de la Mer
ONERA	Office national d'études et de recherches aérospatiales	UERRA	Uncertainties in Ensembles of Regional Re-Analyses
OPG	Orages Points de Grille	UK	United Kingdom
OSTIA	Operational Sea surface Temperature sea Ice Analysis	UMR	Unité Mixte de Recherche
PEARP	Prévision d'Ensemble ARPège	UTC	Temps Universel Coordonné
PI	Prévision Immédiate	UTLS	Haute Troposphère Basse Stratosphère
PIAF	Prévision Immédiate Agrégée Fusionnée	VIIRS	Visible Infrared Imager Radiometer Suite
PICS	Prévision Immédiate intégrée des Impacts des Crues Soudaines	WIRE	Winter Risks for Energy
PNT	Prévision Numérique du Temps	YOPP	Year Of Polar Prediction
PRIMEQUAL	PRogramme de Recherche Interorganisme pour une MEilleure QUALité de l'air		
PROSNOW	Provision of a prediction for Snow management		
RADOME	Réseau d'Acquisition de Données d'Observations Météorologiques Etendu		
RCM	Modèle de Climat Régional		
RCP	Representative Concentration Pathway		

DR: Management structure

October 1, 2019



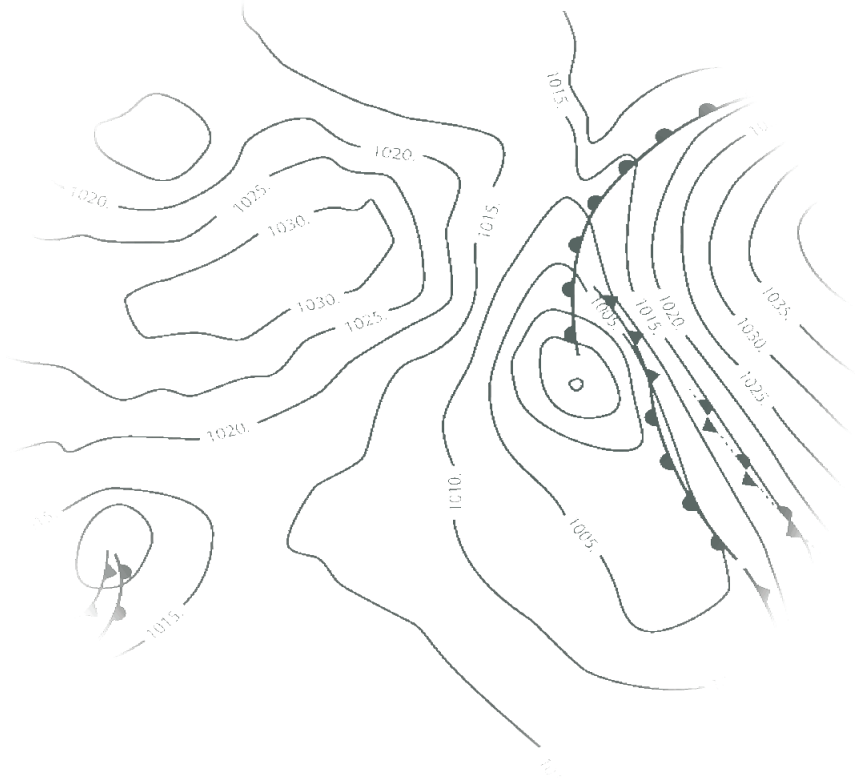
UMR: Joint Research Unit
UMS: Joint Service Unit

Météo-France

73, avenue de Paris
94165 Saint-Mandé Cedex
Phone: +33 (0) 1 77 94 77 94
Fax: +33 (0) 1 77 94 70 05
www.meteofrance.com

Research Department

42, avenue Gaspard Coriolis
31057 Toulouse Cedex 1 France
Phone: +33 (0) 5 61 07 93 70
Fax: +33 (0) 5 61 07 96 00
<http://www.urm-cnrm.fr>
Mail: contact@cnrm.meteo.fr



Création DIRCOM

Météo-France is certified to ISO 9001
by AFNOR Certification
© Météo-France 2020
Copyright december 2020
ISSN : 2116-438X